ÉCLAT

JOURNAL OF MATHEMATICS
LADY SHRI RAM COLLEGE FOR WOMEN
14th EDITION, 2023

Preface

The first 10 volumes of the annual academic journal of the Department of Mathematics were released in print, until 2020, when the e-journal was published for the very first time. The volume of the academic session 2022-23, that is, the XIV volume, marks the recommence of Éclat into e-journal form and continues to propel students into quality undergraduate research. It primarily focuses on undergraduate research and is thrust upon providing a platform for students to experience what research entails. The review research articles published in this volume arise from the mentorship program that was initiated from the 2019-20 academic session. The papers aim to provide theoretical and empirical research from interactions between students and the faculty.

It is to note that in this issue, a paper on the life and contributions of Sofia Kovalevskaya, the first woman in modern Europe to gain a doctorate in Mathematics, has been included in the section "Contribution of Women in Mathematics". The past two years have been full of challenges but we were fortunate enough to resume functioning offline. Inspite of the continuously changing circumstances, our mentors and authors were persistent in their work. As a result of this dedication, for this issue, we received a total of 13 brilliant proposals, and after a rigorous process of selection, 11 proposals were selected. In this volume we present 11 papers: 1 under 'History of Mathematics', 3 under 'Rigour in Mathematics', 2 under 'Extension of Course Content', 4 under 'Interdisciplinary Aspects of Mathematics' and 1 paper under 'Contribution of Women in Mathematics'.

We would like to express our sincere regards to the faculty members, who not only supported the authors during the mentorship program but also in reviewing papers and suggesting relevant additions. We would like to express our thanks to the student team comprising Nikita Sharma and Sneha M A (Batch of 2023) and Aditi Khandelwal and Shaziya Parveen (Batch of 2024) for their assistance in the compilation of this journal and all the authors and mentors who have contributed their articles for this volume. We also thank Muskan Kureel (Batch of 2024) for designing the cover page of this volume. We hope that this journal continues to be an intellectual stimulus for its readers whilst motivating students to make valuable contributions to their subject.

Éclat Editorial Board

CONTENTS

Éclat, A Mathematics Journal
Volume 14, 2022-23 (1-9)

Vastu and Mathematics

Sucheta Nayak and Aditi Khandelwal

Abstract

Vastu is the science of working with energy fields which is used to guide the architects to design buildings. It is a vast topic which covers wide areas which is why this paper focuses on ways in which mathematics is involved in the construction of a house built on the principles of Vastu. Beginning with the measurement units used in ancient societies, the paper describes the role of mathematics at each step in the construction of a house.

Keywords: Vastu, Ayadi, Sankusthapana, Brahmasutra, Yamasutra, Quadrangle, Feng Shui

1 Introduction

Vastu Shastra is an ancient system of architecture developed between 3000-6000 B.C. based on ancient texts that describe principles of layout, measurements, ground preparation and spatial geometry. It is not religious in origin but since Vastu, similar to Yoga and Ayurveda, denotes the connection between the laws and processes that govern the world of nature as well as human body, it has been perceived as religious by the ancient societies. This research paper highlights the possible logics behind the theories of Vastu Shastra.

Vastu is a vast topic and it covers wide areas such as laying out the principles for the design of houses, cities, gardens, roads, water works, shops and many other areas. In this paper, we focus on developing the understanding of how mathematics is involved in the construction of a simple house. The paper is divided into six sections. Section 1 is the introduction to the paper. Section 2 contains the history and the evolution of Vastu. Section 3 contains the definition of terms used throughout the paper. Section 4 discusses the mathematics involved in the construction of a house step-by-step based on Vastu. Section 5 contains a simple illustration of how dimensions are choosen in a given direction. Section 6 is the conclusion.

2 History and Evolution in Vastu Shastra

Vastu Shastra is the science of space and architecture which evolved during Vedic times in India. It is a part of Sthapatya Veda, an Upveda of Atharya Veda, which is around 4000-5000 years old. Through penance and meditation yogis of that period acquired answers to their questions. Hence Vedas are filled with divine knowledge. The principles of the science laid down during those days were purely based on the effect of sunrays during different times of the day. The observations made were noted and concluded only after in-depth screening of the situation.

In around ninth century B.C., the concept of Vastu Shastra was transferred to Tibet, South East and finally to China and Japan which lead to the foundation of what is now known as **Feng Shui**. According to its modern meaning, it covers all buildings irrespective of their use like temples, industries, business buildings, hotels etc. The pink city Jaipur in Rajasthan which was master plan of Rajput king Jai Singh and built by 1727 C.E., is based on Vastu Shastra principles. Similarly,

modern era projects such as Jawahar Kala Kendra in Jaipur, the architect Charles Correa's designed Gandhi Smarak Sangrahalaya in Ahmedabad, apply concepts from the Vastu Shastra. In the design of Chandigarh city, 1950, Le Corbusier combined modern architecture theories with those of Vastu Shastra [5],[6].
In recent times, with the advent of green technology, green lifestyle, and affordable environmental materials, there is a growing focus on green living and hence an understanding of Vastu has become essential since it majorly focuses on the inter-relation between ecology, passive energy, and living beings.

3 Definitions

3.1 Measurement Units

In ancient times, two measurement units were majorly followed, which are:

1. Yavamana[1] : India being an agricultural community, grain was widely used as a measuring unit for small objects. There were majorly 6 varieties of grains out of which yava was considered standard grain for measurement. The average width of yava is 3.75 mm. The octal division is continued to the smallest measurement called paramanu, refer Table 1, which is equal to the size of floating particles visible in sun rays.

8 paramanu	1 trasarenu
8 trasarenu	1 liksa
8 liksa	1 yuka
8 yuka	1 tila
8 tila	1 yuva

Table 3.1: Octal divisions of Yava, tabulated on LaTeX

2. Manusyapramana[2] : This measurement is performed using body parts as a reference.
For Example: Angula is the length of the central phalanx of the middle finger and Vyama is length of arm stretch of a perfect man [2].
Since the anthropometric measurement vary widely from race to race, angula is standardised in relation to yava as 8 times the width of yava, refer Table 2 for the interconversions.

8 yava	1 angula	3 cm
8 angula	1 pada	24 cm
8 pada	1 vyama	192 cm
3 angula	1 parva	9 cm
24 angula	1 hasta	72 cm
4 hasta	1 danda	288 cm

Table 3.2: Octal divisions of Vyama and other important interconversions, tabulated on LaTeX

The following Table 3.3 suggests suitable measuring units for different objects:

[1]yava means barley grain and mana means measurement
[2]meaning Anthropometric measurement

Vastu	Unit	Octal sub-unit
Fine details, carvings, etc.	yava	tila
Icons, pitha, etc.	angula	yava
Building elements	hasta	parva
Building plan	vyama	pada
Building plot	danda	vitasti
Measurement of land	rajju	danda

Table 3.3: Units for measuring different Vastu, tabulated on LaTeX

3.2 Ayadi

Ayadi constitutes six formulae **Aaya**,**Vyaya**,**Yoni**, **Raksha**, **Vara** and **Tithi**. The remainder obtained by using these formulae determines whether it is a gain or loss. If it is a gain, then the structure is said to be proportionate and stable and the dimensions are correct. However if it is a loss, then it means the dimensions are not correct and should be suitably corrected [4].
The formulae are as follows:

1. Aaya is the remainder of (Length × 8 divided by 12).
2. Vyaaya is the remainder of (Breadth × 9 divided by 10).
3. Yoni is the remainder of (Breadth × 3 divided by 8).
4. Raksha is the remainder of (Length × 8 divided by 27).
5. Vara (week) is the remainder of (Height × 9 divided by 7).
6. Tithi (Phase of the moon) is the remainder of (Height × 9 divided by 30).

The length, breadth and height in the Ayadi formulae are in hasta unit and angula subunit.

4 Geometrical formulation and mathematical requirements

4.1 Fixing cardinal direction

The first act to be done in the construction is determining the cardinal direction using sanku[3]. Fixing of gnomon (sanku) is called sankusthapana. Either the entire land or an area of 1 danda square (2.88 m × 2.88 m) should be levelled in the middle of the plot for sankusthapana. The morning time in Suklapaksha of Uttarayana (December 23 to June 22) was considered suitable for this act.
There are two methods for the same:

1. In the first method sanku of 1/2 hasta (32 cm) or slightly more than this height is fixed in the ground.
   Step 1 : With P as centre and one hasta radius, a circle is drawn on the ground.
   Step 2 : The points where the shadows of the tip of the pole touch the circle in the forenoon and in the afternoon are marked as W_1 and E_1.
   Step 3 : In order to get the correct direction, the point where the shadow of the tip of the pole touches the circle next morning (W_2) is also noted. Due to the declination of the sun

[3] a pole like object made of ivory, sandal wood, khadira wood (Acacia catechu), Sami wood (Propsopis julisflora) or saka (Tectona gramdis) wood

(uttarayana and daksinayana), the shadows of the tip of the pole do not fall on the same points next day.
Step 4 : The distance between W_1 and W_2 is divided into 3 parts and the point W_3 nearer to W_1 at a distance equal to one-third of the distance W_2W_1 is joined to E_1 to get the West-East (W-E) direction. Refer Figure 4.1.

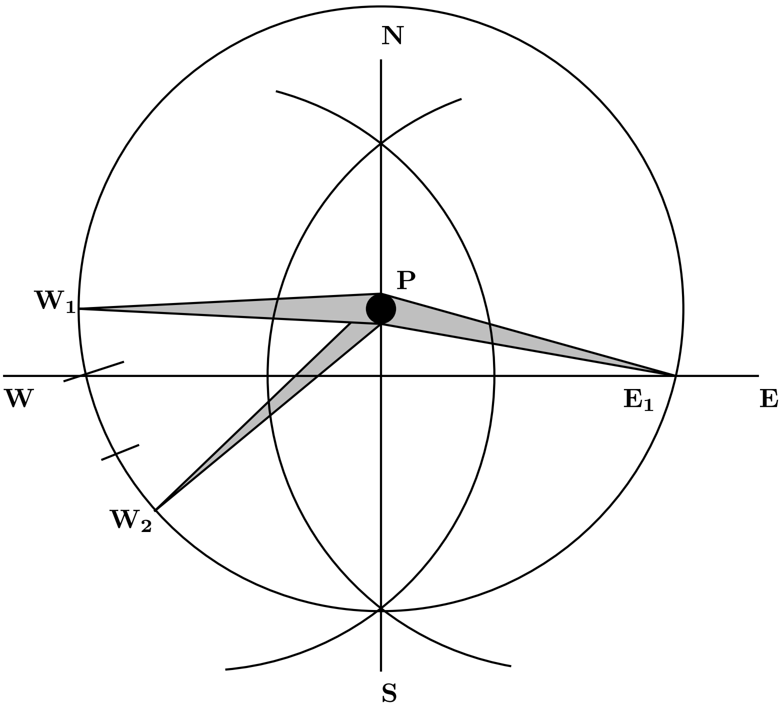

Figure 4.1: Fixing cardinal directions using sun-shadow method, drawn using LaTeX

The South-North (S-N) direction is then marked using geometric principles. The W-E line is called Brahmasutra and the S-N line is called Yamasutra.

2. In the second method, sanku of 12 angula is fixed at centre P.
   Step 1 : Three circles of radius 1/2 hasta, 1 hasta, 3/2 hasta are described with P as centre.
   Step 2 : The points where the shadow of the tip of the pole falls on these 3 circles are marked S_1, S_2, S_3.
   Step 3 : With these 3 points as centres, 3 circles, each of 1/2 hasta radius, are drawn.
   The front and rear (agra and puccha) points (1 and 2; 3 and 4) of the same fish figures are joined and extended to intersect at N. The line joining P and N will give the S-N direction the W-E line is drawn perpendicular to it [2]. Refer Figure 4.2.

Figure 4.2: Fixing cardinal directions using alternate method, drawn using LaTeX

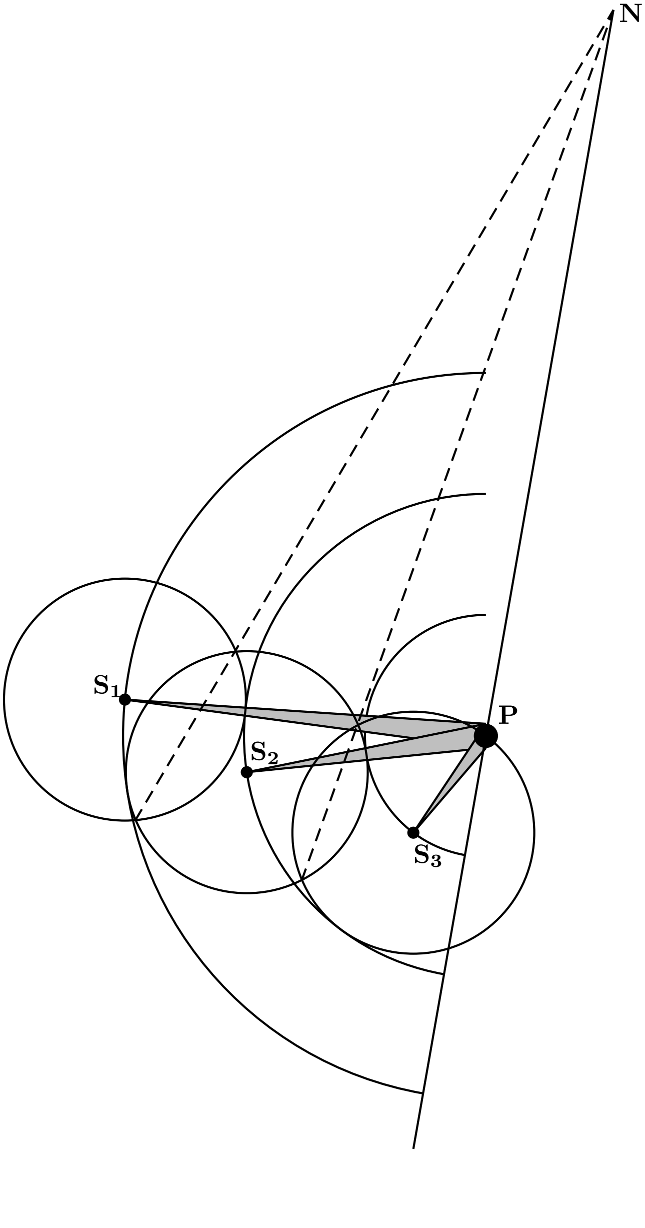

4.2 Possible shapes of plots

The possible shapes of plot for house are as follows [1]:

- Square plot: A plot is square if all the sides are of equal length.
- Rectangular plot: If the opposite sides are equal in length, the plot is called rectangular plot.
- Odd shaped plots: The following alternatives are possible:
  - A square or rectangular plot with one or two sides projecting towards one corner.
  - A plot with atleast one right angle.
- A Trapezoidal plot: In this plot, two sides are parallel to each other and all four sides have varying lengths.
- Quadrangle plot: All sides have varied lengths and none of the angles are 90°.

4.3 Plot angle correction

Amongst all the shapes given above, square is the best geometrical shape in economical and structural considerations followed by rectangle since it requires lesser amount of construction materials on its periphery while providing broader inner area compared to other geometrical figures. In structural terms, "square-shaped and rectangular-shaped buildings can transfer the load safely even where the bearing capacity of soil is low, while other irregular shapes provide large contact areas more than they critically require". The symmetrical shape of rectangular figures also creates a predictable behaviour in terms of structural calculations and constructional methods which involve torsional behaviour problems and stress concentrations. Therefore symmetrical structures can perform better under earthquake or wind forces [3]. Therefore if the plot area is not a proper rectangle or a square then it is corrected according to the following cases:

Case 1: If the plot has an acute angle in Northeast corner it is considered auspicious and should be retained as such. If the projection is in any other corner it is corrected by drawing a side to make a perfect rectangle. If acute angle exists in Northeast corner along with an acute angle in any of the other three corners, retain the acute angle in Northeast and correct the other one.
For Example: In Figure 4.3, the left plot does not require correction whereas right plot requires correction only in the corner at Southwest as illustrated.

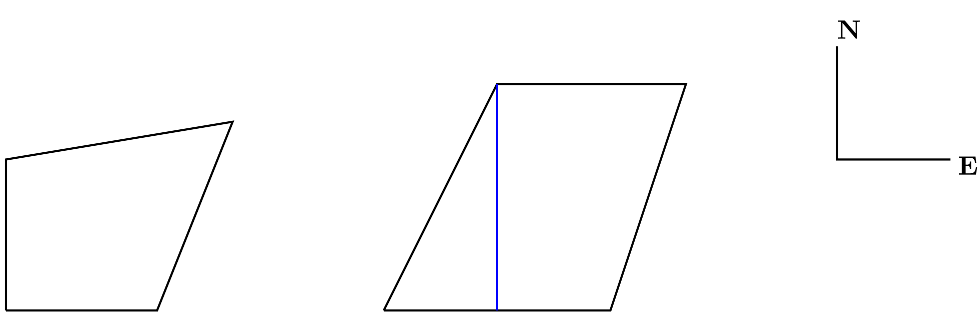

Figure 4.3: Plot angle correction involving acute angles, drawn using LaTeX

Case 2: Trapezoidal plot: In a trapezoidal plot corrections have to be made by reshaping the plot to a rectangle only if the acute angle exists in both Northwest and Southwest or in Southeast and Southwest or in Southeast and Northwest.
For Example: In Figure 4.4, the acute angles are in Southwest and Southeast due to which corrections are made as shown.

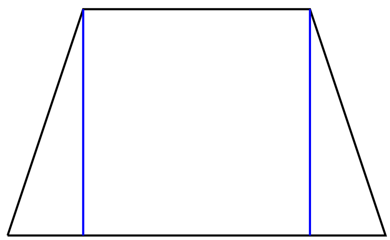

Figure 4.4: Plot angle correction in trapezoidal plot, drawn using LaTeX

Case 3: Quadrangle plot: The maximum rectangle is derived while retaining an acute angle in Northeast direction.
For Example: In Figure 4.5, the plot is corrected as shown [1].

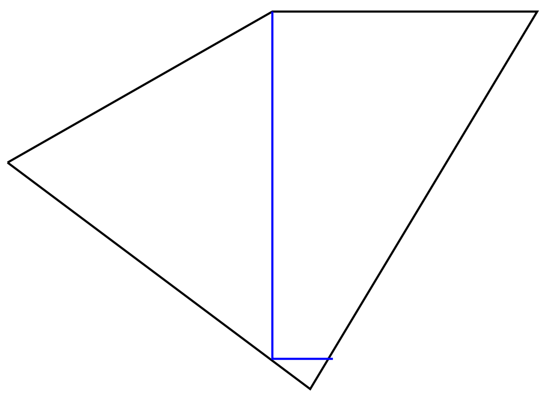

Figure 4.5: Plot correction in quadrangle plot, drawn using LaTeX

4.4 Fixing prime dimensions (Ayadi)

Now we will discuss the dimensions (Ayadi) and orientation of a house as a case study. The first act in the design of a house is the adoption of a perimeter. Hence this is considered as the birth of the Vastu. As the events in life are predicted on the basis of the position of the planets at the time of birth, the characteristics and future effects of the Vastu are based on the prime dimensions viz. breadth, length and height [4].
In ancient times, the units of measurement were not uniform across regions. The units of measurement were Angula (3/4th of an inch) and Hasta (18 inches). However the value of Hasta and Angula differed from person to person. Therefore, by using the Ayadi formulae for fixing the dimensions of a building, one cut down the possibility of creating disproportionate spaces. It is obvious that a

proportionate building will appear aesthetic and will seek attention.

Finally we will fix the breadth, length and height respectively as follows:
The Yoni (origin) and Vyaya (expenditure) formulae are used to determine the width of the building. If the received Yoni is an odd remainder, then it is considered as good Yoni whereas if it is even, then it is considered bad Yoni. Hence 1, 3, 5 and 7 remainders are good Yoni and are associated with East, South, West and North direction respectively. Therefore depending on the direction the building faces, the corresponding Yoni is used to fix the breadth of the building/rooms.

Next, Aaya (Income) and Raksha formulae are used to fix both the length of the building and of the rooms. Aaya or 'aadhayam', means income and 'Vyaya' means expenditure or loss. Therefore, the Aaya should be greater than the Vyaya.
Using the Ayadi formulae it has been concluded that the length of rooms/building should preferably be 1.5 times the breadth or 1.375 times the breadth. This is why generally we find that sites are not square but rectangular with a length 1.375-1.5 times the breadth . For example: Sites have dimensions of 40 m $\times$ 60 m, 30 m $\times$ 40 m, 30 m $\times$ 45 m, and 50 m $\times$ 80 m.

The height is fixed using the Tithi and Vara formulae. The height of the first floor should be less than that of the ground floor. For choosing the correct height of a building, the proportion should also be considered. The ratios of height to breadth and certain aspect of beauty and proportion associated with it are given below. One may opt a particular ratio according to the requirements.

1. Ratio of 1: The building is considered to be aesthetically proportionate. For example: The height to breadth ratio of the Taj Mahal is 1.

2. Ratio of 1.25: The building is considered to have good stability.

3. Ratio of 1.5: The building is considered to have a pleasant appearance.

4. Ratio of 1.75: The building is good in every way and will appear to be both strong and beautiful.

5. Ratio of 2: When the height is twice the breadth, the building will appear pleasing.

5 Illustration

We are constructing a house facing towards west (though this is not the best orientation according to Vastu) then according to the aforesaid facts and formulae one of the suitable measure of breadth can be 20.17 hasta (or 30.25 feet) since the Yoni in the case would be remainder of $(20.17 \times 3)/8 = 4.51 = 5$ (rounding off to nearest integer). The vyaya corresponding to the given breadth = remainder of $(20.17 \times 9)/10 = 1.53 = 2$ (rounding off).
Then the length should be greater than $1.5 \times 20.17 = 30.255$ hasta. A possible measure of length can be 32.33 hasta. Aya corresponding to it is remainder of $(32.33 \times 8)/12 = 6.64 = 7$ (rounding off). Observe that this choice of length has lead to Aya greater than Vyaya , which is considered prosperous according to Vastu. Also, one of the best possible choices of measure of height is 20.17 hasta since the ratio of height and breadth then is equal to 1.

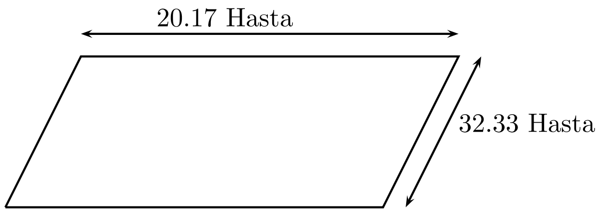

Figure 5.1: Plot area, drawn using LaTeX

6 Conclusion

The paper presented the basics of Vastu Shastra with geometrical explanation. It also discusses an illustration, in which dimensions of house as per the Vastu Shastra are provided. It is to be noted that the above mentioned are not the optimum dimensions. Our illustration involves a simple house, but it can be further used to derive dimensions of highly complicated aesthetically pertinent historical structures. This can also contribute in understanding the then social and scientifically important notions.

References

[1] Hari A.R., *Amazing Science of Vaastu*, Vasan Publications, 8th edition, 2002, pp. 76-88.

[2] Achyuthan A. and Prabhu T.S., *An Engineering Commentary on Manusyalayacandrika*, 1st edition, Vastuvidyapratisthanam Calicut, 1998, pp. 40-97.

[3] Fazeli H. and Goodarzi A., *The Principles of Vastu as a Traditional Architectural Belief System from an Environmental Perspective*, WIT Transactions on Ecology and the Environment, Volume 128, 2010, pp. 102.

[4] Prasad R., Aayadi Vastu, *Vaastu International*, https://www.vaastuinternational.com/Hindi-Vastu/Ayadi-Vastu.html.

[5] Jain S. J., The Origin of Vastu, *Vaastu shastra*, Pankh Vastu Centre, https://www.vaastu-shastra.com/origin-of-vastu-shastra.html.

[6] History of Vastu Shastra, *Vedic Tribe*, 19th March 2021, https://vedictribe.com/vedic-science/vaastu-shastra/history-of-vastu-shastra/.

(Mentor) Dr. Sucheta Nayak, Associate Professor, Department of Mathematics, Lady Shri Ram College for Women, New Delhi
suchetanayak@lsr.du.ac.in

Aditi Khandelwal, B.Sc.(H) Mathematics, 4th Semester, Lady Shri Ram College for Women, New Delhi
aditikhandelwal592@gmail.com

Éclat, A Mathematics Journal
Volume 14, 2022-23 (10-19)

The Jordan Curve Theorem

Mahesh Kumar and Sonam Padma Wangmo

Abstract

Mathematics, amongst the other fields of study, holds a higher place. Its logic seamlessly moulds itself to fit any model. Its appeal to human intellect seems to be hardwired in the very fabric of the human mind and the nature of the field. But there are instances when the two seem to disagree. This paper explores one such example, the case of the Jordan Curve theorem.

Keywords: Jordan Curve, Fixed Point, Path Connected, Arc, Connected Component

1 Introduction

The Jordan Curve Theorem is a curious case of disagreement between the human intuition and mathematical logic. The theorem is a fundamental concept in topology which states that a simple closed curve in a two-dimensional plane divides the plane into two distinct regions, the interior and the exterior. To a layman, it seems to be trivially true but to establish it mathematically has been a difficult task. Over the centuries, mathematicians have disagreed and debated over the proofs they managed to come up with.
Despite its seemingly simple statement, the Jordan Curve Theorem is a complex concept that has opened infinite questions for mathematicians and philosophers alike. At the first glance, the theorem sounds obvious. All of us have almost atleast once experienced the truth of the theorem; for instance we have seen a circle divide the paper in two components. But as we dig deeper into mathematical inquiry, we start questioning the very definition of the curve we are talking about. One of the first questions that arises is 'What is the exterior and interior?' (how do we want to define it?). One characterisation is that of the parity of points; a ray with a fixed direction initiating from points lying in the interior would intersect the curve odd number of times and ray initiating from points lying outside would intersect it even number of times. But this characterisation was however not satisfactory as one can construct a Jordan Curve, which is jagged everywhere, using the knowledge of the Weierstrass's function. Another characterisation that fails, is taking the interior to be on the left when we travel around the curve. The counterexample here is again the example above. Such a curve would not have a defined tangent or a normal and hence while travelling such a curve, the 'left' would not be recognisable. As one can see, the simple trivial ideas we have about geometrical objects are not as simple when it comes to proper mathematical description and characterisation [4].
The aim of this paper is to provide the (undergraduate) reader with a comprehensible proof of the theorem and establish the truth of it using concept of elementary analysis. The second section of the paper would provide the prerequisites which are required for the proof given in the third section.

2 Prerequisites

The following are the definitions and results of elementary analysis which would be used in the later sections of the paper. The paper assumes that the reader has basic knowledge of topological terminologies, notations and basic set theory.

Definition 2.1. *A* Jordan Curve *J in $\mathbb{R}^2$ is the image of the unit circle*

$$C = \{(x, y) : x^2 + y^2 = 1\},$$

under an injective continuous mapping e into $\mathbb{R}^2$.

Definition 2.2. *A metric space (X, d) is said to be* disconnected *if there exists two non-empty subsets A and B of X such that*

1. $X = A \cup B$
2. $A \cap \bar{B} = \phi$ *and* $\bar{A} \cap B = \phi$ *[1, Definition 4.1.1].*

Definition 2.3. *Let (X, d) be a metric space and $A \subseteq X$. Let $\mathcal{G}$ be a collection of open sets in X with the property that $A \subseteq \cup\{O : O \in \mathcal{G}\}$, then $\mathcal{G}$ is said to be an* open cover *of A [1, Definition 5.1.1].*
Given any open cover $\mathcal{G}$ of A, if there exists a finite subcollection $\mathcal{H}$ of $\mathcal{G}$, such that

$$A = \cup_{i=1}^{n} H_i \ \text{ where } \ H_i \in \mathcal{H}$$

then A is said to be compact.

Definition 2.4. *Let (X, d_x) and (Y, d_y) be metric spaces. Let $A \subsetneq X$ and $f : A \to Y$. Then the mapping $g : X \to Y$ is called an* extension *of f if $g(x) = f(x)$ for each $x \in A$ [1, Definition 5.1.1].*

Definition 2.5. *An* arc *from a point a to a point b in $\mathbb{R}^2$ is a homeomorphic mapping $f : I \to \mathbb{R}^2$ where $I = [0, 1]$ such that $f(0) = a$ and $f(1) = b$ [1, Definition 4.3.1].*

Definition 2.6. *A* connected component *of x in a metric space (X, d) is a subset C such that C is the union of all connected subsets of (X, d) that contain x [1, Definition 4.3.1].*

Definition 2.7. *Let X be a metric space. If for every $x_0, x_1 \in X$, there exists a continuous mapping $f : I \to X$ of the unit interval $I = [0, 1]$ such that $f(0) = x_0$ and $f(1) = x_1$, then X is said to be* path connected *[1, Definition 4.3.1].*

Theorem 2.1. *(Special case of Tietze Extension Theorem): Let X be a metric space and $A \subseteq X$ be closed. Let $f : A \to [a, b]$ where $(a < b)$ be a continuous function, then there exists a continuous real-valued function g defined on X which extends f [1, Theorem 3.6.15].*

Theorem 2.2. *(Brouwer's Fixed Point Theorem): Let $f : I \to I$ be a continuous function, where I is a closed disk of a Euclidean space. Then there exists a unique fixed point x in I [6].*

Theorem 2.3. *(Heine Borel Theorem): Let S be a closed and bounded subset of the Euclidean space $\mathbb{R}^2$, then S is compact [7].*

3 Proof of the Jordan Curve Theorem

The following proof is based on the paper by Ryuji Maehara [3]. The two components of the plane produced by a Jordan Curve is characterised as 'bounded component' and 'unbounded component' unlike the other cases where, terms like 'interior' and 'exterior' are used. This makes the approach of this proof different from the other geometrical (visual) proofs. The generalisation that derives from the tools of analysis, leaves very less space for exceptions and contradictions.
The following is the statement of the Jordan Curve theorem.

Theorem 3.1. *The complement of a Jordan curve J in two dimensional Euclidean plane consists of two components, each of which has J as its boundary. Exactly one component of $\mathbb{R}^2 \setminus J$ is bounded and both the components are path connected and open.*

Remark 3.1. Given a Jordan Curve J, the connected components of $\mathbb{R}^2 \setminus J$ if they exist, are open and path connected.

Proof. We know that J is continuous image of a unit circle C (see definition 2.1). And since a unit circle is closed and bounded in $\mathbb{R}^2$, by Heine-Borel theorem C is compact (see theorem 2.3). So, J is compact and closed [1]. Thus $\mathbb{R}^2 \setminus J$ is open in $\mathbb{R}^2$.
We assume that atleast one connected component exists, say U and let $x \in U$. Since $U \subseteq \mathbb{R}^2 \setminus J$ and $\mathbb{R}^2 \setminus J$ is open, there exists a disk $D(x, r)$ such that $D(x, r) \subseteq \mathbb{R}^2 \setminus J$.
Note that $D(x, r)$ is a connected set which contains the point x. By definition U is the union of all the connected sets containing the point x and thus $D(x, r) \subseteq U$.
Hence U is open. Every open connected set of the plane $\mathbb{R}^2$ is also path connected, hence U if it exists is also path connected. □

Remark 3.2. Exactly one of the components of $\mathbb{R}^2 \setminus J$ is unbounded.

Proof. Since J is compact it is hence bounded [1, Corollary 5.3.2].
Thus there exists $r > 0$

$$J \subset D(0, r)$$

which implies that,

$$D(0, r)^C \subset J^C$$

that is,

$$\mathbb{R}^2 \setminus D(0, r) \subset \mathbb{R}^2 \setminus J.$$

Let U be a subset of $\mathbb{R}^2 \setminus J$ be defined as follows,

$$U = \cup\, C_{i \in \Lambda}$$

where $C_{i \in \Lambda}$ is a connected subset of $\mathbb{R}^2 \setminus J$ containing points of the set $\mathbb{R}^2 \setminus D(0, r)$.
It is clear that if it exists, U is a connected component of $\mathbb{R}^2 \setminus J$.

We know that $\mathbb{R}^2 \setminus D(0, r)$ is a connected subset of $\mathbb{R}^2 \setminus J$ containing points of the set $\mathbb{R}^2 \setminus D(0, r)$, so as per the definition

$$\mathbb{R}^2 \setminus D(0, r) \subset U$$

implying

$$U \neq \phi.$$

Thus U exists. Also since $\mathbb{R}^2 \setminus D(0,r)$ is unbounded and $\mathbb{R}^2 \setminus D(0,r) \subset U$,

$$U \text{ is unbounded.}$$

To prove that U is unique, let W be any unbounded connected component of $\mathbb{R}^2 \setminus J$. Then

$$(\mathbb{R}^2 \setminus D(0,r)) \cap W \neq \phi$$

else it would imply that $W \subset D(0,r)$, implying that W is bounded.

Since $\mathbb{R}^2 \setminus D(0,r) \subset U$, and $\mathbb{R}^2 \setminus D(0,r) \cap W \neq \phi$, we have

$$U \cap W \neq \phi,$$

which implies that there exists $x \in W \cap U$. Since U, W are connected components both containing x, so both must be equal due to the definition (see definition 2.6). □

Proceeding further, we just need to prove that the shared boundary of the components of $\mathbb{R}^2 \setminus J$ is J, and that there exists only one bounded component. Then implicitly, we will have that the Jordan Curve divides the plane into exactly two components.

Lemma 1. *Let $h(t) = (h_1(t), h_2(t))$ and $v(t) = (v_1(t), v_2(t))$, $(-1 \leq t \leq 1)$ be continuous paths in the rectangular set $E(a,b;c,d) = \{(x,y)|a \leq x \leq b, c \leq y \leq d\}$ where $a,b,c,d \in \mathbb{R}$ are fixed satisfying*

$$h_1(-1) = a, \quad h_1(1) = b\ , \ v_2(-1) = c, \quad v_2(1) = d.$$

Then $h(s) = v(t)$ for some $s,t \in [-1,1]$, i.e., the two paths meet in $E(a,b;c,d)$.

Proof. Assume on the contrary that, given any $s,t \in [-1,1]$

$$h(s) \neq v(t). \tag{1}$$

Then we have

$$|h_1(s) - v_1(t)| > 0 \text{ or } |h_2(s) - v_2(t)| > 0$$

for all $s,t \in [-1,1]$.

Then let F be a function defined as follows for $(s,t) \in E(-1,1;-1,1)$ in the plane $\mathbb{R}^2$

$$F(s,t) = \left(\frac{v_1(t) - h_1(s)}{M(s,t)}, \frac{h_2(s) - v_2(t)}{M(s,t)}\right)$$

where $M(s,t) = \max\{|v_1(t) - h_1(s)|, |v_2(t) - h_2(s)|\}$. Note that given any $(s,t) \in [-1,1]$

$$M(s,t) > 0$$

because $|v_1(t) - h_1(s)|$ and $|v_2(t) - h_2(s)|$ can never be zero simultaneously and thus one of them will always be greater and non-zero.

Our claim here is, if such a function exits (which is only possible if our assumption (1) holds) then there should be a contradiction. It is known that if a function is continuous, then each of its components are continuous in the given domain and vice versa [1, Example 3.1.13]. Hence h_1, h_2, v_1, v_2 are continuous on $[-1,1]$. The function F is componentwise continuous since $\frac{1}{M(s,t)}$ is continuous and defined (1) and so is $h_1(s) - v_1(t), h_2(s) - v_2(t)$ as h, v are continuous paths.

Observe that for any $(s,t) \in E(-1,1;-1,1)$

$$M(s,t) = |h_1(s) - v_1(t)| \text{ or } |h_2(s) - v_2(t)|,$$

say

$$M(s,t) = |h_1(s) - v_1(t)|$$

then

$$F(s,t) = \left(\frac{v_1(t) - h_1(s)}{|h_1(s) - v_1(t)|}, \frac{h_2(s) - v_2(t)}{|h_1(s) - v_1(t)|}\right)$$

thus

$$F(s,t) = \left(\pm 1, \frac{h_2(s) - v_2(t)}{M(s,t)}\right).$$

In the same manner, when $M(s,t) = |h_2(s) - v_2(t)|$, we have

$$F(s,t) = \left(\frac{v_1(t) - h_1(s)}{M(s,t)}, \pm 1\right).$$

Implying that given any $(s,t) \in E(-1,1;-1,1)$

$$F(s,t) = \left(\pm 1, \frac{h_2(s) - v_2(t)}{M(s,t)}\right) \text{ or } \left(\frac{v_1(t) - h_1(s)}{M(s,t)}, \pm 1\right)$$

and in either cases

$$\left|\frac{v_2(t) - h_2(s)}{M(s,t)}\right| < 1 \text{ or } \left|\frac{v_1(t) - h_1(s)}{M(s,t)}\right| < 1.$$

Then we can state that F is a continuous function from $E(-1,1;-1,1)$ to $E(-1,1;-1,1)$. By *Brouwer Fixed Point theorem*, there exists a fixed point $(s_0,t_0) \in E(-1,1;-1,1)$ such that

$$F(s_0,t_0) = (s_0,t_0).$$

Because of the observation made above, we have $|s_0| = 1$ or $|t_0| = 1$. Assume that $s_0 = -1$, then since $v_1(t_0) \geq a$ and $h_1(s_0) = a$, so;

$$v_1(t_0) - h_1(s_0) \geq 0$$

also

$$M(s_0,t_0) > 0$$

thus

$$\frac{v_1(t_0) - h_1(s_0)}{M(s_0,t_0)} \neq -1.$$

Assume that $s_0 = 1$, then again $\frac{v_1(t_0) - h_1(s_0)}{M(s_0,t_0)} < 0$ implying

$$\frac{v_1(t_0) - h_1(s_0)}{M(s_0,t_0)} \neq 1.$$

Similar contradictions arise when we assume that $|t_0| = 1$. Thus the function F does not have a fixed point, and hence our assumption is wrong. □

Lemma 2. *If $\mathbb{R}^2 \setminus J$ is not connected, then each component has J as its boundary.*

Proof. By the hypothesis we have that, $\mathbb{R}^2 \setminus J$ is disconnected. Thus we can say that the set $\mathbb{R}^2 \setminus J$ contains more than one connected components. Let U be an arbitrary connected component. We have already proved that the connected components of $\mathbb{R}^2 \setminus J$ are open, hence the boundary of the component U is $\bar{U} \cap U^c$. Next we want to show that the boundary $\bar{U} \cap U^c$ of U is not contained in any other connected component of $\mathbb{R}^2 \setminus J$. Let W be a connected component of $\mathbb{R}^2 \setminus J$, disjoint from U. Then

$$W \cap (\bar{U} \cap U^c) = \phi,$$

because if W contains a point z of boundary of U, then by definition of an open set there would exist a neighbourhood of z which is contained in W and intersects U, since every neighbourhood of z intersects U. Thus we would get the contradiction that

$$W = U,$$

because W and U are connected components.
Thus we can say that no connected component of $\mathbb{R}^2 \setminus J$ contains the boundary and hence

$$\bar{U} \cap U^c \subseteq J.$$

Suppose $\bar{U} \cap U^c \neq J$, then there exists an arc $A \subset J$ such that $\bar{U} \cap U^c \subset A$. We then have to work to arrive at a contradiction. We have established the presence of exactly one unbounded component, if we say that there is no bounded component, then $\mathbb{R}^2 \setminus J$ would be connected. So there exists atleast one bounded component of $\mathbb{R}^2 \setminus J$.

Let o be a point in a bounded component. If U itself is bounded, then we choose $o \in U$. Let $\bar{D}(o, r)$ be a large disk with center o such that $J \subset D(o, r)$ and thus

$$A \subset D(o, r).$$

By definition an arc is a homeomorphic image of an interval $[a, b]$. Thus the identity mapping $id : A \to A$ can be extended to a continuous mapping $s : D(o, r) \to A$ (see theorem 2.1). Define $q : \bar{D}(o, r) \to \bar{D}(o, r)$ as follows depending on U:

if U is bounded

$$q(z) = \begin{cases} s(z) & \text{for } z \in \bar{U} \\ z & \text{for } z \in U^c \end{cases}$$

or if U is unbounded

$$q(z) = \begin{cases} s(z) & \text{for } z \in U^c \\ z & \text{for } z \in \bar{U}. \end{cases}$$

Note that $s(z) = z$, for all $z \in \bar{U} \cap U^c$, since s is an extension of the identity function on A and we have assumed that $\bar{U} \cap U^c \subset A$. The mapping $q(z)$ is well defined and continuous, as both mappings s and id are. The mapping s maps each point of the domain to a point on arc A, and under the mapping q

$$q(o) = s(o),$$

because if U is bounded $o \in \bar{U}$, and else if U is unbounded, then $o \in U^c$.

Translating we move the disk $\bar{D}(o, r)$ to the origin. Then define the following mapping p and t:

$$p : \bar{D}(0, r) - \{0\} \to \delta(\bar{D}(0, r)), \quad p(z) = \frac{r.z}{|z|}$$

$$t : \delta(\bar{D}(0,r)) \to \delta(\bar{D}(0,r)), \quad t(z) = -z$$

Next we observe that the composition of functions defined as follows is continuous

$$t \circ p \circ q : \bar{D}(0,r) \to \bar{D}(0,r).$$

Note that $\bar{D}(0,r)$ is homeomorphic to $E(-1,1,;-1,1)$ and thus should contain a fixed point [6]. But the image set lies in the boundary $\delta(\bar{D}(0,r))$, and so fixed point must belong to $\delta(\bar{D}(0,r))$. By construction for any $z \in \delta(\bar{D}(0,r))$

$$q(z) = z \text{ and } p(z) = \frac{r.z}{|z|} = \frac{r.z}{r} = z$$

thus

$$p \circ q(z) = z$$

but

$$t(z) = -z.$$

Which means that the continuous mapping has no fixed point, and thus our assumption that $\bar{U} \cap U^c \subset A$ is wrong and hence

$$\bar{U} \cap U^c = J \qquad ([5],[2]).$$

□

Lemma 3. *$\mathbb{R}^2 \setminus J$ has exactly one bounded component.*

Proof. Since J is compact, it is bounded [1, Theorem 5.2.3]. Thus there exist points $m_1, m_2 \in J$ such that distance between a_1 and a_2 is the largest with respect to the Euclidean metric.

Translating, rotating and scaling the curve J, such that m_1 translates to $a_1 = (-1,0)$ and m_2 to $a_2 = (1,0)$. Now the image of the curve is contained in $E(-1,1;-2,2)$, because the curve J is scaled such that the maximal distance is 2. Let $b_1 = (0,-2)$ and $b_2 = (0,2)$ and τ be the boundary of $E(-1,1;-2,2)$.

Next we show that $\tau \cap J = \{a_1, a_2\}$. Note that

$$a_1, a_2 \in \tau \cap J$$

because of the choice of translation, scaling and rotation. Say there exists a point $\gamma \neq a_1 \text{and} \gamma \neq a_2 \in J$ such that $\gamma \in \tau \cap J$. Consider the following lines segments:
$A = \{(x,y) | y = 2, -1 \leq x \leq 1\}$
$B = \{(x,y) | x = -1, -2 \leq y \leq 2\}$
$C = \{(x,y) | y = -2, -1 \leq x \leq 1\}$
$D = \{(x,y) | x = 1, -2 \leq y \leq 2\}$.
Observe that $\tau = A \cup B \cup C \cup D$. Let $\gamma \in B$, then $\gamma a_1 a_2$ is a right angled triangle with the hypotenuse $\overline{\gamma a_2}$. We thus arrive at a contradiction because by the Pythagoras theorem

$$|a_1 - a_2| < |\gamma - a_2|$$

which is not possible since $|a_1 - a_2|$ is maximal. By symmetry, we arrive at a similar contradiction when $\gamma \in D$. If $\gamma \in A$, then $\gamma = (a,2)$ for $|a| < 1$. When $a = 0$, when $\gamma = (0,2)$

$$|a_1 - \gamma| = |a_2 - \gamma| = \sqrt{5} > |a_1 - a_2| = 2$$

which is not possible since $|a_1 - a_2|$ is maximal. When $a \neq 0$, say $a < 0$ then

$$|a_2 - \gamma| = \sqrt{5 + a^2 - 2a}$$

since $a < 0$, $-2a > 0$ and $a^2 > 0$ thus

$$|a_2 - \gamma| > \sqrt{5} > 2$$

which is not possible since $|a_1 - a_2| = 2$ is maximal. When $a > 0$, considering the distance $|a_1 - \gamma|$ leads to a similar contradiction.

The line segment $\overline{b_1 b_2}$, is then a continuous path in $E(-1, 1; -2, 2)$ and so is any path between the points a_1 and a_2 which intersect with J. Then by Lemma 1, $\overline{b_1 b_2}$ intersects J. Choose $m \in J \cap \overline{b_1 b_2}$ with the largest y co-ordinate. Let the path between a_1 and a_2 in J containing m be J_1, and the other one J_2

Choose the point $n \in J_1 \cap \overline{b_1 b_2}$ with the smallest second coordinate. Again using Lemma 1,

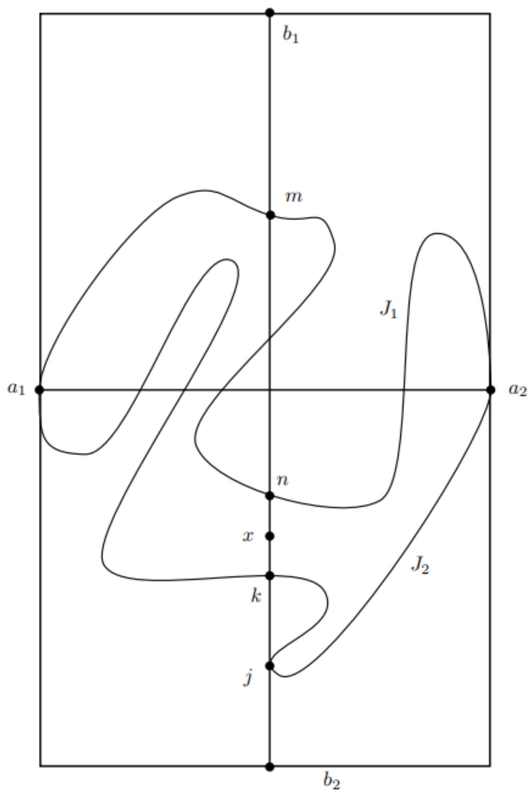

Figure 3.1: Plotting the points on a sample Jordan Curve (source:[5])

the paths J_2 and line $\overline{nb_2}$ intersect. Choose the point k from the $J_2 \cap \overline{nb_2}$ with the largest possible second coordinate and an element j with the smallest possible second coordinate.

Take x to be the midpoint of the line segment $\overline{nk}$. Observe that $x \in \mathbb{R}^2 \setminus J$. Else if we assume that $x \in J$ then either $x \in J_1$ and $x \in J_2$. Consider the case

$$x \in J_1$$

then since x is the mid-point of the line segment $\overline{\mathrm{nk}}$, the second coordinate of x is smaller than n, which is a contradiction considering how n was chosen. Take

$$x \in J_2,$$

then again since x is the mid-point of $\overline{\mathrm{nk}}$, then second coordinate of x should larger than the second coordinate of k, which is not possible.

We claim that the component which contains x is bounded.

Assume on the contrary that the component U containing x is not bounded. Since U is path connected in $\mathbb{R}^2 \setminus J$, there exists a path α in $\mathbb{R}^2 \setminus J$ that connects the point x and an arbitrary point y outside our rectangle $E(-1,1;-2,2)$. Let w be first point at which α meets the boundary τ of $E(-1,1;-2,2)$. Note the the second component of $w \neq 0$, because the intersection of the $x - axis$ $(y = 0)$ and τ contains only the points $a_1, a_2 \in J$. If second coordinate of $w = 0$, then $w = a_1$ or $w = a_2$. But we know that $w \in \alpha \subset \mathbb{R}^2 \setminus J$, we thus arrive at a contradiction.

It is important to observe that α never intersects J, since $\alpha \in \mathbb{R}^2 \setminus J$. Let α_w be the part of α from x to w. If w is on the lower half of τ that is if the second coordinate of w is negative, we can find a path $\widehat{wb_2}$ in τ from w to b_2 which contains neither a_1 nor a_2. Now consider the path $\overline{\mathrm{b_1m}} + \widehat{mn} + \overline{\mathrm{nx}} + \alpha_w + \widehat{wb_2}$. This path does not intersect with J_2, which is a contradiction to Lemma 1.
If w is on the upper half of τ that is if the second coordinate of w is positive, we can find a path $\widehat{wb_1}$in τ from w to b_1 which contains neither a_1 nor a_2. Then the path $b_2x + \alpha_w + \widehat{wb_1}$ does not intersect with the path J_1, which is again a contradiction to Lemma 1.

Suppose that there exists another bounded component W which is not equal to U. The path

$$\beta = \overline{\mathrm{b_1m}} + \widehat{mn} + \overline{\mathrm{nk}} + \widehat{kj} + \overline{\mathrm{jb_2}}$$

does not lie in W since the line segments $\overline{\mathrm{b_1m}}$ and $\overline{\mathrm{jb_2}}$ are contained in the union of J and the unbounded component of $\mathbb{R}^2 \setminus J$, the simple arcs $\widehat{mn}$ and $\widehat{kj}$ are contained in J, and the segment $\overline{\mathrm{nk}}$ is contained in the union of J and the component containing the point x.

Observe that the set W and β cannot contain neither of the points a_1 or a_2 and so we find neighbourhoods U_1 and U_2 of a_1 and a_2 such that these neighbourhoods do not intersect with the path β. Then since boundary of W, $\delta W = J$, so

$$a_1, a_2 \in \delta W.$$

Hence there exists $x \in W \cap U_1$ and $y \in W \cap U_2$, let $\widehat{xy}$ denote a path in W from x to y. Then the path $a_1x + +y\widehat{xy}a_2$ fails to meet β, contradicting Lemma 1 [5].

$\square$

The third lemma (3), proves that there exists exactly one unbounded connected component of $\mathbb{R}^2 \setminus J$. Combining this with the above results that we arrived at, in the course of this paper, we can thus conclude that $\mathbb{R}^2 \setminus J$ consists of exactly two connected components, whose boundary is J as desired.

4. Conclusion

In conclusion, the Jordan Curve Theorem is a fascinating example of how mathematical logic can challenge our intuitive understanding of the world. While the theorem's statement may seem obvious, it has taken centuries for mathematicians to come up with rigorous proofs that satisfy the complexities of the concept. The various characterisations of the components of the curve highlight the subtleties and intricacies involved in mathematical inquiry. As we continue to explore the depths of topology, we are reminded that the seemingly simple ideas we have about geometrical objects are not always straightforward when it comes to a proper mathematical description and characterisation. The Jordan Curve Theorem serves as a testament to the power and beauty of mathematical logic.

References

[1] Shirali S. and Vasudeva H. L., *Metric Spaces*, Springer

[2] Gale D., *The game of hex and the Brouwer fixed-point theorem*, American mathematical monthly, December 1979,pp. 818-827

[3] Maehara R.,*The Jordan curve theorem via the Brouwer fixed point theorem*, American mathematical monthly, 1984, pp. 641-643

[4] Ross F. and William T. R., *The Jordan curve theorem is non-trivial*, Journal of mathematics and the arts, 2009

[5] Luisto R., *The Jordan Curve Theorem*, Essay, University of Helsinki, 2011

[6] *Brouwer fixed point theorem*, Wikipedia, https://en.wikipedia.org/wiki/Brouwer_fixed-point_theorem

[7] *Heine Borel theorem*, Wikipedia, https://en.wikipedia.org/wiki/Heine-Borel_theorem

(Mentor) Dr. Mahesh Kumar, Assistant Professor, Department of Mathematics, Lady Shri Ram College for Women, New Delhi
mahekumar81@gmail.com

Sonam Padma Wangmo, B.Sc(H) Mathematics, 6th Semester, Lady Shri Ram College for Women, New Delhi
sonamwangmo.maths@gmail.com

Éclat, A Mathematics Journal
Volume 14, 2022-23 (20-27)

Prime Avoidance Lemma

Sunil Kumar Yadav, Kriti Agrawal and Richa Shekhar

Abstract

The Prime Avoidance Lemma is one of the fundamental cornerstones of commutative algebra. This paper presents a detailed study, primarily focusing on the proof, variations and consequences of the Prime Avoidance Lemma in the commutative algebra.

Keywords: Rings, Ideals, Prime Ideals, Radical of an Ideal, Spectrum, Prime Avoidance Lemma, Unimodular Rows, Noetherian Rings, Radical Avoidance

1 Introduction

The Prime Avoidance Lemma is one of the most fundamental result in commutative algebra. It states that if an ideal is contained in a finite union of prime ideals, then it is already contained in one of them. It is useful for establishing dichotomies, in particular, if an ideal is not contained in finitely many prime ideals, then it has an element which is not contained in any of the finitely many prime ideals. The lemma plays a significant role in commutative algebra and can be refined to extend the implementation in non-commutative algebra. This fundamental concept has several applications in abstract algebra. This review research paper will study the significance, variations, consequences and applications of the Prime Avoidance Lemma in the world of commutative algebra.

The paper is divided into 6 sections. Section 1 contains the introduction to the paper. Section 2 contains the preliminaries needed before delving deeper into the topic. Section 3 discusses what exactly the Prime Avoidance Lemma is. Section 4 contains the proofs of the lemma using different methods. Section 5 contains the applications and consequences of the lemma and Section 6 is the conclusion.

2 Preliminaries

This section consists of the basic definitions and notations used throughout the article. For details, one may refer ([1],[3],[4]).

Definition 2.1. A **ring** is a non-empty set R with two binary operations, namely, addition(+) and multiplication(.) satisfying the following conditions:

(i) $(R, +)$ is an Abelian group

(ii) $a.(b.c) = (a.b).c$ for all $a, b, c \in R$

(iii) $a.(b + c) = a.b + b.c$ and $(b + c).a = b.a + c.a$ for all $a, b, c \in R$.

Definition 2.2. A ring R is said to be **commutative** if commutative law holds in R with respect to multiplication, i.e., $a.b = b.a$ for all $a, b \in R$.

Definition 2.3. A non-empty subset S of a ring R is said to be a **subring** of R if S itself forms a ring with respect to the operations of R.

Definition 2.4. Let R be a ring and I be a non-empty subset of R, then I is said to be an **ideal** of R if following conditions are fulfilled:

(i) $(I, +)$ is a subgroup of R

(ii) For every $a \in I$ and for every $r \in R$, $a.r \in I$ and $r.a \in I$.

Definition 2.5. Let R be a commutative ring. A proper ideal I of R is said to be a **prime ideal** of R if $a.b \in I$ for $a, b \in R$, then either $a \in I$ or $b \in I$.

Definition 2.6. Let R be a commutative ring and I be a proper ideal of R. Then I is said to be a **maximal ideal** of R if there is no proper ideal of R containing I. In other words, if there exists an ideal J of R such that $I \subseteq J \subseteq R$, then $J = I$ or $J = R$.

Definition 2.7. Let R be a ring and I be an ideal of R. The **radical of I** in R is the ideal which is the intersection of all prime ideals containing I.

The following Venn diagram is another way of understanding the definition of the **radical of an ideal**:

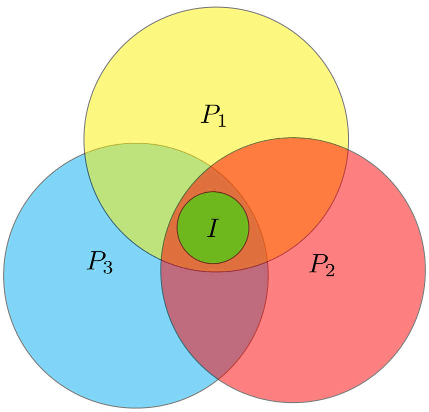

Figure 2.1: Drawn in LaTeX

In figure 2.1, P_1, P_2, P_3 represent prime ideals containing the ideal I and the intersection portion represents the radical of I.

Definition 2.8. Let R be a ring. The **prime spectrum** or simply **spectrum** of R is denoted by $\mathrm{Spec}(R)$ and defined as the set of all prime ideals of R, i.e.,

$$\mathrm{Spec}(R) = \{P : P \text{ is a prime ideal in } R\}$$

.

Definition 2.9. Let R be a ring and let $P \in \mathrm{Spec}(R)$. The **height** of P, denoted by $\mathrm{ht}(P)$, is the supremum of the lengths of chains of prime ideals $P_0 \subset P_1 \subset P_2 \subset \ldots \subset P_r = P$ of R which end at P. If no such number exists, then $\mathrm{ht}(P)$ is ∞.

Definition 2.10. A ring is called **Noetherian** if it satisfies the following equivalent conditions:

1. R satisfies the ascending chain condition on ideals.

2. Every ideal of R is finitely generated.

3. Every set of ideals contains a maximal element.

3 What is Prime Avoidance Lemma?

In this section of the article, we shall state the Prime Avoidance Lemma and its refinements (refer [2], [6]).

Lemma 3.1. *The Prime Avoidance Lemma states that if an ideal I in a commutative ring R is contained in a finite union of prime ideals, then it is already contained in one of them, i.e., if $P_1, P_2, P_3, \ldots, P_n \in \operatorname{Spec}(R)$, where R is a commutative ring and I is any ideal in R such that*

$$I \subseteq \bigcup_{i=1}^{n} P_i, \text{ then } I \subseteq P_i \text{ for some } i, \text{ where } i = 1, 2, 3, \ldots, n.$$

It is also useful to study the contrapositive statement of the Prime Avoidance Lemma which is stated as follows: Let $P_1, P_2, P_3, \ldots, P_n \in \operatorname{Spec}(R)$, where R be a commutative ring and I is any ideal in R such that $I \nsubseteq P_i$ for any $i = 1, 2, 3, \ldots, n$, then

$$I \nsubseteq \bigcup_{i=1}^{n} P_i.$$

This implies if $I \nsubseteq P_i$ for each $i = 1, 2, 3, \ldots, n$ then there exists an element $x \in I \setminus \bigcup_{i=1}^{n} P_i$, i.e., if $I \nsubseteq P_i$ for all i, then there exists an element $x \in I$ which avoids all the P_i's. Hence, the name Prime Avoidance Lemma. The following Venn diagram is a representation of the Prime Avoidance Lemma:

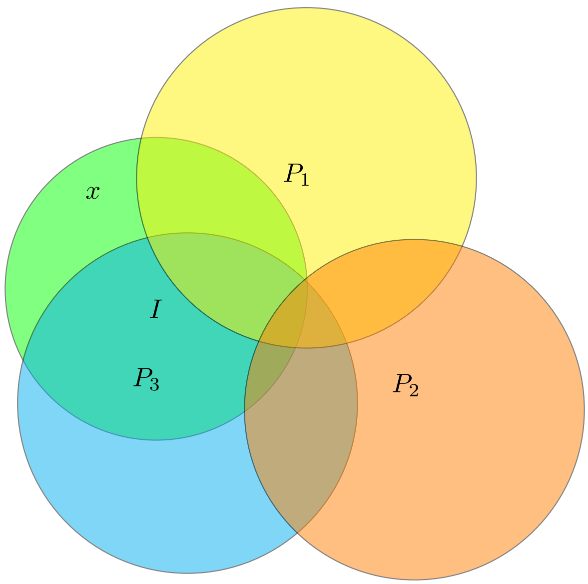

Figure 3.1: Drawn in LaTeX

In figure 3.1, P_1, P_2, P_3 represent prime ideals and the ideal I is not contained in any of these prime ideals. Clearly, we can find an element $x \in I$ which does not belong to any of the prime ideals, P_1, P_2, and P_3.

4 Approaches to Prove the Prime Avoidance Lemma

The following section illustrates proofs of some of the forms of the Prime Avoidance Lemma.

4.1 Via Principle of Mathematical Induction

Lemma 4.1. *: Let R be a commutative ring and $P_1, P_2, P_3, \ldots, P_n \in \operatorname{Spec}(R)$. Let I be any ideal in R such that $I \subseteq \bigcup_{i=1}^{n} P_i$, then $I \subseteq P_i$ for some i, where $i = 1, 2, 3, \ldots, n$.*

Proof. To prove the lemma, it is sufficient to prove the contrapositive statement of the lemma which is given as follows: let $P_1, P_2, P_3, \ldots, P_n \in \operatorname{Spec}(R)$, where R is a commutative ring and I be any ideal in R such that $I \nsubseteq P_i$ for each $i = 1, 2, 3, \ldots, n$ then $I \nsubseteq \bigcup_{i=1}^{n} P_i$. To prove this, we use the principle of mathematical induction on n.
For $n = 1$, we have $I \nsubseteq P_1$. This implies, there exists $a_1 \in I$ such that $a_1 \notin \mathrm{P}_1$. Hence the result holds for $n = 1$.
For $n = 2$, consider $I \nsubseteq P_1$ and $I \nsubseteq P_2$. If intersections $I \cap P_1$ and $I \cap P_2$ contains only the trivial element, 0, then clearly $I \nsubseteq P_1 \cup P_2$. Suppose $I \cap P_1$ and $I \cap P_2$ is not trivial. We can always choose $a_1 \in I \cap P_1$ such that $a_1 \notin P_2$ and $a_2 \in I \cap P_2$ such that $a_2 \notin P_1$. Now, we claim that $a_1 + a_2 \notin P_1 \cup P_2$. This implies either $a_1 + a_2 \in P_1$ or $a_1 + a_2 \in P_2$. If $a_1 + a_2 \in P_1$, then $a_1 + a_2 - a_1 \in P_1$. This implies that $a_2 \in P_1$, which is not possible. So, $a_1 + a_2 \notin P_1$. By the same argument, we can say that $a_1 + a_2 \notin P_2$. Thus, there exists $a_1 + a_2 \in I$ such that $a_1 + a_2 \notin P_1 \cup P_2$. So, $I \nsubseteq P_1 \cup P_2$. Hence the result is true for $n = 2$.
Suppose that the result is true for $n = k$ where $k > 2$, i.e., if $I \nsubseteq P_j$ for $j = 1, 2, 3, \ldots, k$ then $I \nsubseteq \bigcup_{j=1}^{k} P_j$ this implies that there exists $a_j \in I$ such that $a_j \notin \bigcup_{j=1}^{k} P_j$.
Now, we prove the result for $n = k + 1$. Let $P_1, P_2, P_3, \ldots, P_{k+1} \in \operatorname{Spec}(R)$ and $I \nsubseteq P_j$ for all $j = 1, 2, 3, \ldots, k + 1$. As discussed earlier, we can choose $a_i \in I$ such that $a_i \notin \bigcup_{j \neq i} P_j$. Then we have the following cases:
Case 1: If $a_i \notin P_i$ for any $i = 1, 2, 3, \ldots, k + 1$ then, $a_i \notin \bigcup_{j=1}^{k+1} P_j$. So, $I \nsubseteq \bigcup_{j=1}^{k+1} P_j$.
Case 2: If $a_i \in P_i$ choose $a = a_1 a_2 \ldots a_k + a_{k+1}$. If $a \in P_j$ for $j < k+1$ then, $a_{k+1} = a - a_1 a_2 \ldots a_k \in P_j$. Therefore, $a_{k+1} \in P_j$, which is not possible. If $a \in P_{k+1}$, then $a_1 a_2 \ldots a_k = a - a_{k+1} \in P_{k+1}$. Since, P_{k+1} is a prime ideal $a_t \in P_{k+1}$ for some $t \leq k$ but, this is not possible since $a_i \notin \bigcup_{j \neq i} P_j$. Thus, we have an element $a \in \mathrm{I}$ such that $a \notin \bigcup_{j=1}^{k+1} P_j$ which implies $I \nsubseteq \bigcup_{j=1}^{k+1} P_j$. Therefore, the result is true for $n = k + 1$. Hence by the principle of mathematical induction, result is true for all $n \geq 1$ [4]. □

4.2 Refinement of the Prime Avoidance Lemma

Lemma 4.2. *If R is a ring, $P_1, P_2, \ldots P_r \in \operatorname{Spec}(R)$ and $I = \langle a_1, a_2, \ldots, a_n \rangle$ be an ideal of R such that $I \nsubseteq P_i$ where $1 \leq i \leq r$, then there exists $b_2, b_3, \ldots, b_n \in R$ such that the element $c = a_1 + a_2 b_2 + \cdots + a_n b_n \notin \bigcup_{i=1}^{r} P_i$.*

Proof. Without loss of generality, we may assume that $P_i \not\subseteq P_j$ for $i \neq j$. We prove the lemma by using induction on r. If $r = 1$, then $I \not\subseteq P_1$ implies $a_i \notin P_1$ for some $1 \leq i \leq n$. We may assume that $a_1 \notin P_1$. So, by taking $b_2 = 0 = b_3 = \cdots = b_n$, we have $c = a_1 + a_2b_2 + a_3b_3 + \cdots + a_nb_n \notin P_1$ and we are done.
Suppose the lemma is true for $r-1$, that is, if $I \not\subseteq P_i$ for $1 \leq i \leq r-1$, then there exists $c_2, c_3, \ldots, c_n \in R$ such that $d = a_1 + a_2c_2 + a_3c_3 + \cdots + a_nc_n \notin \bigcup_{i=1}^{r-1} P_i$.
Now, we have to prove the lemma for r. If $d \notin P_r$, then by taking $b_i = c_i$ for all $2 \leq i \leq n$, we are done. So assume that $d \in P_r$. If $a_i \in P_r$ for all $i = 2, 3, \ldots, n$, then we have $a_1 = d - \sum_{i=2}^{n} a_ic_i \in P_r$. This implies that $I \subseteq P_r$, which is not possible. So we must have $a_i \notin P_r$ for some $2 \leq i \leq n$. Without loss of generality, we may assume that $a_2 \notin P_r$. Since $P_i \not\subseteq P_j$ for $i \neq j$, we can choose $x \in \bigcap_{i=1}^{r-1} P_i$ such that $x \notin P_r$.
Claim: The element $c = d + xa_2$ neither belongs to $\bigcup_{i=1}^{r-1} P_i$ nor belongs to P_r. If $c = d + xa_2 \in \bigcup_{i=1}^{r-1} P_i$, then we have $d = c - xa_2 \in \bigcup_{i=1}^{r-1} P_i$ which is not possible. Therefore, $c = d + xa_2 \notin \bigcup_{i=1}^{r-1} P_i$. If $c = d + xa_2 \in P_r$, then we have $c - d = xa_2 \in P_r$. This implies $a_2 \in P_r$ as $x \notin P_r$. Again, this is not possible. This implies $c = d + xa_2 \notin \bigcup_{i=1}^{r-1} P_i$. So, by taking $b_2 = x + c_2, b_i = c_i$ for all $i = 3, 4, \ldots, n$, we are done. Hence, by Principle of Mathematical Induction, the result is true for all r. □

4.3 Prime Avoidance Lemma of E-Davis

Corollary 4.3. *Let R be a commutative ring with unity and $P_1, P_2, P_3, \ldots, P_n \in \operatorname{Spec}(R)$. Let I be an ideal of R, x is an element of R and $xR + I \not\subseteq P_i$ for each i, then there exists $y \in I$ such that $x + y \notin P_i$ for each $i = 1, 2, 3, \ldots, n$.*

Proof. Without loss of generality, we may assume that $P_i \not\subseteq P_j$ for $i \neq j$. For any $x \in R$, we have the following cases:
Case 1: If $x \notin P_i$ for each $i = 1, 2, 3, \ldots, n$. Since $xR + I \not\subseteq P_i$ for each $i = 1, 2, 3, \ldots, n$. Clearly, there exists $y \in I$ such that $x + y \notin P_i$ for each $i = 1, 2, 3, \ldots, n$.
Case 2: If $x \in P_i$ for each $i = 1, 2, 3, \ldots, n$. In this case, we use induction on n. If $n = 1$, we have $xR + I \not\subseteq P_1$, then there exists $y \in I$ such that $y \notin P_1$ which implies $x + y \notin P_1$ and we are done. Suppose that the result is true for $n = k$, i.e., if $xR + I \not\subseteq P_i$ for each $i = 1, 2, 3, \ldots, k$, then, there exists $y \in I$ such that $x + y \notin P_i$ for each i.
Now, we prove the result for $n = k + 1$. Let $P_1, P_2, P_3, \ldots, P_{k+1}$ are prime ideals and I is any ideal of R. We know that $xR + I \not\subseteq P_i$ for each $i = 1, 2, 3, \ldots, k + 1$. By induction hypothesis, there exists $y \in I$ such that $x + y \notin P_i$ for $i = 1, 2, \ldots, k$. If $x + y \notin P_{k+1}$, then $x + y \notin P_i$ for each $i = 1, 2, 3, \ldots, k + 1$. If $x + y \in P_{k+1}$. We know that, $xR + I \not\subseteq P_{k+1}$. Let $M = xR + I$ and $M \not\subseteq P_{k+1}$. We can find $MP_1P_2 \cdots P_k \not\subseteq P_{k+1}$ then there exists $y_1 \in MP_1P_2 \cdots P_k$ such that $y_1 \notin P_{k+1}$. By induction hypothesis, for $x + y_1 \in R$ and $(x + y_1)R + I \notin P_{k+1}$ there exists $y \in I$ such that $x + y_1 + y \notin P_{k+1}$. Hence, the result holds for $n = k + 1$. By principle of mathematical induction, the result holds for all $n \geq 1$ [6]. □

5 Applications of Prime Avoidance Lemma

There are several applications of Prime Avoidance Lemma. This section presents some of the results that utilize the concept of Prime Avoidance Lemma [7].

5.1 Prime Absorbance Lemma

Lemma 5.1. *If a finite intersection of ideals is contained in a prime ideal, then one of them is already contained in the prime ideal, i.e., if $I_1, I_2, \ldots, I_n$ are ideals of R and $P \in R$ is a prime ideal with the property that $\bigcap_{i=1}^n I_i \subseteq P$, then $I_i \subseteq P$ for some i.*

Proof. On the contrary, assume that $I_i \nsubseteq P$ for all i. Therefore, there exists an element $a_i \in I_i \setminus P$ for all i. Thus, we have $a_1 a_2 \cdots a_n \in \bigcap_{i=1}^n I_i$. Also, $a_1 a_2 \cdots a_n \notin P$ as P is a prime ideal. This is a contradiction as $\bigcap_{i=1}^n I_i \subseteq P$. Therefore, if $\bigcap_{i=1}^n I_i \subseteq P$, then $I_i \subseteq P$ for some i. □

The Venn diagram of Prime Absorbance Lemma is as follows:

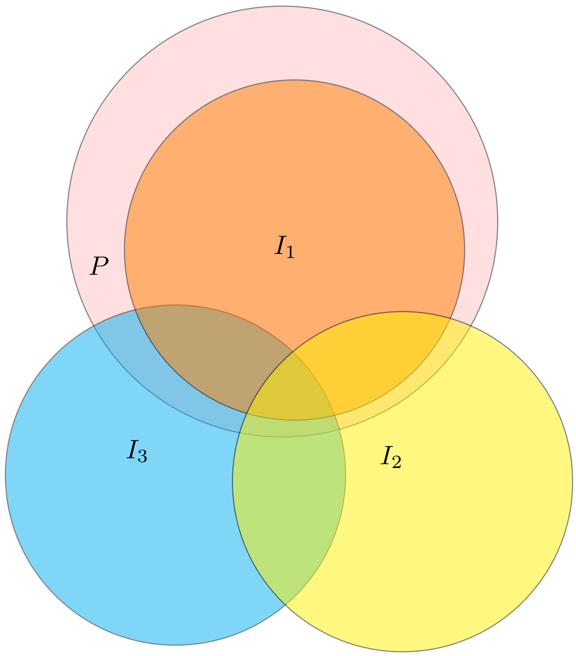

Figure 5.1: Drawn in LaTeX

Now, we shall state and prove some important results of the Prime Absorbance Lemma.

Corollary 5.2. *Let R be a ring and P be a prime ideal of R. Let I_1 and I_2 be two ideals of R such that $I_1 \cap I_2 \subseteq P$. Then $I_1 \subseteq P$ or $I_2 \subseteq P$.*

Proof. Let $I_1 \cap I_2 \subseteq P$. Suppose $I_1 \nsubseteq P$. Then we have to show that $I_2 \subseteq P$. Since $I_1 \nsubseteq P$, there exists $x \in I_1 \setminus P$. For any $y \in I_2$, the element $xy \in I_1 \cap I_2$. This implies $xy \in P$ as $I_1 \cap I_2 \subseteq P$. Since $x \notin P$, this implies $y \in P$ and hence, $I_2 \subseteq P$. Similarly, one can show that if $I_1 \cap I_2 \subseteq P$ and $I_2 \nsubseteq P$, then $I_1 \subseteq P$. □

Corollary 5.3. *Let R be a ring and P be a prime ideal of R. Let I_1 and I_2 be two ideals of R such that if $P = I_1 \cap I_2$, then $P = I_1$ or $P = I_2$.*

5.2 Completion of Unimodular Rows

Let R be a ring. A row $[a_1, a_2, \ldots, a_n] \in R^n$ is said to be unimodular row of length n if the ideal $\langle a_1, a_2, \ldots, a_n \rangle = R$. The set of unimodular rows of length n is denoted by $\mathrm{Um}_n(R)$. A unimodular row $[a_1, a_2, \ldots, a_n]$ is said to be completable if there exists a matrix in $GL_n(R)$ whose first row is $[a_1, a_2, \ldots, a_n]$. Let $[a_1, a_2, \cdots, a_n]$, $[b_1, b_2, \ldots, b_n] \in R^n$. We say that the row $[a_1, a_2, \ldots, a_n]$ is equivalent to the row $[b_1, b_2, \ldots, b_n]$ over $GL_n(R)$ if there exists a matrix $M \in GL_n(R)$ such that

$$M \begin{bmatrix} a_1 \\ a_2 \\ \vdots \\ a_n \end{bmatrix} = \begin{bmatrix} b_1 \\ b_2 \\ \vdots \\ b_n \end{bmatrix}.$$

The Prime Avoidance Lemma plays an important role to prove the lemma given by Horrocks' which states that if (R, m) be a local ring and $[F_1(X), F_2(X), \ldots, F_n(X)]$ be a unimodular row in $R[X]$ with one entry monic, then $[F_1(X), F_2(X), \ldots, F_n(X)]$ is completable. For more details, one can follow [4].

5.3 Noetherian Rings

Theorem 5.4. *Let A be a Noetherian ring and $[a_1, a_2, \ldots, a_n, a]$ in A^{n+1}. Then there exists $[b_1, b_2, \ldots, b_n]$ in A^n such that if $I = \langle a_1 + ab_1, \ldots, a_n + ab_n \rangle$, then $ht(I_a) \geq n$, i.e., if $P \in$ Spec (A), $I \subset P$ and $a \notin P$, then $ht(P) \geq n$.*

Proof. Case 1: If a belongs to every minimal prime ideal of A, then a belongs to every prime ideal of A. Hence, we have nothing to prove here.
Case 2: Let $P_1, P_2, \ldots, P_r$ be the minimal prime ideals of A which do not contain a. Since $a \notin P_i$, $\langle a_1, a \rangle \not\subseteq P_i$. By the Prime Avoidance Lemma, we know that $\langle a_1, a \rangle \not\subseteq \bigcup_{i=1}^{r} P_i$. Hence, there exists $b_1 \in A$ such that $a_1 + b_1 a \notin \bigcup_{i=1}^{r} P_i$. For $k < n$, we have elements $b_1, b_2, \ldots, b_k$ so we choose b_{k+1} as follows:
Suppose that $Q_1, Q_2, \ldots Q_s \in \mathrm{Spec}(A)$ are the minimal prime ideals containing the ideal $\langle a_1 + b_1 a, \ldots, a_k + b_k a \rangle$ but $a \notin Q_i, 1 \leq i \leq s$. If there exists no such prime ideal with the above property, we shall choose $b_{k+1} = 0$ and $b_i = 0$ for $i \geq k+1$. Otherwise, since $a \notin Q_i$, $\langle a_{k+1}, a \rangle \not\subseteq \bigcup_{i=1}^{s} Q_i$, so we shall choose $b_{k+1} \in A$ such that $a_{k+1} + b_{k+1} a \notin \bigcup_{i=1}^{s} Q_i$. Easily we can check that the elements $b_1, b_2, \ldots, b_n$ satisfy the required property [4]. □

5.4 Radical Avoidance

Theorem 5.5. *Let R be a commutative ring. If an ideal I of R is contained in the union of a finite family $\{I_k\}$ of radical ideals of R, then $I \subseteq I_k$ for some k.*

Proof. Suppose I is not contained in any of the I_k. So, there exists $a \in I$ such that $a \notin I_k$ for each k. Then I_k does not meet the multiplicative set $\{1, a, a^2, \ldots\}$, so there is a prime ideal P_k of R containing I_k that does not contain a. Then $I \not\subseteq P_k$ for any k. This implies that $I \not\subseteq \bigcup_k P_k$ by the Prime Avoidance Lemma. But it is given that $I \subseteq \bigcup_k P_k$ which is a contradiction. Hence our assumption was wrong. I is contained in I_k for some k [5]. □

6 Conclusion

Through this review research paper, we have attempted to present a comprehensive study of one of the building blocks of commutative algebra. We have stated and proved the Prime Avoidance

Lemma. We have also discussed its refinements and variations tracing the evolution of the lemma over the years. The application of Prime Avoidance Lemma goes a long way in proving various concepts of the commutative algebra. We have presented some of the important results and applications in commutative algebra in which the concept of Prime Avoidance Lemma has been applied.

References

[1] Dummit D. S. and Foote R. M., *Abstract Algebra*, 3rd edition, John Wiley and Sons Inc., 2004, pp. 656-673.

[2] Constantinescu A., *Algebra 1**, Freie Universität Berlin, 2019-2020, pp. 18-19.

[3] Gallian J.A., *Contemporary Abstract Algebra*, University of Minnesota, 9th edition, Cengage Learning India, 2013, pp. 249-253.

[4] Basu R. and Sridharan R.,*On Forster's Conjecture and Related Results*, Punjab University Research Journal (Science), 2007, pp. 3-7, 24-29, 44.

[5] Chen J. and Tarizadeh A.,*Avoidance and Absorbance*, Journal of Algebra, Volume 582, 2021, pp. 2-4.

[6] Prime Avoidance Lemma, *HandWiki*, https://handwiki.org/wiki/Prime_avoidance_lemma.

[7] Applications of the Prime Avoidance Lemma, *MathOverflow*, https://mathoverflow.net/questions/255813/applications-of-the-prime-avoidance-lemma.

(Mentor) Dr. Sunil Kumar Yadav, Assistant Professor, Department of Mathematics, Lady Shri Ram College for Women, New Delhi
skymath.bhu@gmail.com

Kriti Agrawal, B.Sc.(H) Mathematics, 6th Semester, Lady Shri Ram College for Women, New Delhi
kritiagrawal1502@gmail.com

Richa Shekhar, B.Sc.(H) Mathematics, 6th Semester, Lady Shri Ram College for Women, New Delhi
shekharricha07@gmail.com

Éclat, A Mathematics Journal
Volume 14, 2022-23 (28-35)

The $\left(\frac{G'}{G}\right)$ Expansion Method to Find the Exact Travelling Wave Solutions of (3+1)- Dimensional Painlevé Integrable Extension of Mikhailov-Novikov-Wang Equation

Kuldeep, Shaziya Parveen and Teena

Abstract

In this paper, we apply the $\left(\frac{G'}{G}\right)$- expansion method to find the soliton solutions of a (3+1)- dimensional Painlevé integrable extension of Mikhailov-Novikov-Wang Equation. The $\left(\frac{G'}{G}\right)$- expansion method is a powerful yet rather simple method to find the exact travelling wave solutions of nonlinear evolution equations. These soliton solutions may further help in understanding some crucial physical phenomena. Maple software has been used to derive the analytic solutions and to graphically represent them in 3D.

Keywords: Mikhailov-Novikov-Wang Equation, Solitons, Nonlinear Evolution Equation, Exact Solutions

1 Introduction

In physics and engineering, the majority of natural phenomena can be modelled using nonlinear evolution equations (NLEEs). The solutions to the NLEEs are hence of paramount importance in understanding these phenomena. One of the significant classes of the analytic solutions of the NLEEs are the exact travelling wave solutions or solitons. The solitons are essential in understanding and description of various physical processes.

Many dominant methods have been proposed to solve the NLEEs like the Bäcklund transformation [5], Hirota's method [7], tanh-function method [3], extended tanh-function method [2], homogeneous balance method ([6],[8]), variational iteration method [13], Adomian Decomposition method [1], Jacobi elliptic function expansion method [9], F expansion method [11], auxiliary equation method, Fan sub-equation method, extended Fan sub-equation method, modified extended Fan sub-equation method and so on.

Extensive research has been done for finding the exact solutions of (1+1)- dimensional integrable NLEEs like Boussinesq equation, KdV equation, Mikhailov-Novikov-Wang equation (MNWEq) that describe some crucial dynamical physical phenomena.

Higher dimensional integrable NLEEs are used to model various physical processes in nonlinear optics, oceanography, fluid flow, etc. The MNWEq is of great importance in research and its solutions can help in understanding nonlinear wave phenomenon.

2 (3+1)- dimensional Painlevé integrable extension of the Mikhailov-Novikov-Wang Equation

In this paper, we use the $\left(\frac{G'}{G}\right)$- expansion method proposed by Wang et al [9]. Our work aims to apply the $\left(\frac{G'}{G}\right)$- expansion method to find new exact travelling wave solutions of the following (3+1)- dimensional Painlevé integrable extension of the Mikhailov-Novikov-Wang Equation [10],

$$R + \beta_1 u_{xt} + \beta_2 u_{yt} + \beta_3 u_{zt} = 0, \tag{1}$$

where $u = u(x, y, z, t)$ and,

$$R = 24u_x^2 u_{xx} - 4u_{xx}u_t - 8u_x u_{xt} + 2u_x u_{xxxx} + 4u_{xx}u_{xxx} + u_{tt} - u_{xxxt},$$

is the standard integrable (1+1)- dimensional Mikhailov-Novikov-Wang Equation [4].

The equation that we use here, MNWE2, was formally introduced by Wazwaz et al (2022) [11]. It is an integrable extension to the standard MNWEq. The extended MNWEq is obtained by adding a suitable set of partial derivatives, in this case $\{u_{xt}, u_{yt}, u_{zt}\}$, to the standard MNWEq. The resultant extended MNWEq is integrable and hence possesses a rich set of exact solutions.

3 $\left(\frac{G'}{G}\right)$-Expansion Method

The following section explains the modified $\left(\frac{G'}{G}\right)$- expansion method for finding travelling wave solutions of NLEEs [12].

We consider the following (3+1)- dimensional nonlinear evolution equation of the standard form-

$$P\left(u, u_t, u_x, u_{tt}, u_{xx}, u_{xt}, \ldots\right) = 0, \tag{2}$$

where $u = u(x, y, z, t)$ is an unknown function and P is a polynomial in $u(x, y, z, t)$ and its partial derivatives. It contains nonlinear as well as higher order derivatives of u.

Step 1: We start by considering the following wave transform-

$$u\left(x, y, z, t\right) = u\left(\xi\right), \tag{3}$$
$$\xi = x + y + z - Vt,$$

where t denotes time (temporal coordinate), x, y and z are spatial coordinates and V is the speed of the travelling wave, which is to be determined.
The travelling wave transform enables us to convert the equation (2) from a NLEE to an ordinary differential equation (ODE) of the form-

$$P\left(u, -Vu', u'', V^2u''', \ldots\right) = 0, \tag{4}$$

where u', u'', u''' are derivatives of u with respect to ξ and P is a polynomial in $u = u(\xi)$ and its derivatives.

Step 2: Now suppose that the solution of the ODE (4) can be expressed as a polynomial in $\left(\frac{G'}{G}\right)$, such that,

$$u(\xi) = \alpha_m \left(\frac{G'}{G}\right)^m + \ldots, \tag{5}$$

where $m = 0, 1, 2, ...$ and $\alpha_m \neq 0$.
Here $G = G(\xi)$ is the solution of the following second order linear ordinary differential equation-

$$G''(\xi) + \lambda G'(\xi) + \mu G(\xi) = 0, \tag{6}$$

where λ and μ are real constants.

We determine the constant m in equation (5) by considering the homogenous balance between the highest order derivative and the most nonlinear term appearing in the ODE (4).

Step 3: Substituting equation (5) into the ODE (4) and collecting the terms having the same power of $\left(\frac{G'}{G}\right)$, we obtain a polynomial in $\left(\frac{G'}{G}\right)$. Thereafter, we equate the coefficients of this polynomial to zero which generates a set of algebraic equations containing the undetermined terms $\alpha_m, ..., \alpha_0, V, \lambda$ and μ.

Step 4: Solving the above mentioned set of algebraic equations we obtain the values of the constants $\alpha_m, ..., \alpha_0, V, \lambda$ and μ. Now, using the auxiliary solution of equation (6) we can derive the general solution of the ODE (4).

4 Application of the $\left(\frac{G'}{G}\right)$-expansion method to MNWE2

Consider the following NLEE (1),

$$24u_x^2 u_{xx} - 4u_{xx}u_t - 8u_x u_{xt} + 2u_x u_{xxxx} + 4u_{xx}u_{xxx} + u_{tt} - u_{xxxt} + \beta_1 u_{xt} + \beta_2 u_{yt} + \beta_3 u_{zt} = 0,$$

We can change the given NLEE to an ODE by the variable transformation given in equation (3). Further, integrating the ODE with respect to ξ yields the following equation,

$$C + V^2u' + Vu''' + 6V(u')^2 + 2u'''u' + (u'')^2 + 8(u')^3 - V\beta_1 u' - V\beta_2 u' - V\beta_3 u', \tag{7}$$

where C is the constant of integration.

Considering the homogenous balance between the highest order derivates and most nonlinear term, we get $m = 2$. Hence $u = u(\xi)$ can be written as a polynomial in $\left(\frac{G'}{G}\right)$ as done in equation (5),

$$u(\xi) = \alpha_2 \left(\frac{G'}{G}\right)^2 + \alpha_1 \left(\frac{G'}{G}\right) + \alpha_0. \tag{8}$$

Differentiating equation (8) we obtain,

$$u'(\xi) = -\frac{\left(\alpha_1 G(\xi) + 2\,\alpha_2 \frac{d}{d\xi} G(\xi)\right)\left(\mu\,(G(\xi))^2 + \lambda\, G(\xi)\frac{d}{d\xi}G(\xi) + \left(\frac{d}{d\xi}G(\xi)\right)^2\right)}{(G(\xi))^3}$$

$$u''(\xi) = 2\,\frac{\left(3\,\alpha_2\left(\frac{d}{d\xi}G(\xi)\right)^2+2\,G(\xi)(\lambda\,\alpha_2+1/2\,\alpha_1)\frac{d}{d\xi}G(\xi)+(G(\xi))^2(\mu\,\alpha_2+1/2\,\lambda\,\alpha_1)\right)\left(\mu\,(G(\xi))^2+\lambda\,G(\xi)\frac{d}{d\xi}G(\xi)+\left(\frac{d}{d\xi}G(\xi)\right)^2\right)}{(G(\xi))^4}$$

$$u'''(\xi) = \frac{-6\left[4\alpha_2\left(\frac{d}{d\xi}G(\xi)\right)^3+5G(\xi)\left(\lambda\alpha_2+\frac{\alpha_1}{5}\right)\left(\frac{d}{d\xi}G(\xi)\right)^2+\frac{8\left(\frac{1}{2}\lambda^2\alpha_2+\mu\alpha_2+\frac{3}{8}\lambda\alpha_1\right)G(\xi)^2\left(\frac{d}{d\xi}G(\xi)\right)}{3}\right.}{G(\xi)^5}$$
$$\left.+\frac{G(\xi)^3\left(\mu\lambda\alpha_2+\frac{1}{6}\lambda^2\alpha_1+\frac{1}{3}\mu\alpha_1\right)}{(G(\xi))^5}\right]\frac{\left(\mu G(\xi)^2+\lambda\,G(\xi)\,\frac{d}{d\xi}G(\xi)+\left(\frac{d}{d\xi}G(\xi)\right)^2\right)}{(G(\xi))^5}$$

Putting $u'(\xi), u''(\xi), u'''(\xi)$ in equation (7) and collecting the same order terms of $\left(\frac{G'}{G}\right)$ we obtain a polynomial in $\left(\frac{G'}{G}\right)$. As done in Step 3, we equate the coefficients of the polynomial to zero and obtain a set of algebraic equations containing the undetermined terms.

Suppose $l_0, l_1, l_2, \ldots, l_9$ are coefficients of $\left(\frac{G'}{G}\right)^0, \left(\frac{G'}{G}\right)^1, \left(\frac{G'}{G}\right)^2, \ldots, \left(\frac{G'}{G}\right)^9$ respectively, we have,

$$\begin{aligned}l_0:\ & 4\,\mu^4\alpha_2{}^2+\left(16\,\lambda\,\alpha_1\alpha_2-8\,\alpha_1{}^3+4\,\alpha_1{}^2\right)\mu^3+\left(\left(3\,\lambda^2+6\,V\right)\alpha_1{}^2-2\,V\alpha_1-6\,V\lambda\,\alpha_2\right)\mu^2\\ & -V\alpha_1\left(\lambda^2+V-\beta_1-\beta_2-\beta_3\right)\mu+C.\end{aligned}$$

$$\begin{aligned}l_1:\ & 48\,\alpha_2\left(\lambda\,\alpha_2-\alpha_1{}^2+\alpha_1\right)\mu^3+\left(-24\,\lambda\,\alpha_1{}^3+24\,\lambda\,\alpha_1{}^2+24\,\left(5/2\,\lambda^2+V\right)\alpha_2\alpha_1-16\,V\alpha_2\right)\mu^2\\ & +\left(\left(6\,\lambda^3+12\,V\lambda\right)\alpha_1{}^2-8\,V\lambda\,\alpha_1-2\,V\alpha_2\left(7\,\lambda^2+V-\beta_1-\beta_2-\beta_3\right)\right)\mu\\ & -V\lambda\,\alpha_1\left(\lambda^2+V-\beta_1-\beta_2-\beta_3\right).\end{aligned}$$

$$\begin{aligned}l_2:\ & \left(-24\,\lambda^2\mu-24\,\mu^2\right)\alpha_1{}^3+\left(3\,\lambda^4+\left(6\,V+42\,\mu\right)\lambda^2-144\,\alpha_2\lambda\,\mu^2+12\,\mu\,\left(V+2\,\mu\right)\right)\alpha_1{}^2\\ & +\left(72\,\mu\,\alpha_2\lambda^3-7\,V\lambda^2+48\,\mu\,\alpha_2\left(V+5\,\mu\right)\lambda-V^2+\left(-8\,\mu+\beta_1+\beta_2+\beta_3\right)V-96\,\mu^3\alpha_2{}^2\right)\alpha_1\\ & -2\,\left(4\,V\lambda^3-66\,\mu^2\alpha_2\lambda^2+V\left(V+26\,\mu-\beta_1-\beta_2-\beta_3\right)\lambda-12\,\mu^2\alpha_2\left(V+4\,\mu\right)\right)\alpha_2.\end{aligned}$$

$$\begin{aligned}l_3:\ & -64\,\mu^3\alpha_2{}^3+48\,\lambda\,\mu\,\left(-6\,\mu\,\alpha_1+\tfrac{17\,\lambda^2}{6}+V+9\,\mu\right)\alpha_2{}^2\\ & +\Big(28\,\alpha_1\lambda^4+\left(-144\,\mu\,\alpha_1{}^2+\left(24\,V+360\,\mu\right)\alpha_1-38\,V\right)\lambda^2-144\,\alpha_1{}^2\mu^2+48\,\mu\,\left(V+4\,\mu\right)\alpha_1\\ & -2\,V\left(V+20\,\mu-\beta_1-\beta_2-\beta_3\right)\Big)\alpha_2+12\,\lambda\,\alpha_1\left(\left(-2/3\,\alpha_1{}^2+\tfrac{11\,\alpha_1}{6}\right)\lambda^2-4\,\mu\,\alpha_1{}^2+\left(V+6\,\mu\right)\alpha_1-V\right).\end{aligned}$$

$$\begin{aligned}l_4:\ & -192\,\lambda\,\mu^2\alpha_2{}^3+\left(-288\,\mu\,\left(\lambda^2+\mu\right)\alpha_1+48\,\lambda^4+\left(24\,V+600\,\mu\right)\lambda^2+48\,V\mu+312\,\mu^2\right)\alpha_2{}^2+\\ & 48\,\lambda\,\left(\left(-\lambda^2-6\,\mu\right)\alpha_1{}^2+\left(7/2\,\lambda^2+V+11\,\mu\right)\alpha_1-\tfrac{9\,V}{8}\right)\alpha_2+6\,\alpha_1\Big(\left(-4\,\lambda^2-4\,\mu\right)\alpha_1{}^2\\ & +\left(17/2\,\lambda^2+V+6\,\mu\right)\alpha_1-V\Big).\end{aligned}$$

$$l_5: -192\,\mu\,\left(\lambda^2+\mu\right)\alpha_2{}^3+48\,\lambda\,\left(\left(-2\,\alpha_1+11/2\right)\lambda^2-12\,\mu\,\alpha_1+V+17\,\mu\right)\alpha_2{}^2$$
$$+\left(\left(-144\,\alpha_1{}^2+348\,\alpha_1\right)\lambda^2-144\,\mu\,\alpha_1{}^2+\left(24\,V+240\,\mu\right)\alpha_1-24\,V\right)\alpha_2-24\,\lambda\,\alpha_1{}^2\left(\alpha_1-2\right).$$

$$l_6: \left(-64\,\lambda^3-384\,\lambda\,\mu\right)\alpha_2{}^3+\left(\left(-288\,\lambda^2-288\,\mu\right)\alpha_1+516\,\lambda^2+24\,V+352\,\mu\right)\alpha_2{}^2$$
$$-144\,\lambda\,\left(\alpha_1-\tfrac{19}{9}\right)\alpha_1\alpha_2-8\,\alpha_1{}^3+16\,\alpha_1{}^2.$$

$$l_7: -192\,\left(\left(\lambda^2+\mu\right)\alpha_2{}^2+3/2\,\left(\alpha_1-3/2\right)\lambda\,\alpha_2+1/4\,\alpha_1{}^2-1/2\,\alpha_1\right)\alpha_2.$$

$$l_8: -\,192\,\lambda\,\alpha_2{}^3+\left(-96\,\alpha_1+132\right)\alpha_2{}^2.$$

$$l_9: -\,64\,\alpha_2{}^3.$$

Solving the above system of algebraic equations, we get the following suitable value for the constants-

$$[C=0,\quad \mu=\frac{1}{4}\left(\lambda^2+V\right),\quad \alpha_1=2,\quad \alpha_2=0,\quad \beta_1=-\beta_2-\beta_3],$$

where $\lambda,\mu,\alpha_0,\beta_2$ and β_3 are arbitrary constants.

Substituting the given values in equation (8), we obtain-

$$u(\xi)=2\left(\frac{G'}{G}\right)+\alpha_0, \tag{9}$$
$$\xi=x+y+z-(-\lambda^2+4\mu)t.$$

Solving equation (6) and substituting the value of $\left(\frac{G'}{G}\right)$ in equation (9), we obtain the following soliton solutions of the (3+1)- dimensional Painlevé integrable extension of the Mikhailov-Novikov-Wang Equation (1):

1. When $V>0$:

$$u(x,y,z,t)=\frac{\sqrt{V}\left(c_2\cos\left(\frac{1}{2}\sqrt{V}(x+y+z-Vt)\right)-c_1\sin\left(\frac{1}{2}\sqrt{V}(x+y+z-Vt)\right)\right)}{c_1\cos\left(\frac{1}{2}\sqrt{V}(x+y+z-Vt)\right)+c_2\sin\left(\frac{1}{2}\sqrt{V}(x+y+z-Vt)\right)}+\alpha_0.$$

2. When $V<0$:

$$u(x,y,z,t)=\frac{\sqrt{V}\left(c_2\cosh\left(\frac{1}{2}\sqrt{V}(x+y+z-Vt)\right)-c_1\sinh\left(\frac{1}{2}\sqrt{V}(x+y+z-Vt)\right)\right)}{c_1\cosh\left(\frac{1}{2}\sqrt{V}(x+y+z-Vt)\right)+c_2\sinh\left(\frac{1}{2}\sqrt{V}(x+y+z-Vt)\right)}+\alpha_0,$$

where c_1 and c_2 are arbitrary constants.

5 Graphical Representation

By taking different values of arbitrary constants $c_1,c_2,\lambda,\mu,\alpha_0$ we get the following graphs-

CASE 1: When V>0

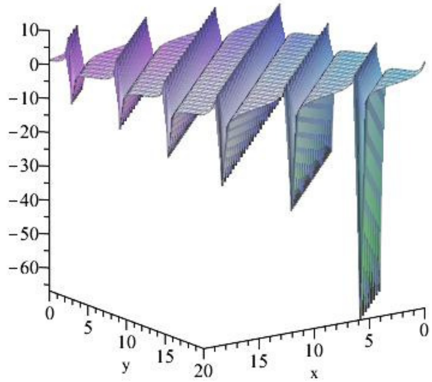

Figure 5.1: Graph of $u(x, y, z, t)$ when $(c_1 = 1; c_2 = 1; \lambda = 1; \mu = 0.5; \alpha_0 = 1; y = 0; z = 0)$ drawn using Maple

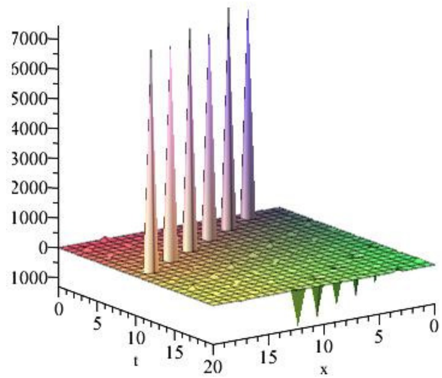

Figure 5.2: Graph of $u(x, y, z, t)$ when $(c_1 = 1; c_2 = 1; \lambda = 0.5; \mu = 0.5; \alpha_0 = 1; y = 1; z = 1)$ drawn using Maple

Figure 5.1 is the graph of a dark soliton characterized by the peaks in the negative z direction. Figure 5.2 is the graph of a bright soliton characterized by the peaks in the positive z direction.

CASE 2: When V<0

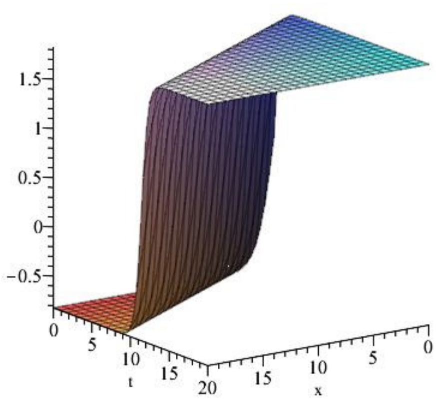

Figure 5.3: Graph of $u(x, y, z, t)$ when $(c_1 = 2; c_2 = 0; \lambda = 1; \mu = 2; \alpha_0 = 0.5; y = 0; z = 0)$ drawn using Maple

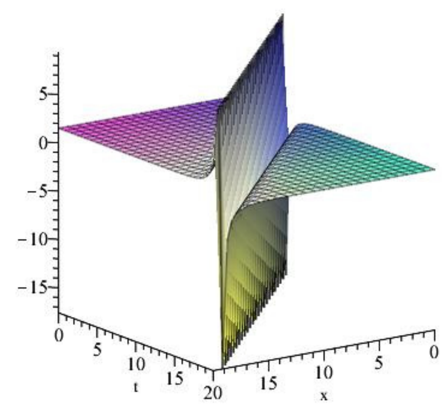

Figure 5.4: Graph of $u(x, y, z, t)$ when $(c_1 = 1; c_2 = 3; \lambda = 1; \mu = 0.5; \alpha_0 = 1; y = 0; z = 0)$ drawn using Maple

Figure 5.3 and Figure 5.4 depict a kink type soliton for the particular chosen value of arbitrary constants. The kink wave soliton changes its asymptotic position from one to another and tends to take the value of constant at infinity.

6 Conclusion

In this paper, the generalised and extended $\left(\frac{G'}{G}\right)$-expansion method has been successfully applied to find the exact travelling wave solution of (3+1)- dimensional Painlevé integrable extension to the Mikhailov-Novikov-Wang Equation. By applying appropriate constraints on the coefficients, we obtain the general solution of the equation. It contains plenty of arbitrary constants and hence yields a rich set of exact soliton solutions. These solutions can further be used in understanding the mechanism of some complicated nonlinear physical phenomena occurring in wave interactions.

References

[1] Pamuk S., *An Application for Linear and Nonlinear Heat Equations by Adomian's Decomposition Method*, Applied Mathematics and Computation, Volume 163, No. 1, 2005, pp. 89-96.

[2] Parkes E.J. and Duffy B.R., *An Automated tanh-function Method for Finding Solitary Wave Solutions to Nonlinear Evolution Equations*, Computer Physics Communications, Volume 98, Issue 3, 1996, pp. 288-300.

[3] Zhang W., *A Generalised tanh-function Type Method and the* $\left(\frac{G'}{G}\right)$*- Expansion Method for Solving Nonlinear Partial Differential Equations*, Applied Mathematics, Volume 4, No. 10A, 2013, pp. 11-16.

[4] Demiray S.T. and Bayrakci U., *A Study on the Solutions of (1+1)-Dimensional Mikhailov-Novikov-Wang Equation*, Mathematical Modelling and Numerical Simulation With Applications, Volume 2, No. 5, 2022, pp. 1-8.

[5] Rogers C. and Shadwick W.F., *Backlund Transformations*, Academic Press, New York, 1982.

[6] Wang M.L., *Exact Solutions for a Compound KdV- Burgers Equation*, Physics Letter A, Volume 213, 1996, pp. 279.

[7] Hirota R., *Exact Solution of the Korteweg-De Vries Equation for Multiple Collisions of Solitons*, Physical Review Letters, Volume 27, 1971, pp. 1192-1194.

[8] Barman H.K., Roy R., Mahmud F., Akbar M.A. and Osman M.S., *Harmonizing Wave Solutions to the Fokas–Lenells Model Through the Generalised Kudryashov Method*, International Journal for Light and Electron Optics, Volume 229, 2021, Article No. 166294.

[9] Liu S.K., Fu Z., Liu S. and Qiang Zhao, *Jacobi Elliptic Function Expansion Method and Periodic Wave Solutions of Nonlinear Wave Equations*, Physics Letters A, Volume 289, Issues 1–2, 2001, pp. 69-74.

[10] Wazwaz A.M., Alhejaili W. and El-Tantawy S.A., *New (3+1)-Dimensional Painlevé Integrable Extensions of Mikhailov-Novikov-Wang Equation: Variety of Multiple Soliton Solutions*, Romanian J Physics, Volume 67, 2022, Article 115.

[11] Yildirim Y., *Optical Solitons With Biswas-Arshed Equation by F-expansion Method*, International Journal for Light and Electron Optics, Volume 227, 2021, pp. 227.

[12] Wang M., Li X. and Zhang J., *The* $\left(\frac{G'}{G}\right)$*-Expansion Method and Travelling Wave Solutions of Nonlinear Evolution Equations in Mathematical Physics*, Physics Letters A, Volume 372, 2008, pp. 417–423.

[13] Abdou M.A. and Soliman A.A., *Variational Iteration Method for Solving Burger's and Coupled Burger's Equations*, Journal of Computational and Applied Mathematics, Volume 181, 2005, pp. 245-251.

(Mentor) Kuldeep, Assistant Professor, Department of Mathematics, Lady Shri Ram College for Women, New Delhi
kuldeepkr09@gmail.com

Shaziya Parveen, B.Sc.(H) Mathematics, 4th Semester, Lady Shri Ram College for Women, New Delhi
shaziyaparveen297@gmail.com

Teena, B.Sc.(H) Mathematics, 4th Semester, Lady Shri Ram College for Women, New Delhi
teena.maths2021@gmail.com

Éclat, A Mathematics Journal
Volume 14, 2022-23 (36-47)

Introduction to the Mahalanobis distance

Monika Singh, Akshi Sharma and Jigyasa Srivastava

Abstract

This paper attempts to provide an insight into the concept of Mahalanobis distance (MD). The Mahalanobis distance in the real coordinate space is examined and interpreted in relation to the Euclidean distance (ED), where ED doesn't take into account the correlation between the correlated variables, while MD takes the same into consideration. It further discusses one of the most significant applications of MD i.e., multivariate outlier detection.

Keywords: Mahalanobis distance, Euclidean distance, Correlation, Multivariate outlier detection

1 Introduction

The discovery of Mahalanobis distance[1] (MD) dates back to 1936. It was proposed by a renowned Indian mathematician and statistician, Prasanta Chandra Mahalanobis[4], whose birth anniversary on 29^{th} June is celebrated as National Statistics Day. This concept was prompted by the problem of identifying the similarities of skulls based on anthropometrical measurements in 1927, in context of his study on racial likeness. During the course of his study, he found a way of comparing and grouping populations using a multivariate distance measure. This distance measure was termed as the Mahalanobis distance.

The Mahalanobis distance is the most widely used metric in multivariate statistics. The classical method to compute distance is Euclidean distance (ED) measure, which is the shortest possible distance between any two points in uni-dimensional or multi-dimensional space. The problem with ED measure is that it doesn't take into account the correlation between the correlated variables while MD takes the same into consideration, since it is calculated using the inverse of variance-covariance matrix [for definition, see Subsection 2.1] of the data set of interest.

The formula for calculating Mahalanobis distance between a point and a distribution denoted by MD, is given by:

$$MD := \sqrt{(A-\mu)\Sigma^{-1}(A-\mu)^T}, \tag{1}$$

where A is the row matrix of values of the variables, μ is the row matrix of the mean of the distributions, Σ is the variance-covariance matrix, T indicates the transpose of the matrix and Σ^{-1} denotes the inverse of the variance-covariance matrix.

The paper is organised as follows: Section 2 discusses the computation of MD and ED for correlated and uncorrelated data set of two variables respectively. Section 3 provides graphical representation of ED and MD. Section 4 gives the interpretation of eigenvalues and eigenvectors of variance-covariance matrix. Section 5 outlines in brief the analytical interpretation[2] of ED and MD. Section 6 highlights the applications[3] of MD. Section 7 is the conclusion and is followed by references.

Following is a little digression to briefly mention about P.C. Mahalanobis.

1.1 About P.C. Mahalanobis

P.C. Mahalanobis (1893-1972), the father of Indian statistics was born in Calcutta (now Kolkata), India. Mahalanobis received his early schooling at the Brahmo Boys' School, Kolkata, then did his Bachelor's in Physics from University of Calcutta under Presidency College in 1912. He also attended the King's College in Cambridge, where he met mathematical genius, Srinivasa Ramanujan[5]. His career in statistics was greatly influenced by the nobel laureate Rabindranath Tagore[6] who took keen interest in Mahalanobis's statistical works. P.C. Mahalanobis has been credited for receiving many honours for his remarkable contributions in statistics and to its applications in various fields. He is the founder of Indian Statistical Institute (ISI), the statistics Journal, *Sankhya* and Central Statistical Organisation (CSO) which was formed for coordinating all statistical activities of the government. In recognition to the notable contributions made by him, Prof. P.C. Mahalanobis National Award in Official Statistics is annually awarded to Official statisticians for their outstanding and meritorious contributions in the area of Official statistics in India.

2 Computation of ED and MD

2.1 For Correlated data

Let x and y denote the score and attendance of the students; respectively, out of 100. Suppose x_{S_i}, y_{S_i} denote the score and attendance of the i^{th} student and μ_x, μ_y denote the mean of the variables respectively.
The Table 1 includes the simulated correlated data set of two variables x_{S_i} and y_{S_i}. The formula for calculating correlation coefficient denoted by ρ_{xy}, is given by :

$$\rho_{xy} := \frac{\sum (x_{S_i} - \mu_x)(y_{S_i} - \mu_y)}{\sqrt{\sum (x_{S_i} - \mu_x)^2 \sum (y_{S_i} - \mu_y)^2}}. \tag{2}$$

Here, $\rho_{xy} = \mathbf{0.8860}$. This implies that the variables are in positive correlation to each other and are nearly perfectly correlated[1].
Mahalanobis distance (MD):

$$MD_{S_i} = \sqrt{(A-\mu)\Sigma^{-1}(A-\mu)^T}, \tag{3}$$

where A is the row matrix of values of score and attendance for i^{th} student i.e.,

$$A = \begin{bmatrix} x_{S_i} & y_{S_i} \end{bmatrix},$$

μ is the row matrix of the mean of variables x and y respectively i.e.,

$$\mu = \begin{bmatrix} \mu_x & \mu_y \end{bmatrix}$$

[1]Correlation Coefficient, $\rho_{xy} \neq -1, 1$ since in that case determinant of variance-covariance matrix will be zero.

and matrix Σ is the variance-covariance matrix i.e.,

$$\Sigma = \begin{bmatrix} \text{variance}(x) & \text{covariance}(x,y) \\ \text{covariance}(y,x) & \text{variance}(y) \end{bmatrix},$$

$$\Sigma = \begin{bmatrix} 148.8286 & 192.8800 \\ 192.8800 & 365.5524 \end{bmatrix}.$$

$$\Sigma^{-1} = \begin{bmatrix} 0.021250628 & -0.011212677 \\ -0.011212677 & 0.008651841 \end{bmatrix}.$$

Now by formula (3),

$$MD^2_{S_1} = \begin{bmatrix} 26.4 & 37.1333 \end{bmatrix} \begin{bmatrix} 0.021250628 & -0.011212677 \\ -0.011212677 & 0.008651841 \end{bmatrix} \begin{bmatrix} 26.4 \\ 37.1333 \end{bmatrix}.$$

Therefore,

$$MD_{S_1} = 2.1647.$$

Student (S_i)	**Score (/100)** (x_{S_i})	**Attendance (/100)** (y_{S_i})	$x_{S_i} - \mu_x$	$y_{S_i} - \mu_y$	$(x_{S_i} - \mu_x)^2$	$(y_{S_i} - \mu_y)^2$	$(x_{S_i} - \mu_x)(y_{S_i} - \mu_y)$
S_1	92.0	78.0	26.4	37.1333	696.9600	1378.8820	980.3191
S_2	86.0	58.0	20.4	17.1333	416.1600	293.5500	349.5193
S_3	69.0	54.0	3.4	13.1333	11.5600	172.4836	44.6532
S_4	73.0	45.0	7.4	4.1333	54.7600	17.0842	30.5864
S_5	69.0	41.0	3.4	0.1333	11.5600	0.0178	0.4532
S_6	66.0	38.0	0.4	-2.8667	0.1600	8.2180	-1.1467
S_7	71.0	65.0	5.4	24.1333	29.1600	582.4162	130.3198
S_8	55.0	14.0	-10.6	-26.8667	112.3600	721.8196	284.7870
S_9	57.0	19.0	-8.6	-21.8667	73.9600	478.1526	188.0536
S_{10}	63.0	52.0	-2.6	11.1333	6.7600	123.9504	-28.9466
S_{11}	65.0	38.0	-0.6	-2.8667	0.3600	8.2180	1.7200
S_{12}	58.0	37.0	-7.6	-3.8667	57.7600	14.9514	29.3870
S_{13}	58.0	36.0	-7.6	-4.8667	57.7600	23.6868	36.9869
S_{14}	43.0	6.0	-22.6	-34.8667	510.7600	1215.6870	787.9874
S_{15}	59.0	32.0	-6.6	-8.8667	43.5600	78.6184	58.5202
Mean	$\mu_\mathbf{x} = \mathbf{65.6}$	$\mu_\mathbf{y} = \mathbf{40.8667}$	**0**	**0**			
Standard Deviation	$\sigma_\mathbf{x} = \mathbf{12.1995}$	$\sigma_\mathbf{y} = \mathbf{19.1194}$					
Variance	$\sigma^2_\mathbf{x} = \mathbf{148.8286}$	$\sigma^2_\mathbf{y} = \mathbf{365.5524}$					

Table 1: Simulated data of the correlated variables

Euclidean Distance (ED):

$$ED_{S_i} := \sqrt{(x_{S_i} - \mu_x)^2 + (y_{S_i} - \mu_y)^2}, \tag{4}$$

Hence,

$$ED_{S_1} = \sqrt{696.9600 + 1378.8820} = 45.5614.$$

Similarly, for remaining students ED and MD can be evaluated [see Table 2].

Student(S_i)	ED_{S_i}**(Approx.)**	MD_{S_i}**(Approx.)**
S_1	45.5614	2.1647
S_2	26.6404	2.0953
S_3	13.5663	0.9890
S_4	8.4761	0.9208
S_5	3.4026	0.5878
S_6	2.8945	0.3874
S_7	24.7301	1.9279
S_8	28.8822	1.6225
S_9	23.4971	1.3230
S_{10}	11.4329	1.6766
S_{11}	2.9288	0.2346
S_{12}	8.5271	0.9782
S_{13}	9.0247	0.8941
S_{14}	41.5505	1.8938
S_{15}	11.0534	0.5420

Table 2: Evaluated ED and MD for the correlated data set

2.2 For Uncorrelated data

Let x and y denote the number of movies watched and intelligence of the students; respectively, out of 10. Suppose x_{S_i}, y_{S_i} denote the number of movies watched and intelligence of the i^{th} student and μ_x, μ_y denote the mean of the variables respectively.
The Table 3 includes the simulated uncorrelated data set of two variables x_{S_i} and y_{S_i}.
By formula (2), the correlation coefficient for this data set is $-\mathbf{0.2901}$ which implies that the variables are nearly perfectly uncorrelated.
Mahalanobis distance (MD):
The variance-covariance matrix and its inverse are calculated as follows:

$$\Sigma = \begin{bmatrix} 9.1667 & -1.2500 \\ -1.2500 & 2.5000 \end{bmatrix}.$$

$$\Sigma^{-1} = \begin{bmatrix} 0.117073 & 0.058537 \\ 0.058537 & 0.429268 \end{bmatrix}.$$

Therefore, by (3)

$$MD_{S_1} = 2.0708.$$

Student(S_i)	**No. of movies watched (/10)** (x_{S_i})	**Intelligence (/10)** (y_{S_i})	$x_{S_i}-\mu_x$	$y_{S_i}-\mu_y$	$(x_{S_i}-\mu_x)^2$	$(y_{S_i}-\mu_y)^2$	$(x_{S_i}-\mu_x)(y_{S_i}-\mu_y)$
S_1	1.0	6.0	-4.5	-1.5	20.25	2.25	6.75
S_2	2.0	7.0	-3.5	-0.5	12.25	0.25	1.75
S_3	5.0	10.0	-0.5	2.5	0.25	6.25	-1.25
S_4	7.0	8.0	1.5	0.5	2.25	0.25	0.75
S_5	8.0	7.0	2.5	-0.5	6.25	0.25	-1.25
S_6	10.0	5.0	4.5	-2.5	20.25	6.25	-11.25
S_7	4.0	9.0	-1.5	1.5	2.25	2.25	-2.25
S_8	9.0	6.0	3.5	-1.5	12.25	2.25	-5.25
S_9	3.0	8.0	-2.5	0.5	6.25	0.25	-1.25
S_{10}	6.0	9.0	0.5	1.5	0.25	2.25	0.75
Mean	$\mu_{\mathbf{x}} = \mathbf{5.5}$	$\mu_{\mathbf{y}} = \mathbf{7.5}$	**0**	**0**			
Standard Deviation	$\sigma_{\mathbf{x}} = \mathbf{3.0277}$	$\sigma_{\mathbf{y}} = \mathbf{1.5811}$					
Variance	$\sigma^{\mathbf{2}}_{\mathbf{x}} = \mathbf{9.1667}$	$\sigma^{\mathbf{2}}_{\mathbf{y}} = \mathbf{2.5000}$					

Table 3: Simulated data of the uncorrelated variables

Euclidean distance (ED):
Since for student S_1 i.e., for i=1, $\frac{(x_{S_1}-\mu_x)}{\sigma_x} = -1.4863$ and $\frac{(y_{S_1}-\mu_y)}{\sigma_y} = -0.94868$.
This implies,

$$ED_{S_1} = \sqrt{(-1.4863)^2 + (-0.94868)^2} = 1.7632.$$

Similarly, for remaining students ED and MD can be evaluated [see Table 4].

Student(S_i)	ED_{S_i}**(Approx.)**	MD_{S_i}**(Approx.)**
S_1	1.7633	2.0708
S_2	1.1985	1.3416
S_3	1.5898	1.6106
S_4	0.5877	0.6903
S_5	0.8842	0.8296
S_6	2.1701	1.9113
S_7	1.0702	0.9762
S_8	1.4954	1.3218
S_9	0.8842	0.8296
S_{10}	0.9630	1.0544

Table 4: Evaluated ED and MD for the uncorrelated data set

3 Graphical representation of ED and MD

3.1 Euclidean distance

For the simulated correlated data of $(x_{S_i} - \mu_x)$ and $(y_{S_i} - \mu_y)$ in Table 1, the ED for each student is calculated by the formula,

$$ED_{S_i} = \sqrt{(x_{S_i} - \mu_x)^2 + (y_{S_i} - \mu_y)^2}.$$

Therefore,

$$ED^2_{S_i} = (x_{S_i} - \mu_x)^2 + (y_{S_i} - \mu_y)^2,$$

which represents the circle with centre (μ_x, μ_y) and radius ED_{S_i}.
The Figure 3.1 plots the simulated data of $(x_{S_i} - \mu_x)$ and $(y_{S_i} - \mu_y)$.

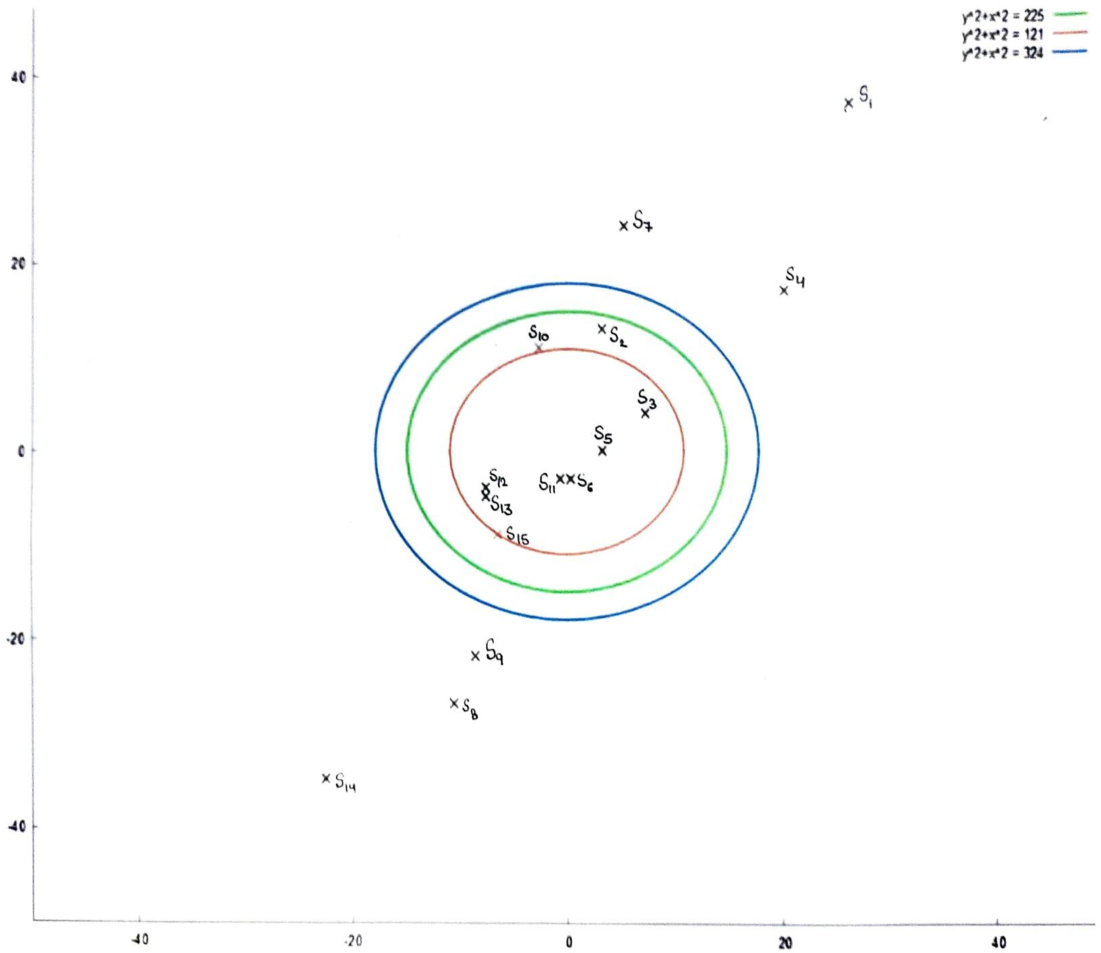

Figure 3.1: Plot of $(x_{S_i} - \mu_x)$ and $(y_{S_i} - \mu_y)$ data together with the circles representing equal EDs drawn in wxMaxima

3.2 Mahalanobis distance

For the simulated correlated data of $(x_{S_i} - \mu_x)$ and $(y_{S_i} - \mu_y)$ in Table 1, MD for each student is calculated by the formula,

$$MD = \sqrt{(A-\mu)\Sigma^{-1}(A-\mu)^T}.$$

Here,

$$\begin{aligned}
\Sigma &= \begin{bmatrix} \sigma_x^2 & \rho_{xy}\ \sigma_x\ \sigma_y \\ \rho_{xy}\ \sigma_x\ \sigma_y & \sigma_y^2 \end{bmatrix}, \\
\Sigma^{-1} &= \begin{bmatrix} \frac{\sigma_y^2}{|\Sigma|} & \frac{-\rho_{xy}\ \sigma_x\ \sigma_y}{|\Sigma|} \\ \frac{-\rho_{xy}\ \sigma_x\ \sigma_y}{|\Sigma|} & \frac{\sigma_x^2}{|\Sigma|} \end{bmatrix},
\end{aligned}$$

where $|\Sigma| = \sigma_x^2\ \sigma_y^2(1-\rho_{xy}^2)$ is the determinant of the Σ.
Now, by the formula

$$MD_{S_i}^2 = (A-\mu)\Sigma^{-1}(A-\mu)^T,$$

$$\begin{aligned}
MD_{S_i}^2 &= [x_{S_i} - \mu_x \quad y_{S_i} - \mu_y] \begin{bmatrix} \frac{\sigma_y^2}{\sigma_x^2\sigma_y^2(1-\rho_{xy}^2)} & \frac{-\rho_{xy}\sigma_x\sigma_y}{\sigma_x^2\sigma_y^2(1-\rho_{xy}^2)} \\ \frac{-\rho_{xy}\sigma_x\sigma_y}{\sigma_x^2\sigma_y^2(1-\rho_{xy}^2)} & \frac{\sigma_x^2}{\sigma_x^2\sigma_y^2(1-\rho_{xy}^2)} \end{bmatrix} \begin{bmatrix} x_{S_i} - \mu_x \\ y_{S_i} - \mu_y \end{bmatrix} \\
&= [x_{S_i} - \mu_x \quad y_{S_i} - \mu_y] \begin{bmatrix} \frac{1}{\sigma_x^2(1-\rho_{xy}^2)} & \frac{-\rho_{xy}}{\sigma_x\sigma_y(1-\rho_{xy}^2)} \\ \frac{-\rho_{xy}}{\sigma_x\sigma_y(1-\rho_{xy}^2)} & \frac{1}{\sigma_y^2(1-\rho_{xy}^2)} \end{bmatrix} \begin{bmatrix} x_{S_i} - \mu_x \\ y_{S_i} - \mu_y \end{bmatrix} \\
&= \left[\frac{x_{S_i} - \mu_x}{\sigma_x^2(1-\rho_{xy}^2)} - \frac{\rho_{xy}(y_{S_i} - \mu_y)}{\sigma_x\sigma_y(1-\rho_{xy}^2)} \quad \frac{y_{S_i} - \mu_y}{\sigma_y^2(1-\rho_{xy}^2)} - \frac{\rho_{xy}(x_{S_i} - \mu_x)}{\sigma_x\sigma_y(1-\rho_{xy}^2)}\right] \begin{bmatrix} x_{S_i} - \mu_x \\ y_{S_i} - \mu_y \end{bmatrix} \\
&= \left[\frac{(x_{S_i} - \mu_x)^2}{\sigma_x^2(1-\rho_{xy}^2)} - \frac{2\rho_{xy}(x_{S_i} - \mu_x)(y_{S_i} - \mu_y)^2}{\sigma_x\sigma_y(1-\rho_{xy}^2)} + \frac{(y_{S_i} - \mu_y)^2}{\sigma_y^2(1-\rho_{xy}^2)}\right] \\
&= \frac{(x_{S_i} - \mu_x)^2}{\sigma_x^2(1-\rho_{xy}^2)} - \frac{2\rho_{xy}(x_{S_i} - \mu_x)(y_{S_i} - \mu_y)^2}{\sigma_x\sigma_y(1-\rho_{xy}^2)} + \frac{(y_{S_i} - \mu_y)^2}{\sigma_y^2(1-\rho_{xy}^2)}.
\end{aligned}$$

This equation represents the equation of a translated and rotated ellipse[2]. After substituting the evaluated σ_x, σ_y and ρ_{xy} for the correlated data set in Table 1, the equation gets deduced to the following form,

$$MD_{S_i}^2 = 0.03125(x_{S_i} - \mu_x)^2 - 0.03533(x_{S_i} - \mu_x)(y_{S_i} - \mu_y) + 0.01272(y_{S_i} - \mu_y)^2. \tag{5}$$

The Figure 3.2 plots the simulated correlated data of $(x_{S_i} - \mu_x)$ and $(y_{S_i} - \mu_y)$.

[2] $A(x-h)^2 + B(x-h)(y-k) + C(y-k)^2 = 1$, where $A > 0$, $C > 0$ and $B^2 - 4AC < 0$.

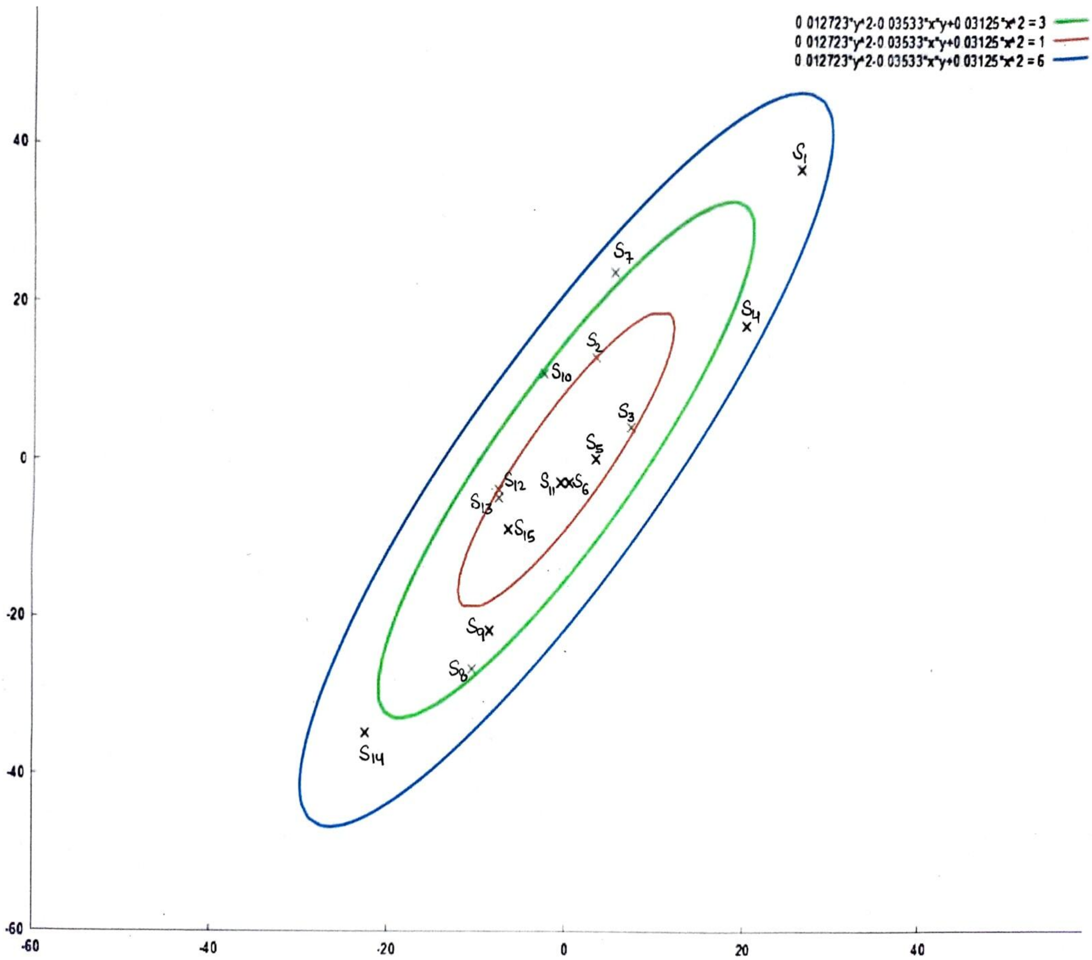

Figure 3.2: Plot of $(x_{S_i} - \mu_x)$ and $(y_{S_i} - \mu_y)$ data together with the ellipses representing equal MDs drawn in wxMaxima

Remark 3.1: If the simulated data is uncorrelated i.e., $\rho_{xy} = 0$, then by (5),

$$MD_{S_i}^2 = \left(\frac{x_{S_i} - \mu_x}{\sigma_x}\right)^2 + \left(\frac{y_{S_i} - \mu_y}{\sigma_y}\right)^2, \tag{6}$$

which is the $ED_{S_i}^2$ of normalized simulated data[**?**]. Hence,

$$MD_{S_i}^2 = ED_{S_i}^2.$$

Remark 3.2: For the simulated uncorrelated data in Table 3, ED_{S_i} and MD_{S_i} are almost same and hence the graphical representation of this data would be same.

4 Eigenvalues and Eigenvectors of Σ

For correlated data in Table 1,

$$\Sigma = \begin{bmatrix} 148.8286 & 192.8800 \\ 192.8800 & 365.5524 \end{bmatrix}.$$

To compute the eigenvalues of variance-covariance matrix, we need to compute $|\Sigma - \lambda I| = 0$
i.e., $\lambda^2 - 514.3810\lambda + 17201.9575 = 0$.
This implies, $\lambda_1 = 478.4257$ and $\lambda_2 = 35.9553$.
To compute the eigenvectors[3] corresponding to the eigenvalues λ_1 and λ_2, we need to find v_1 and v_2 such that $\Sigma v_1 = \lambda_1 v_1$ and $\Sigma v_2 = \lambda_2 v_2$ respectively. Therefore, eigenvectors corresponding to eigenvalues λ_1 and λ_2 are

$$\begin{bmatrix} 1 \\ 1.7088 \end{bmatrix} \text{ and } \begin{bmatrix} 1 \\ -0.5852 \end{bmatrix},$$

respectively.
The Figure 4 shows the $(x_{S_i} - \mu_x)$ and $(y_{S_i} - \mu_y)$ data together with the ellipses representing equal MDs and eigenvectors of variance-covariance matrix drawn in wxMaxima

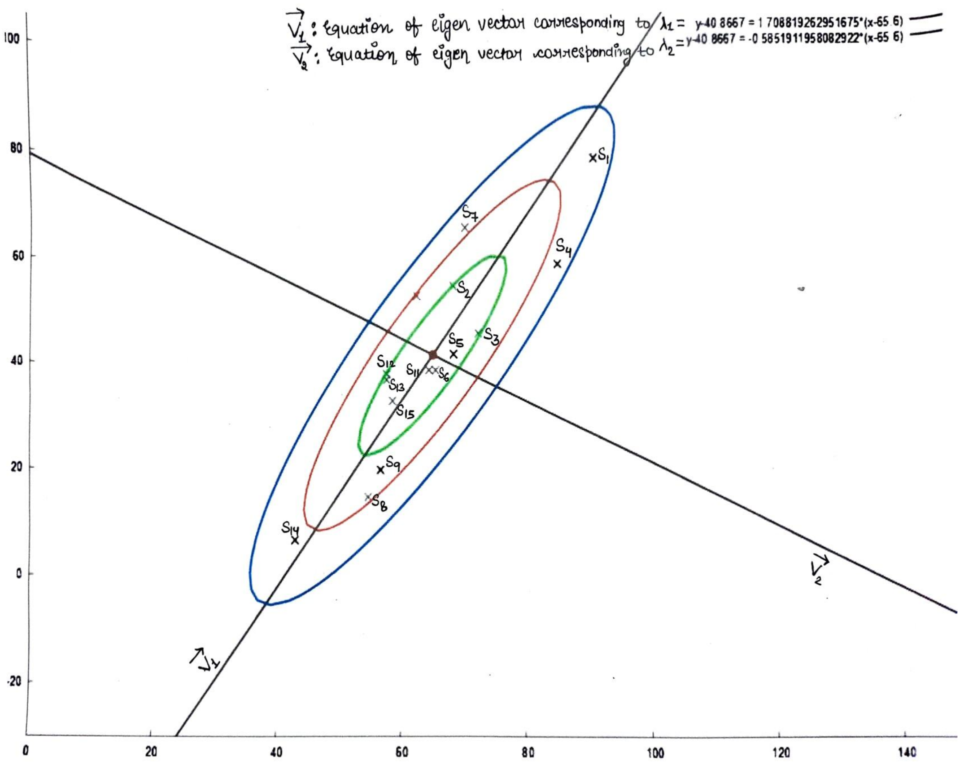

Figure 4: Plot of $(x_{S_i} - \mu_x)$ and $(y_{S_i} - \mu_y)$ data alongwith the ellipses and eigenvectors of variance-covariance matrix drawn in wxMaxima

[3]An eigenvector is a non-zero vector that satisfies the equation, $Av = v\lambda$, where A is a square matrix, v is a column matrix and λ is the eigenvalue corresponding to the given eigenvector.

From the Figure 4, it can be clearly seen that the eigenvectors of variance-covariance matrix coincides with the axes of the ellipses representing equal MDs.

5 Analytical interpretation of ED and MD

The MD of S_{10} and S_{15} in Table 2 from mean are 1.6766 and 0.5420 respectively while their ED from the mean are nearly equal i.e., 11.4329 and 11.0534 respectively. Since, S_{10} is lying in the direction where there is less correlation, the chance that a new measurement would be on that side of the plot, is lesser than when it would be in the position of S_{15}. The MD takes into account this probability due to correlation within two variables and attributes to S_{10}, a larger distance than to S_{15}, while the ED does not.

6 Applications of MD

Some of the fields of Applied Sciences where MD plays a significant role include Image Processing, Neurocomputing, Precision-medicine, Chemometrics, Pattern and Face recognition, etc. Precisely, any application that incorporates multivariate statistical analysis is bound to use MD for better results. The underlying idea behind all these applications is same i.e., the detection of multivariate outliers[2] which in simple terms is defined as the classification of a sample from the pool of references and detecting whether that sample belong to the references or not.
Outliers are those data that deviate from general behaviour of majority of data. In the field of multivariate statistics, MD finds major applications for detection of outliers. A few outliers are always enough to distort the results of the data by altering the performance of mean. Therefore, it is a growing concern in several scientific domains. A general understanding of the same is provided below with its graphical interpretation.

6.1 Multivariate outlier detection

To detect multivariate outliers, two points are considered say, $A(90.6, 65.8667)$ and $B(90.6, 15.8667)$. We shall call point A as the test point A and point B as the test point B. To detect the outlier, we shall use correlated data set given in Table 1. Let $C(\mu_x, \mu_y)$ be $C(65.6, 40.8667)$.
The $ED_{(A,C)}$ between the test point A and C is 35.3553 and $ED_{(B,C)}$ between the test point B and C is 35.3553. The $MD_{(A,C)}$ between the test point A and C is 2.1618 and the $MD_{(B,C)}$ between the test point B and C is 5.7188. Note that, $ED_{(A,C)} = ED_{(B,C)} = 35.3553$. This implies that both the test points are at equal distance from C but $MD_{(A,C)} \neq MD_{(B,C)}$ i.e., while computing distance through MD measure, $MD_{(A,C)}$ is less than $MD_{(B,C)}$. This implies that the test point A is closer to the distribution than B, implying B to be an outlier.
From the Figure 6.1, which illustrates the plot of $(x_{S_i} - \mu_x, y_{S_i} - \mu_y)$ of the correlated data [see Table 1], it can be verified that the distance between the distribution and the test point A is not equal to that of the distance between the distribution and the test point B which implies that the test point B must be an outlier. Here, the Mahalanobis distance is taking into account the correlation of the data set of interest whereas ED does not.

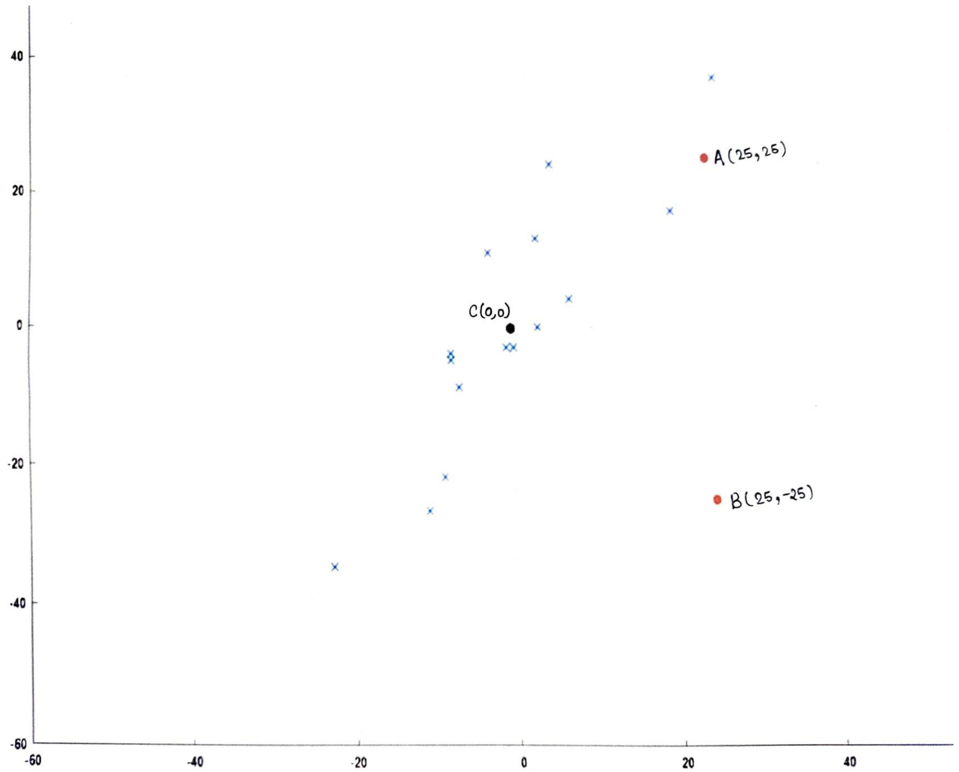

Figure 6.1: Plot of $(x_{S_i} - \mu_x)$ and $(y_{S_i} - \mu_y)$ data, mean and centered-test points drawn in wxMaxima

7 Conclusion

In this paper, the Mahalanobis distance as a multivariate distance and it's advantages relative to the Euclidean distance were reviewed. The paper has made it clear that when dealing with correlated multivariate data, the Mahalanobis distance is more suitable than the Euclidean distance because it takes the correlation into account and in case of uncorrelated variables, MD reduces to the formula of familiar ED with unit variance. Moreover, it has been shown how MD is used as a tool for detecting multivariate outliers and is the multivariate analogue of the univariate distance measured in standard deviations which provide a way of measuring distances that takes into account the scale of the data.

References

[1] Mahalanobis P. C., *On the Generalized Distance in Statistics*, National Institute of Sciences of India, Volume 2, 1936, pp. 49-55.

[2] Maesschalck R. D., Rimbaud D. J., Massart D. L., *The Mahalanobis distance*, Chemometrics and Intelligent Laboratory Systems, Volume 50, Issue 1, 2000, pp. 2-8.

[3] Sharma A.,*analyticsindiamag*, July 10, 2018,
https://analyticsindiamag.com/understanding-mahalanobis-distance-and-its-use-cases/

[4] J J O'Connor and E F Robertson, *MacTutor*,
https://mathshistory.st-andrews.ac.uk/Biographies/Mahalanobis/

[5] J. J. O'Connor and E. F. Robertson, *MacTutor*,
https://mathshistory.st-andrews.ac.uk/Biographies/Ramanujan/

[6] J. J. O'Connor and E. F. Robertson, *Poetry Foundation*,
https://www.poetryfoundation.org/poets/rabindranath-tagore

[7] Wicklin R., *sas*, February 15, 2012,
https://blogs.sas.com/content/iml/2012/02/15/what-is-mahalanobis-distance.html

(Mentor) Dr. Monika Singh, Associate Professor, Department of Mathematics, Lady Shri Ram College for Women, New Delhi
monikasingh@lsr.du.ac.in

Akshi Sharma, B.Sc.(H) Mathematics, 4th Semester, Lady Shri Ram College for Women, New Delhi
akshisharma.maths2021@gmail.com

Jigyasa Srivastava, B.Sc.(H) Mathematics, 4th Semester, Lady Shri Ram College for Women, New Delhi
jigyasasrivastava.maths2021@gmail.com

Éclat, A Mathematics Journal
Volume 14, 2022-23 (48-54)

Modelling Abstainers as Threats to Elections

Bhavneet Kaur, Hritika Meena and Sanskriti Sharma

Abstract

Through the course of this paper, we have tried to quantify the subjective nature of forces that act towards moulding and influencing the electoral process of democracy in unwanted ways. Such a study can potentially cater to the eradication of unsuspected stumbling blocks that sway a democracy away from a fundamental feature, that is, elections. This is also an attempt to highlight the significance of mathematics in analyzing an otherwise politically oriented subject. Psephologists might benefit from this attempt.

Keywords: Abstainers, Equilibrium, Stability Analysis, Feasible Region, Jacobian

1 Historical Background

Historically, the cultures of the Ancient Near East and the Ancient Greek have been credited with employing modelling as a method of abstract representations as done in cave paintings with counting and "writing" numbers (e.g., as marks on bones) being the first recognizable models, documented in about 3000 B.C. Astronomy and Architecture were other significant areas where models played a role. By 2000 B.C. the Babylonian, Egyptian and Indian cultures were substantially versed with mathematics and utilized mathematical models to improve their daily life. India, China and Islamic countries like Persia developed methods similar to modelling, keeping in mind the importance of mathematical models in solving real world problems.
A prominent mathematician of late eighteenth century Abu Abd-Allah had modelled numerous real-life problems related to commerce, legacy, surveying and irrigation in his famous book *de numero Indorum*. Algorithms like the Runge-Kutta method or the Fast Fourier Transform paved way for augmenting compatible computer models. The advancements in technology, storage capacity and efficiency in computers have made optimization modelling very attractive and demanding [4].

2 Introduction

The present paper is an application of the epidemiological model or SIR model which models the populations of susceptible, infected and recovered population. Here, the narrative shifts to the population in an arbitrary democratic state comprising of three classes of population that interact, intervene and influence the existence of one another in an electoral system which is expected to be free and fair.
These populations are that of **Potential electors, Abstainers and Registered Voters.** The

rising political turmoil around the globe and instability of regimes is also a result of unstable and fragile electoral systems. While people in democracies have been given the right to vote and elect their representatives, it is an alarming call of the present day and times that abstinence on part of a cluster of population that is all powerful to influence the democratical structure and framework of the electoral system of a nation has the potential of influencing the potential voters, thus, leading to cracks and crevices in the basic democratic structure of institutions. Hence, with this paper, we have tried to present forth an attempt at gauging and analysing the prospective depths and lengths of the influence of abstainers on the entire population of potential voters and we have also tried to project the differences that are likely to prevail in case of absence of abstaining behaviour [1].

3 Definitions

Potential Electors: The portion of the population which is eligible to cast a vote but are not yet registered on the electoral list.
Abstainers: The segment of the population which is not willing to take part in the democratic elections of the nation and moreover is able to influence potential electors to abstain from taking part in the democratic electoral processes.
Registered Voters: People who are eligible to vote and are registered on the electoral lists.

The following table explains the notations that have been invoked throughout the paper.

$\mathbf{P(t)}$	Number of potential voters at a time t
$\mathbf{A(t)}$	Number of abstainers at a time t
$\mathbf{R(t)}$	Number of registered voters at a time t
Λ	Rate at which the number of individuals increase in the class of potential voters
β	Rate at which the potential voters acquire abstaining behavior due to negative influence of abstainers
μ	Rate of natural death of potential voters, abstainers, registered voters
γ	Rate at which abstainers cease to boycott elections and join the class of registered voters.
α	Rate at which potential electors get themselves registered and join the class of registered voters.

Table 3.1: Notations that have been used throughout the paper.

The system of non-linear differential equations which governs the dynamics of the model is given by:

$$\frac{dP}{dt} = \Lambda - \beta\frac{AP}{N} - (\alpha + \mu)P$$

$$\frac{dA}{dt} = \beta\frac{AP}{N} - (\gamma + \mu)A$$

$$\frac{dR}{dt} = \alpha P + \gamma A - \mu R, \tag{1}$$

where $P(0) \geq 0, A(0) \geq 0$ and $R(0) \geq 0$ are the given initial states.

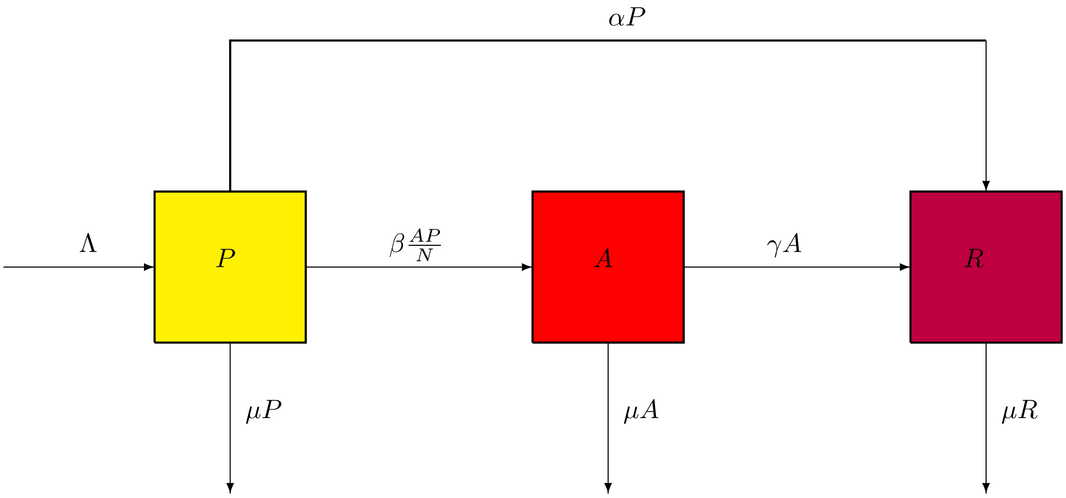

Figure 3.1: Compartmental Diagram

3.1 Stability Analysis and Sensitivity of the Model Parameters

In this section, we will compute the non-abstaining equilibrium point of the system of the non-linear differential equations.

3.1.1 Abstaining-free equilibrium point : To calculate abstaining-free equilibrium point, we solve the system of equation. Hence the abstaining free-equilibrium point is given by,

$$E^0 = \left(\frac{\Lambda}{(\alpha + \mu)}, 0, \frac{\alpha\Lambda}{\mu(\alpha + \mu)}\right).$$

Reproduction Number : Since this model follows from the epidemiological model, we shall retain the meaning of $\mathcal{R}$ as used there. $\mathcal{R}$ gives the average number of secondary infections as induced by an infected person in an absolutely susceptible population. Similarly, in this model of tracing abstaining behaviour, $\mathcal{R}$ gives the average number of abstainers as influenced by the existing abstainers while they interact with the population of potential electors. We obtain $\mathcal{R}$ by employing the method of next-generation [2].

Step 1: Let $x = (A, R, P)$, then System (1) can be re-written as:

$$\frac{dx}{dt} = \mathcal{F}(\S) - \mathcal{G}(\S),$$

where,

$$\mathcal{F}(\S) \quad = \quad \begin{pmatrix} \frac{\beta PA}{N} \\ 0 \\ 0 \end{pmatrix},$$

$$\mathcal{G}(\S) \quad = \quad \begin{pmatrix} (\gamma + \mu)A \\ -\alpha P - \gamma A + \mu R \\ -\Lambda + \frac{\beta AP}{N} + (\alpha + \mu + P) \end{pmatrix}.$$

Step 2: We shall now compute the Jacobian matrices of $\mathcal{F}(\S)$ & $\mathcal{G}(\S)$ at the abstaining free equilibrium point E^0.

$$J\mathcal{F}(E^0) \quad = \quad \begin{pmatrix} \frac{\mu\beta}{\alpha+\mu} & 0 & 0 \\ 0 & 0 & 0 \\ 0 & 0 & 0 \end{pmatrix},$$

$$J\mathcal{G}(E^0) \quad = \quad \begin{pmatrix} \gamma + \mu & 0 & 0 \\ -\gamma & \mu & -\alpha \\ \frac{\mu\beta}{\alpha+\mu} & 0 & 0 \end{pmatrix}.$$

3.1.2 Local Stability Analysis : In this section, we aim at determining the local stability of the abstaining-free equilibrium. We shall perform this by employing the method of *Eigenvalues stability Analysis*.

Step 1: Let

$$\begin{aligned} \frac{dP}{dt} &= \Lambda - \beta\frac{AP}{N} - (\alpha + \mu)P &= f(P, A, R), \\ \frac{dA}{dt} &= \beta\frac{AP}{N} - (\gamma + \mu)A &= g(P, A, R), \\ \frac{dR}{dt} &= \alpha P + \gamma A - \mu R &= h(P, A, R). \end{aligned}$$

Step 2: We need to construct a Jacobian matrix of partial differentials of f, g, h with respect to P, A and R.

$$J(P, A, R) \quad = \quad \frac{\partial(f,g,h)}{\partial(P,A,R)} \quad = \quad \begin{pmatrix} \frac{\partial f}{\partial P} & \frac{\partial f}{\partial A} & \frac{\partial f}{\partial R} \\ \\ \frac{\partial g}{\partial P} & \frac{\partial g}{\partial A} & \frac{\partial g}{\partial R} \\ \\ \frac{\partial h}{\partial P} & \frac{\partial h}{\partial A} & \frac{\partial h}{\partial R} \end{pmatrix},$$

Substituting the values of partial differentials $f_P, f_A, f_R, g_P, g_A, g_R, h_P, h_A, h_R$ in the above matrix, we get:

$$J(P, A, R) \quad = \quad \begin{pmatrix} -(\alpha+\mu) & \frac{\mu\beta}{\alpha+\mu} & 0 \\ 0 & \frac{\mu\beta}{\alpha+\mu} - (\gamma+\mu) & 0 \\ \alpha & \gamma & -\mu \end{pmatrix}$$

Hence, this equilibrium is attained when there is no prevalence of abstainers in the population. Now

$$J - KI = \begin{bmatrix} -(\alpha+\mu+K) & -\frac{\mu\beta}{(\alpha+\mu)} & 0 \\ \\ 0 & \frac{\mu\beta}{(\alpha+\mu)} - (\gamma+\mu) - K & 0 \\ \\ \alpha & \gamma & -(\mu+K) \end{bmatrix},$$

where K is the eigenvalue.
Now, to evaluate K, we need to solve $|(J - KI)| = 0$.

$$|(J - KI)| = (\mu+K)(\alpha+\mu+K)\left(-\frac{\mu\beta}{\alpha+\mu} + (\gamma+\mu+K)\right)$$

On solving $|(J - KI)| = 0$ we get the following three values of K :

$$\begin{aligned} K_1 &= -\mu, \\ K_2 &= -(\alpha+\mu), \\ K_3 &= (\gamma+\mu)(R_0 - 1). \end{aligned}$$

Clearly, all eigenvalues of the characteristic equation will be negative if $R_0 < 1$. Hence, the equilibrium point E^0 is locally asymptotically stable when $R_0 < 1$ and unstable if $R_0 > 1$.

Lemma 1. *The feasible region ψ is defined by :*

$$\psi = \{(P(t), A(t), R(t)) \in \mathbb{R}^3_+, P(t) + A(t) + R(t) \leq \frac{\Lambda}{\mu}\}$$

3.1.3 Global Stability Analysis : Now, we will discuss the global asymptotic stability of abstaining-free equilibrium E^0.

Theorem 2. *If $R_0 \leq 1$, then the free equilibrium E^0 of system of differential equation is globally asymptotically stable on ψ.*

Proof. To prove the global stability of the free equilibrium E^0, we construct the following Lyapunov function (which is a positive definite function) $V : \psi \to R$,

$$V(P,A) = \frac{1}{2}((P - P^0) + A)^2 + \frac{(\alpha + \gamma + 2\mu)N}{\beta} A.$$

Then, the derivative of V with respect to time is given by,

$$\begin{aligned} \frac{dV}{dt}(P,A) &= (P - P^0 + A)(\Lambda - (\alpha+\mu)P - (\gamma+\mu)A) + \frac{(\alpha+\gamma+2\mu)N}{\beta}\frac{dA}{dt} \\ &= -(\alpha+\mu)(P-P^0)^2 - (\gamma+\mu)A^2 - (\alpha+\gamma+2\mu).\frac{(\gamma+\mu)N}{\beta}(1-R_0)A. \end{aligned}$$

Thus, $\frac{dV}{dt}(P,A) \leq 0$ for $R_0 \leq 1$.

Further, if $R \leq 1$, then $\frac{dV}{dt}(P,A) = 0 \Leftrightarrow P = P^0$ and $A = 0$.
Hence, by LaSalle's invariance principle [3], we get the free equilibrium point E^0 is globally asymptotically stable on ψ. □

4 Conclusion

While abstinence on part of a group of voters in democratic electoral systems is a majorly political and sociological phenomenon/practice, this paper sheds light on the potential and prospect of optimal utilisation of mathematics in solving this pervasive real world problem. Unlike the other popular multidisciplinary applications of mathematical modelling (lake pollution modelling, seismology, biomathematics, etc.), application of modelling in political and sociological phenomena (as the one talked about in this paper) is yet to gather mass attention and requires contributions in the form of academic research to be able to get highlighted. This review research paper is an effort in this direction. Methods employed here are those already in common use among scholars of mathematics.

Exploiting Jacobian matrices and characteristic equations has helped in the analysis of local stability points of the system while a Lyapunov function has been used in computation and analysis of the global stability of the model. Thereupon, these stability analyses aided in dealing with the troublesome possibility of a hike in abstinence behaviour during elections.

Wider and deeper academic work on and around this sort of application of mathematical modelling can pave the path towards popularisation of the application of mathematical methods in solving problems of the society, the people.

References

[1] Balatif O. , Khajji B. and Rachik M, *Mathematical Modeling, Analysis, and Optimal Control of Abstinence Behavior of Registration on the Electoral Lists.*

[2] Driessche P. V. and Watmough J., *Reproduction Numbers and Sub-threshold Endemic Equilibria for Compartmental Models of Disease Transmission*, Mathematical Biosciences, Volume 180, 2002 , pp. 29–48.

[3] LaSalle J. P., *The Stability of Dynamical Systems*, Regional Conference Series in Applied Mathematics, Volume 25, 1976.

[4] Schichl H., *Models and History of Modelling*

(Mentor) Dr. Bhavneet Kaur, Associate Professor, Department of Mathematics, Lady Shri Ram College for Women, New Delhi
bhavneetkaurbakshi@lsr.du.ac.in

Hritika Meena, B.Sc.(H) Mathematics, 4th Semester, Lady Shri Ram College for Women, New Delhi
hritikameena.maths2021@gmail.com

Sanskriti Sharma, B.Sc.(H) Mathematics, 4th Semester, Lady Shri Ram College for Women, New Delhi
sanskritisharma.maths2021@gmail.com

Éclat, A Mathematics Journal
Volume 14, 2022-23 (55-65)

An Application of Artificial Bee Colony Optimization in Feature Selection

Yograj Singh, Sonia Raj Saxena and Vartika Bhardwaj

Abstract

Feature Selection is the method of minimising the input variable to your model by using only necessary data and discarding the excess one. This paper gives an in-depth description of an application of Artificial Bee Colony Optimization which is a nature inspired algorithm in solving feature selection problems. A comparative analysis would be further conducted to investigate the performance based on various iterations. We aim to implement feature selection problem using sphere function in MATLAB and examine the results.

Keywords: Nature Inspired Algorithms, Sphere Function, Artificial Bee Colony Optimization, Feature Selection Problems, Greedy Selection, Foraging Behaviour

1 Introduction

Machine Learning is a procedure of analysing data and initiating the construction of a model. Systems can thus take insights from data and make decisions with little human interruption. But while developing the model only few set of variables in whole dataset are applicable and remaining are irrelevant. *"Feature selection is a way of selecting the subset of the most relevant features from the original features set by removing the redundant, irrelevant, or noisy features"* [5]. In today's era when everyone is expecting faster results it has become very crucial to choose most appropriate features and washing out the less important ones which is done using feature selection in machine learning. It minimises the training time and helps in the rephasement of the model. Nature Inspired Algorithms are very efficient in looking for optimised solutions to multi-modal problems. Artificial Bee Colony (ABC) Algorithm can be effectively used in solving feature selection problems since it has strong robustness, greater convergence and high flexibility. This method can be successfully used for solving complex problems. In the sections discussed below the basic concepts of some of the important terms have been described, followed by the detailed explanation of ABC Algorithm and its application and implementation in MATLAB.

2 Prerequisites

2.1 Nature Inspired Algorithms

Nature-inspired algorithms are a collection of problem solving strategies derived from natural processes. In the last decade a latest version of nature inspired optimization algorithms has emerged.

After swarm models, scientists focused their research on natural phenomenons which has given rise to a new category of equally effective algorithms as compared to genetic algorithms and swarm schemes. These algorithms could be used in different problem areas using possible approaches. The ability to adapt the ever changing environment makes it a hub for solving complex problems.
Nature Inspired Optimization Algorithms are meta-heuristic which imitate the behaviour of naturally occurring species, like ants, bees, flies, bats, termites etc., and provide suitable ways for solving many complex optimization problems [3].

2.2 Food Sources

They serve as a metaphor for the solutions to the issues or the problems at hand. The amount of nectar produced by each food source depends on how well the challenge is solved [1].

2.3 Employed Bees

In the vicinity of the old food supply, employed bees look for new food sources that contain more nectar than the old ones. Despite being random, this search makes use of information already known from other food sources [1].

2.4 Onlooker Bees

They pick up the locations of the food sources by observing the employed bees' waggle dance. In reality, this is accomplished by employing a Roulette Wheel Selection Algorithm, which selects food sites with a higher chance if they have more nectar [1].

2.5 Scout Bees

Over a predetermined number of trails, scout bees randomly select their food sources to replace those that have been abandoned or are unusable [1].

2.6 Waggle Dance

Bees communicate to their hive mates the location of the food sources by performing the bee dance, often known as the "waggle dance" which they use to navigate [1].

2.7 Foraging Behaviour

The most important feature of the honey swarm is foraging behaviour. In this process, bee leaves the hive and starts looking for food. When a bee gets a food source, she withdraws the nectar till $30 - 120$ minutes based on richness, distance of food source from hive and stores it in her stomach. Then with enzymes secretion, honey making process starts and she excretes nectar in empty cells after reaching hive. Then, she allocates her information with other bees in the form of various types of dance [1].

3 Sphere Function

There are several test functions that are frequently used in the literature, one of the widely used out of them is the sphere function. These test functions, often known as fake landscapes, are helpful in applied mathematics for evaluating how well an algorithm performs or how well a suggested algorithmic adjustment performs.

Sphere function displays a single objective function, making it appropriate for single-objective optimization. Hence, the traditional methods of optimization are substantially faster at solving this function. The sphere function is however uni-modal. This indicates that it has a single global optimum and exhibits a single "mode". It also shows convex behaviour and is a continuous function. The range of the function is usually from $[-5.12, 5.12]$.

Sphere function is depicted as given below:

$$f(\mathbf{x}) = \sum_{i=1}^{D} {x_i}^2$$

Here D is the dimension of the sphere function. The sphere function has the same number of local minima as the dimension and a global one too. However the global minima occurs at $(0, 0, 0, \ldots, \text{upto}\, D)$ i.e., $f(0, 0, 0, \ldots) = 0$ [4].

Figure 3.1 is the maxima plot of two dimensional sphere function.

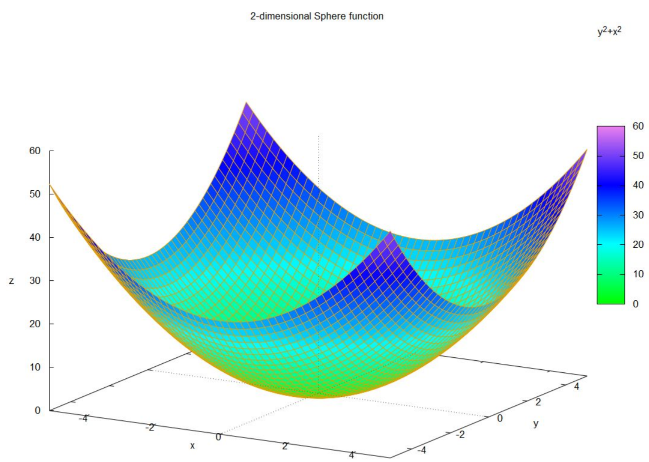

Figure 3.1: Sphere Function plotted on Maxima

4 Artificial Bee Colony Optimization

The Artificial Bee Colony (ABC) method, an optimization method that replicates honey bee foraging behaviour, has been effectively used to solve a number of real-world issues. The swarm intelligence algorithms include ABC, which was developed by Karaboga in 2005 [8]. Since bees live in a colony, we label the optimization problem as the problem of finding the best food sources. The ABC algorithm mainly requires the given five components that are food sources, employed bees, onlooker bees, scout bees and the waggle dance. All of these are thus effectively utilised for the working of the method [7].
The whole process can thus be evaluated in the form of the given phases:

- *Initialisation Phase*
  During the initialization phase, enough amount of food sources for every employed bee are generated. Depending on the kind of issue we are attempting to solve, different food sources will be produced. The randomly generated bees are dispersed throughout the solution space. It may be more effective for some solution spaces if researchers distribute them evenly throughout the area.

- *Employed Bee Phase*
  In the employed bees phase, each bee ventures outside to look for a food source. The procedure involves the bees scouting the area for food sources, and if they discover one with more nectar, their current food source is substituted by the newer, superior one.

- *Onlooker Bee Phase*
  When the employed bees return home, they begin their waggle dance. With a little error, each onlooker bee estimates how much nectar each bee drank from its source. Consequently, each onlooker bee will choose the food source according to its estimation of the nectar it produces. The likelihood that an onlooker bee will gather up nectar increases with its elevation. One way to think of the onlooker bees is as extra explorers around the most promising food sources. They essentially do the same tasks as the bees in use, except they are focused closer to potential food sources. Therefore, the onlooker bee phase helps the quick development of the best food sources while the employed bees ensure that we do not give up on solutions too soon. We can converge more quickly and keep our options open if we do it this way.

- *Scout Bee Phase*
  In the scout bee phase, the food source's neighbourhood is abandoned once it has been sufficiently investigated. We increase the trial counter each time a food supply is investigated. In order to replace it with a new, random food source, we remove it from the array of food sources when the trial count surpasses the maximum specified number. Just like during the initialization phase, the scouts just identify a random food source; they do not need to confirm that it is superior to the old food source or that it is nearby. To avoid being trapped in local minima, think of the scouting phase as adding fresh regions to investigate [7].

4.1 Steps of Artificial Bee Colony Optimization

1. *Initialization Phase*
   Every vector of the population of food sources, $\overrightarrow{x_m}|$'s, are commenced ($m = 1 \ldots ; SN|\underline{SN}$) population size by scout bees and control parameters are set. Since each food source, ($\overrightarrow{x_m}|$) is a solution vector to the optimization problem, each $\overrightarrow{x_m}|$ vector holds n variables, ($x_{mi}, i = 1 \ldots n|$) , which are to be optimized so as to get the minimum value of the objective function. The following definition might be used for initialization purposes:

   $$x_{mi} = l_i + rand(0, 1) * (u_i - l_i)$$

   where $l_i|$ and $u_i|$ are the lower and upper bound of the parameter $x_{mi}|$, respectively.

2. *Employed Bees Phase*

   - Generate a new solution
     $X_{new} = X + \phi(X - X_p)$
     $\phi \in [-1, 1]$
   - Calculate fitness value using formula given below:

   $$fit_m(\overrightarrow{x_m}) = \left\{ \begin{array}{cc} \frac{1}{1+f_m(\overrightarrow{x_m})} & \text{if } f_m(\overrightarrow{x_m}) \geq 0 \\ 1 + |f_m(\overrightarrow{x_m})| & \text{if } f_m(\overrightarrow{x_m}) < 0 \end{array} \right\}$$

   - Apply greedy selection
     (accept new solution if it is better)
     $f_{new} < f_{old}$

3. *Onlooker Bee Phase*

   - Calculate probabilities

   $$p_m = \frac{fit_m(\overrightarrow{x_m})}{\sum_{m=1}^{SN} fit_m(\overrightarrow{x_m})}$$

   - Select the random number (r)
     If $r <$ probability
     Then new solution is generated with the help of partner solution X_p given by
     $X_{new} = X + \phi(X - X_p)$
     $\phi \in [-1, 1]$
   - Calculate new fitness using the above fitness formula and apply greedy selection

4. Memorize the best solution

5. Scout Bee Phase

   - Find the abandoned solution (based on the value of limit)

- Generate a new solution randomly to replace them

  The ABC algorithm foretells that employed bees with poorly improving solutions are likely to become scouts and their solutions will therefore be abandoned. Users specify the limit of trials, or “abandonment criteria”, and it is followed by the ABC algorithm. As a result, the converted scouts start looking for new solutions at random. For instance, if solution $\overrightarrow{x_m}$ has been abandoned, the revised solution discovered by the scout who was the employed bee of $\overrightarrow{x_m}$ can be defined by Initialization phase [8].

5 Description

The aim of this paper is to implement Artificial Bee Colony Algorithm in MATLAB. In our paper we have taken the most widely used sphere function to solve the feature selection problems. Feature selection is basically about understanding the necessity for any approach before putting it into practise. In order to lessen overfitting in the model, it is a technique for decreasing the input variable for the framework by selecting only pertinent data. The dataset is used to choose features by either including the crucial features or removing the superfluous features, without altering the dataset's original features [2]. In order to achieve better results with machine learning, a high-quality input dataset that has been pre-processed is required. To hone our model and aid in its learning, we gather a vast amount of data. The dataset typically includes some corrupt, unnecessary and valuable data. However, the model performs better when the best characteristics are chosen. It is simpler to select the proper statistical measure for feature selection the more we are familiar with the datatypes of variables.

Numerous studies have previously been conducted to find the most effective techniques in the extremely complex and wide topic of feature selection in machine learning. Feature selection is not only a variable shrinkage process and target is not just to perform arbitrary cardinality reduction for a data set, rather it searches for optimum subset of features. The main target of Feature Selection problem is to find trade offs between various conflicting objectives. The optimal feature selection approach has no set rules. The optimum strategy for a given problem will be determined by a machine learning specialist who can mix and develop different approaches.

For fundamental analysis of feature selection problem in our paper, we have considered maximum iterations as 100 and taken initial trial to be zeros and applied ABC algorithm in MATLAB.

5.1 Implementation of ABC in MATLAB

Some initial assumptions are made to implement ABC code in MATLAB. We considered 100 iterations and two dimensional sphere function with its well known lower and upper bound. Following is the Artificial Bee Colony Algorithm code in MATLAB [6]:

```
format short;
clear all;
clc;

FoodSource=100;
D=2;
lb=[-5.12 5.12];
ub=[5.12 5.12];
max_iter=100;
N=FoodSource./2;
limit=(N.*D);
trial=zeros(N,1);

for i=1:N
for j = 1:D
pos(i,j) = lb(:,j) + rand.*(ub(:,j)-lb(:,j));
end
end
fx = fns1(pos);
fx1 = fns(pos);

for iter = 1:max_iter
for i=1:N
Xnew = pos(i,:);
p2c = ceil(rand*D);
partner = ceil(rand*N);
while(partner==i)
partner=ceil(rand*N);
end
X = pos(i,p2c);
Xp = pos(partner,p2c);
Xnew(p2c) = X + (rand-0.5).*2.*(X-Xp);

for j = 1:D
if Xnew(j)>ub(j)
Xnew(j) = ub(j);
elseif Xnew(j)<lb(j)
Xnew(j) = lb(j);
end
end

fnew = fns1(Xnew);
if fnew < fx(i,:)
pos(i,:) = Xnew;
fx(i, :) = fnew;
trial(i) =0;
else
trial(i)=trial(i) +1;
end
end

prob = fx./sum(fx);
for i=1:N
if(rand<prob(i))
```

```
Xnew = pos(i,:);
p2c = ceil(rand*D);
partner = ceil(rand*N);
while(partner==i)
partner=ceil(rand*N);
end
X = pos(i,p2c);
Xp = pos(partner,p2c);

Xnew(p2c) = X + (rand-0.5).*2.*(X-Xp);
end

for j = 1:D
if Xnew(j)>ub(j)
Xnew(j) = ub(j);
elseif Xnew(j)<lb(j)
Xnew(j) = lb(j);
end
end

fnew = fns1(Xnew);
if fnew < fx(i,:)
pos(i,:) = Xnew;
fx(i, :) = fnew;
trial(i) =0;
else
trial(i)=trial(i) +1;
end
end

[fxval, fxind] = min(fx);
Gbest = pos(fxind,:);
Xbest(iter,:) = Gbest;
Fbest(iter) = fxval;
Fbest1(iter)= fns1(Gbest);

H= find(trial>limit);
if length(H)>0

for j = 1:D
pos(H,j) = lb(:,j) + rand.*(ub(:,j) - lb(:,j));
end
fx(H,:)=fns1(pos(H,:));
end
plot(Fbest,'r','LineWidth',2);
xlabel('Iteration');
ylabel('Fitness Value');
grid on;
end
```

```
#fns file

function out =fns(X)
x1 = X(:,1);
x2 = X(:,2);
fx = x1.^2+x2.^2;

for i=1:size(fx,1)
if fx(i,:)>=0
fit(i,:) = 1./(1+fx(i,:));
elseif fx(i,:)<0
fit(i,:) = 1+abs(fx(i,:));
end

end

out = fit;

#fns1 file

function out = fns1(X)
x1 = X(:,1);
x2 = X(:,2);

out = x1.^2+x2.^2;
end
```

Figure 5.1: ABC Algorithm in MATLAB

Figure 5.2 is the Fitness Value vs Iterations plot which indicates the convergence point for sphere function in ABC algorithm.

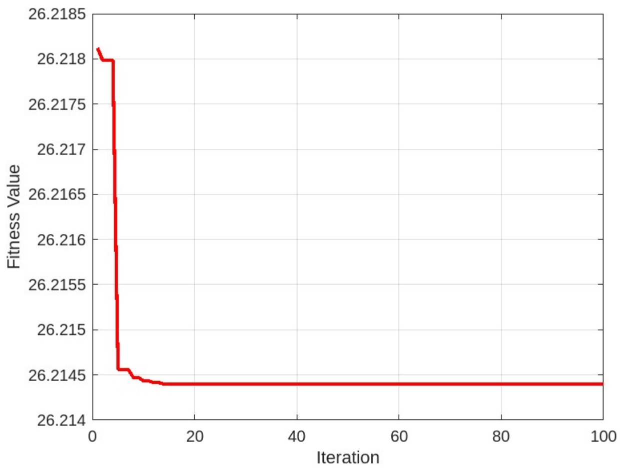

Figure 5.2: Fitness Value vs Iterations drawn in MATLAB

Convergence point in Artificial Bee Colony Optimization is comparatively achieved faster than other nature inspired algorithms.

6 Conclusion

Major developments have taken place in the field of nature inspired algorithms. Among various methods developed in this regard we have taken Artificial Bee Colony Optimization into consideration due to its faster convergence rate and foraging behaviour of honey bees.

This refined proposal was implemented in MATLAB using minimum codes with bare complexity and runtime as low as possible. After a series of phases of ABC we got 26.2181 as the point of convergence of two dimensional sphere function that can be utilised for solving feature selection problems.

References

[1] Andrushia A.D. and Patricia A.T, *Nature Inspired Optimization Techniques for Image Processing Applications*, Volume 150, Springer, 2018, pp. 223 − 231.

[2] Cai J., Luo J., Wang S. and Yang S., *Neurocomputing*, Volume 300, Elsevier, 2018, pp. 70 − 794.

[3] Khurma R.A., Aljarah I., Sharieh A., Elaziz M.A., Damasevicius R. and Krilavičius T., *A Review of the Modification Strategies of the Nature Inspired Algorithms for Feature Selection Problem*, Volume 10, 2022, pp. 7 − 9.

[4] Molga M. and Smutnicki C., Test functions for optimization needs, April 3, 2005, pp. 1 − 3.

[5] Brownieee J., How to Choose a Feature Selection Method For Machine Learning, *Machine Learning Mastery*, November 27, 2019, https://machinelearningmastery.com/feature-selection-with-real-and-categorical-data/.

[6] Yarpiz, Artificial Bee Colony (ABC) in MATLAB, Version 1.0.0.0, *Mathworks*, December 26, 2022, https://in.mathworks.com/matlabcentral/fileexchange/52966-artificial-bee-colony-abc-in-matlab.

[7] Ram N., Implementing Artificial Bee Colony Algorithm to Solve Business Problems, *Towards Data Science-Medium*, March 5, 2022, https://towardsdatascience.com/implementing-artificial-bee-colony-algorithm-to-solve-business-problems-cb754f3b925.

[8] Karaboga D., Artificial Bee Colony algorithm, *Wikipedia*, 2010, https://en.wikipedia.org/wiki/Artificialbeecolonyalgorithm.

(Mentor) Yograj Singh, Assistant Professor, Department of Mathematics, Lady Shri Ram College for Women, New Delhi
yograjchauhan26@gmail.com

Sonia Raj Saxena, B.Sc.(H) Mathematics, 6th Semester, Lady Shri Ram College for Women, New Delhi
sr4113882@gmail.com

Vartika Bhardwaj, B.Sc.(H) Mathematics, 6th Semester, Lady Shri Ram College for Women, New Delhi
vartikabhardwajmath@gmail.com

Éclat, A Mathematics Journal
Volume 14, 2022-23 (66-73)

Application of Group Theory in Molecular Biological System

Sunil Kumar Yadav, Divya Kesarwani and Mansi

Abstract

Biology is mostly expressed in terms of protein, carbohydrates and other chemicals. In this paper we investigate that biology can also be expressed mathematically, especially in cell cycle and binucleated cells. Here by using the symmetry of a square and with the help of cell experiment we cast the cell cycle into the group theory.

Keywords: Cell Cycle, Group, Abelian Group, Binucleated Cell, Cell Fusion

1 Introduction

Group theory is an area of abstract algebra that was created to explore and interact with symmetrical abstract concepts. In this paper, we will explore symmetry of cell cycle and check that it is natural application of group theory, in addition to this, we will explore the group operations of some actual manipulations of the cells. For this, various experiments were conducted by Potu N. Rao and Robert T. Johnson to address the questions about the regulation of mitosis and DNA synthesis. Here with the help of cell fusion experiment [2], we form the Cayley table with the fusion of different phases of cell cycle (i.e., $G1$, S, $G2$, and M) as the operation of a group. Afterwards, by using the Cayley table obtained, we will prove whether different phases in the cell cycle and binucleated cells form a group or not. Additionally, we will also check the properties of the group and based on those observations, we would be able to appreciate the significance of group theory in real life.

The paper is divided into 5 sections. The paper's introduction is in Section 1. Section 2 contains the preliminaries needed before delving deep into the topic. Section 3 discusses about how group theory is involved in cell cycle. Section 4 contains cell fusion experiment and Section 5 is the conclusion.

2 Preliminaries

This section consists of the basic definitions and notations used throughout the paper. For better understanding, one may refer ([1], [3]).

Definition 2.1. A group G is a nonempty set with a binary operation $*$ that satisfies the following three conditions:

1. Associativity: For $a, b, c \in G$, $(a * b) * c = a * (b * c)$.

2. Existence of identity: There is an identity element $e \in G$, such that $a * e = a = e * a$, $\forall\, a \in G$.

3. Existence of inverse: For any $a \in G$, there is an element $b \in G$, such that $a * b = e = b * a$.

Definition 2.2. A group $(G, *)$ is said to be an **Abelian group** if commutative law holds in G with respect to operation $*$, i.e., $a * b = b * a, \quad \forall\, a, b \in G$.

According to biology, cell division is a very important process in all living organisms. DNA replication and cell expansion happen simultaneously with a cell's division. For proper cell division and the production of offspring cells with intact genomes, all of these steps take place in a coordinated manner [1].

Definition 2.3. The series of processes by which a cell duplicates its DNA, synthesises its other components of the cell and ultimately divides into two daughter cells is termed as **cell cycle**.

The cell cycle is further divided into two basic phases namely, **Interphase** and **Mitosis phase** (***M*** phase). The phase in between two succeeding M phases is called interphase. When a cell is in the interphase, it is preparing for division by going through orderly processes of cell growth and DNA replication. The interphase is further divided into three phases which are ***G*1 Phase (Gap 1)**, ***S* Phase (Synthesis)** and ***G*2 Phase (Gap 2)**.

Definition 2.4. ***G*1 phase** corresponds to the interval between mitosis and initiation of DNA replication. During $G1$ phase the cell is metabolically active and continuously grows but does not replicate its DNA.

Definition 2.5. ***S*** or **Synthesis** phase marks the period during which DNA synthesis or replication takes place.

Definition 2.6. During the ***G*2 phase**, proteins are synthesised in preparation for mitosis while cell growth continues.

Definition 2.7. The ***M* Phase** represents the phase when the actual cell division or mitosis occurs. This is the most dramatic period of cell cycle, involving a major reorganisation of virtually all components of the cell.

Definition 2.8. All cells that contain two nuclei are called **binucleated cells**.

3 Cell Cycle and Group Theory

Cell cycle is an illustration of a natural application of group theory due to its cyclic symmetry that governs the process. The steps in the cell cycle include $G1 \to S \to G2 \to M$, and back to $G1$ (see figure 3.1). $G0$ [1] can occasionally be so short as to be nonexistent, thus we don't take that condition into account. Using the notion of a group, the cell cycle can be expressed in terms of group theory [3]. To cast the cell cycle into group theory we will use symmetry of squares and the definition of a group. Here is the illustration of cell cycle and it's rotations:

[1] $G0$ or quiescent phase is the stage wherein cells remain metabolicially active but do not proliferate unless called to do so. Such cells are used for replacing the cells lost during injury [1].

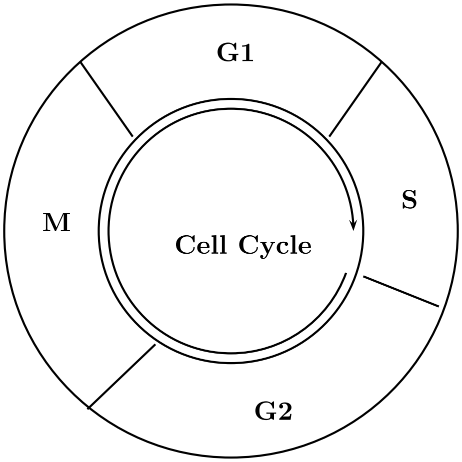

Figure 3.1: Cell Cycle, drawn on LaTeX

Now by applying the symmetries of the square, we get four rotations as follows:

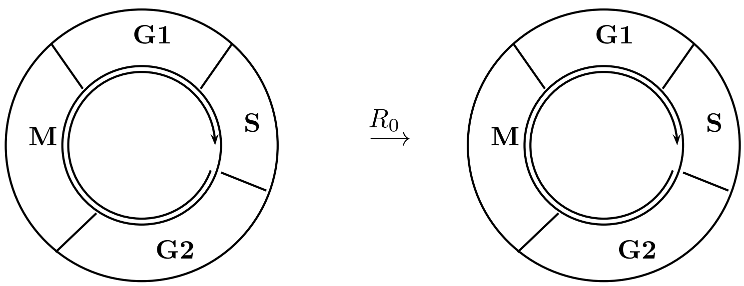

Figure 3.2: Rotation of cell cycle by 0°, drawn on LaTeX

Writing the rotations for the cell cycle as permutation: $R_0 = \begin{pmatrix} G1 & S & G2 & M \\ G1 & S & G2 & M \end{pmatrix}$.

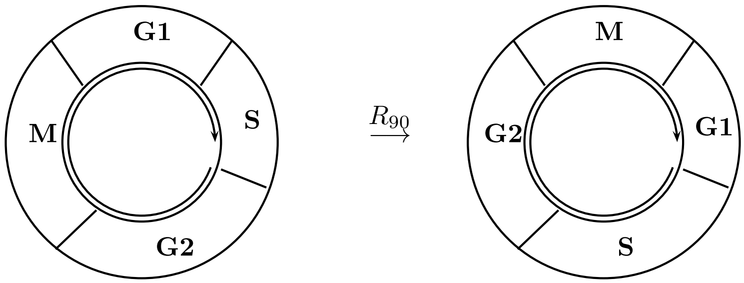

Figure 3.3: Rotation of cell cycle by 90°, drawn on LaTeX

Writing the rotations for the cell cycle as permutation: $R_{90} = \begin{pmatrix} G1 & S & G2 & M \\ M & G1 & S & G2 \end{pmatrix}$.

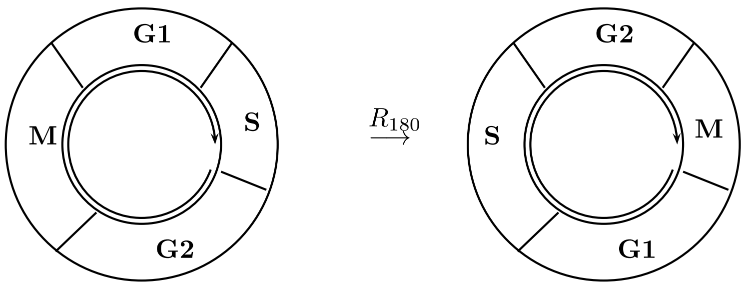

Figure 3.4: Rotation of cell cycle by 180°, drawn on LaTeX

Similiarly, $R_{180} = \begin{pmatrix} G1 & S & G2 & M \\ G2 & M & G1 & S \end{pmatrix}$.

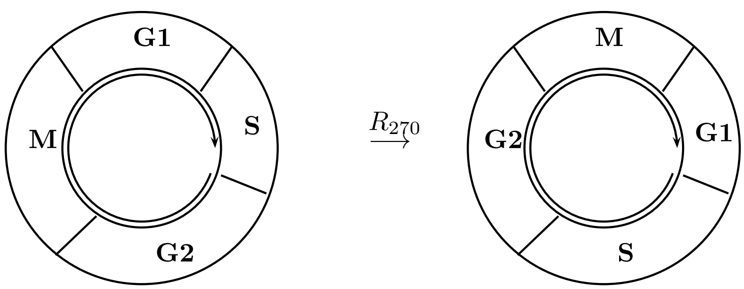

Figure 3.5: Rotation of cell cycle by 270°, drawn on LaTeX

Similiarly, $R_{270} = \begin{pmatrix} G1 & S & G2 & M \\ M & G1 & S & G2 \end{pmatrix}$.

-	G1	S	G2	M
G1	G1	S	G2	M
S	S	G2	M	G1
G2	G2	M	G1	S
M	M	G1	S	G2

Table 3.1: Cayley table for the cell cycle, tabulated on LaTeX

3.1 Observations

Now we check whether the set C=$\{G1, G2, S, M\}$ forms an abelian group under the rotation composition, for that we refer to the Cayley table 3.1 for the cell cycle.

- **Closure Property:** It is clear from the Cayley table that closure property holds in C [2].
- **Associativity:** Similarly, one can check associative law holds in C. For example,

$$G1 * (S * G2) = M = (G1 * S) * G2.$$

- **Existence of identity:** From the Cayley table, we can conclude that $G1$ is the *identity element*.
- **Existence of inverse:** From the Cayley table, it can be seen that inverse of $G1, S, G2$ and M are $G1, M, G2$ and S respectively.
- **Commutativity:** Since the Cayley table of C is symmetric over the diagonal, it is commutative.
  Hence C is an *Abelian group*.
- **C is isomorphic to $\mathbf{Z_4}$:** By referring to table 3.2 and table 3.3 can be seen that Z_4 and C behave similarly, hence group C is isomorphic to the cyclic group Z_4 i.e.,

$$C \cong Z_4$$

-	G1	S	G2	M
G1	G1	S	G2	M
S	S	G2	M	G1
G2	G2	M	G1	S
M	M	G1	S	G2

Table 3.2: Cayley table for C, tabulated on LaTeX

-	0	1	2	3
0	0	1	2	3
1	1	2	3	0
2	2	3	0	1
3	3	0	1	2

Table 3.3: Cayley table for Z_4, tabulated on LaTeX

[2] natural group of cell cycle

4 Cell fusion experiment

In this section, we check whether a converged state of binucleated cell forms a group or not, using the experiment conducted by Potu N. Rao and Robert T. Johnson. They carried out three types of experiments involving fusion of S with $G2$ cells, $G1$ with S cells and $G1$ with $G2$ cells to research how DNA synthesis and mitosis are regulated. One member of each cell pair was labelled with ^3H-thymidine previous to fusion, to permit its identification in the resulting hybrid [2]. The following effects of fusion were studied:

1. Initiation of DNA synthesis in $G1$ and $G2$ nuclei after fusion with cells in $G1, S$ or $G2$.

2. Suppression of DNA synthesis in S and $G1$ nuclei after fusion with cells in $G1, S$ or $G2$.

3. Accleration in progression into mitotic cycle of $G1$ and S nuclie by the $G2$ and, conversely the delay in progression into mitotic cycle of $G2$ nucleus after fusion with cells in $G1$ and S.

4.1 Experiment 1: $S/G2$ fusion

A prelabelled S population was fused with an unlabelled $G2$ population and the pattern of DNA synthesis and mitotic accumulation were studied in the fused cells. Since the $G2$ population had completed DNA synthesis before cell fusion, no change was observed. Moreover, the $G2$ component did not inhibit the DNA synthesis of the S nucleus.
The mitosis accumulation was also studied, $G2$ population was first to enter into mitosis followed by S class of binucleated $S/G2$ class of cells.

4.2 Experiment 2: $G1/S$ fusion

A prelabelled S population was fused with an unlabelled $G1$ population, that results in the induction of DNA synthesis in the $G1$ nucleus of the $G1/S$ fused cell.
This was further confirmed by the mitotic accumulation for binucleated $G1/S$ class of cells. The induction of DNA synthesis in the $G1$ nucleus of the $G1/S$ cells resulted in earlier initiation of mitosis in the $G1/S$ cells than in the $G1$ cells.

4.3 Experiment 3: $G1/G2$ fusion

A prelabelled $G2$ population was fused with an unlabelled $G1$ population. The $G2$ component of the $G1/G2$ cell had no effect on the normal course of DNA synthesis in the $G1$ nucleus.
The mitotic accumulation function was also studied, the $G2$ component did not affect the $G1$ nucleus in its progression through the mitotic cycle. However the $G2$ nucleus of binucleated $G1/G2$ cell was delayed in entering into mitosis by its $G1$ component.

4.4 Results of cell fusion experiment

Following are the results of the cell fusion experiments:

1. Fusion of S phase cell with $G2$ cell: The $G2$ nucleus did not inhibit S phase nucleus in DNA synthesis.

2. Fusion of S phase cell with $G1$ cell: The $G1$ nucleus entered S phase and started DNA synthesis.

3. Fusion of $G1$ phase cell with $G2$ phase: The $G1$ and $G2$ phase cell nucleus did not influence each other.

4. Fusion of M phase with interphase cell: All interphase nucleus enter M phase.

Using above results, we have the following Cayley table:

	G1	S	G2	M
G1	G1	S	G1/G2	M
S	S	S	S	M
G2	G1/G2	S	G2	M
M	M	M	M	M

Table 4.1: Cayley table for converged stated of binucleated cells, tabulated on LaTeX

- Here, we formed the Cayley table 4.1 for the converged state of binucleated cells. Usually, it takes time for the fusion reaction to occur and for the cell to settle to stable attractor[3]. But, by applying the concepts of groups, we can quickly analyse the results and immediately determine the reaction from the Cayley table of converged state of binucleated cell and it will take less time to predict the results.

4.5 Observations

Now we check whether the set B=$\{G1, G2, S, M\}$ forms a group under the operation of fusion of different phases of a cell cycle, for that we refer to the Cayley table 4.1 for the converged state of binucleated cells.

- **Closure Property:** From the Cayley table, we observe that closure property holds for converged state of binucleated cell.

- **Associative Law:** From Cayley table one can see associative law holds in B.

- **Existence of Identity:** From the Cayley table, we observe that there does not exist any identity element for the set B.

- **Existence of Inverse:** Since there does not exist identity of the set B, so we cannot talk about the inverse of the set B.

- **Commutative law:** The Cayley table shows that commutative law holds in the set B.

  It is clear from the Cayley table that we cannot have a group structure on the set B=$\{G1, G2, S, M\}$. This implies converged state of binucleated cell does not form group under fusion of different phases of cell cycle.

[3]An attractor is a set of states invariant under the dynamics, towards which neighboring states in given basin of attraction asymptotically approach in the course of dynamic evolution, an attractor is stable when it is in single state

5 Conclusion

Through this paper, we proved that the cell cycle forms an abelian group under the rotation composition. The cell cycle group is also isomorphic to Z_4. We have also discussed the cell fusion experiment and shown that the converged state of binucleated cells does not form a group under the fusion of different phases of the cell cycle. Thus, we may conclude that mathematics is applied in biological areas; this new field is called biomathematics. We have shown that the Cayley Table, a collection of experimental results, is directly related to biological studies. Although they both offer the same information, mathematics does it in a far more ordered manner. Additionally, we learned how crucial the Cayley table is for predicting the results of many experiments.

References

[1] *Biology* NCERT class 11 chapter 10th, 2020, pp.162-164

[2] Rao P.N., Johnson R.T., *Mammalian Cell Fusion: Studies on the Regulation of DNA Synthesis and Mitosis*, Nature, 1970, pp 159-64. doi: 10.1038/225159a0.

[3] Rietman E.A., Karp R.L. and Tuszynski J.A., *Review and Application of Group Theory to Molecular Systems Biology*, Theoretical Biology and Medical Modelling, volume 8, 2011, Article No. 21. https://doi.org/10.1186/1742-4682-8-21

(Mentor) Dr. Sunil Kumar Yadav, Assistant Professor, Department of Mathematics, Lady Shri Ram College for Women, New Delhi
skymath.bhu@gmail.com

Divya Kesarwani, B.Sc.(H) Mathematics, 4th Semester, Lady Shri Ram College for Women, New Delhi
kesarwanidivya2003@gmail.com

Mansi, B.Sc.(H) Mathematics, 4th Semester, Lady Shri Ram College for Women, New Delhi
kmansi10qwer@gmail.com

Éclat, A Mathematics Journal
Volume 14, 2022-23 (74-82)

3 Persons, 2 Cuts: A Maximin Envy-Free Cake-Cutting Algorithm

Nitin Sharma, Deepti Bhardwaj and Naga Siva Gayatri Dittakavi

Abstract

This paper describes a 3-person, 2-cut envy-free cake-cutting algorithm. Unlike the algorithms that require continuously moving knives, it specifies an algorithm that results in a division that is maximin. Additionally, value functions are used to find a maximally equitable division. Using a Maximin envy-freeness, a maximally equitable division, we arrive at an efficient resource allocation algorithm.

Keywords: Value Functions, Maximin Envy-Free Allocation, Maximally Equitable Division

1 Introduction

This paper attempts to elaborate the cake cutting procedure through an algorithm. Suppose a person P cuts the cake which is a heterogeneous divisible good, into two equal parts according to his/her preference. Person Q then chooses the piece which he/she thinks is at least as valuable as the other piece. This division is envy-free as both P and Q receive the piece that they think is more valuable.

John Selfridge and John Conway, circa 1960, described the division of cake between three persons (or referred as players) but was never published. This algorithm in 1960 was described by Brams and Taylor (1996) which required upto five cuts but the portions that players received may not be connected or contagious.

After some twenty years, Stromquist (1980) gave an algorithm for the division which gave the players connected pieces but was not discrete. After this Barbanel and Brams (2004) found a simpler 3-person moving knife algorithm which included a player and a referee, to move two knives simultaneously. It also provided 'squeezing' procedure which gave most valuable division.

Besides these algorithms, the algorithm that works for n players has also been developed. One such algorithm was given by Brams and Taylor (1995) which uses a finite number of cuts but this number is unbounded. In 2016, Aziz and Mackenzie [1] also gave an algorithm which does not require moving knives and is finite and bounded. This was also modified and extended (Dehghani et al., 2018) [6] and a more simplified 4-person cake cutting algorithm was found (Amanatidis et al., 2018) [3].

In this paper we tend to review the 3-person cake cutting algorithm and obtain the envy-free allocation.

2 Using a Value-function approach

We use value-functions to approach the above resource allocation problem. To explore potential solutions, the following assumptions will have to be made:

1. Each division of the cake is indicated by points on the interval [0,1]. Two cuts on the interval give us 3 divisions (or three subintervals). Each player has a probability density function over the cake, and this is their value function. This value function is absolutely continuous- it takes only non-negative values, is positive somewhere on each subinterval, and has (Riemann) integral equal to 1.

2. Each player, independent of the other players, place marks on the interval that defines the two points that trisect the cake into three equally valuable pieces for each player. Let the players be P, Q, and R.

3. Let the two marks trisecting the cake into 1/3rd and 2/3rd pieces for P be marked as p_1 and p_2. Let the same for Q be q_1 and q_2, and R's marks be r_1 and r_2. To avoid ties, let's assume that each player's marks on [0,1] are unique.

4. After the players have placed their 1/3rd and 2/3rd marks, the algorithm then determines, whichever player's mark is the closest to 0 (again, without ties). Assume that player is P, so except for P, the other players value it as being less than 1/3rd. Now P receives the leftmost piece [0, p_1].

Now we follow a case based approach to see whether Q and R most value different pieces, which may either be [p_1,p_2] or [p_2,1] or they value the same piece. The players' marks may or may not lead to an immediate envy-free division.

Case 1: Q and R most value different pieces:

$$0 - 1$$
$$p_1 \quad q_1 \quad r_1 \quad r_2 \quad q_2 \quad p_2$$

Suppose Q values the middle piece [p_1,p_2], at more than 1/3rd, and the left and right pieces at less than 1/3rd , and R values the right piece [p_2,1] at more than 2/3rd. Since Q and R prefer different pieces, and P receives the left piece, the allocation is envy-free.

Case 2: Q and R most value the middle piece:

$$0\text{-}\ 1$$
$$p_1 \quad q_1 \quad r_1 \quad r_2 \quad q_2 \quad p_2$$

This is a combination that may not result in an envy-free combination, since Q and R both prefer the same piece. Whoever, Q or R receives the middle piece will be envied by the other player.

Case 3: Q and R most value the right piece:

$$0\text{-}\ 1$$
$$p_1 \quad q_1 \quad r_1 \quad r_2 \quad q_2 \quad p_2$$

In a similar fashion, when Q and R both value the rightmost piece [p_2,1] more, at more than 2/3rd and the left and middle pieces at less than 1/3rd, whoever of Q or R receives the right piece will be envied by the other player.

Clearly, making cuts at p_1 and p_2 in Cases 75 and 76 does not produce an envy-free allocation, whichever of Q or R gets the middle piece in Case 75 or the right piece in Case 76. Consider, the following case of marks by the players:

$$0\text{-}\ 1$$
$$p_1 \quad q_1 \quad r_1 \quad r_2 \quad q_2 \quad p_2$$

Once P receives [0,p_1] and Q receives (in this case) [p_1,p_2], they will not envy each other. To P, the three pieces are equal, and Q values [p_1,p_2] at more than 1/3rd. But it is unclear whether giving [p_2,1] to R will cause R to be envious. We cannot be sure whether R values this piece more than 1/3. It may also be a possibility that R values the middle piece more than 1/3rd.

In conclusion, we do not have sufficient information from the players' marks alone whether R values the right piece more than the middle piece.

But an efficient solution to this ambiguous case is the moving-knives solution that uses the "squeezing procedure", Barbanel and Brams, 2004 [4]. P continuously moves two parallel knives, reducing a piece that both Q and R prefer until one of these players indicates that this piece ties with one of P's continuously increasing pieces.

But the algorithm given by Brams and Landweber [2] does not use the squeezing procedure, and instead, directly determines the two points on [0,1] at which to cut the cake so that a tie occurs with one of the two enlarged pieces that P values equally. It then assigns the tied enlarged piece to the player for whom the squeezed piece ties, and the other player gets the squeezed piece, which they still think is the most valuable. Thereby, all the players receive at least tied-for-most valuable pieces, making the resultant allocation envy-free.

Unless the marks are as illustrated in Case 75, wherein each player most values a different piece, there is insufficient information to determine an envy-free allocation. When this is the case, each player independently submits to a referee its value function.

3 Example

Let us assume that P and Q have the given piecewise linear value functions that are symmetric and V-shaped:

$$V_P(x) = \begin{cases} -4x + 2 & \text{for } x \in [0, 1/2] \\ 4x - 2 & \text{for } x \in [0, 1/2] \end{cases}$$

$$V_Q(x) = \begin{cases} -2x + 3/2 & \text{for } x \in [0, 1/2] \\ 2x - 1/2 & \text{for } x \in [1/2, 1] \end{cases}$$

Here we can see in figure 3.1 that both the functions have maxima at $x = 0$ and $x = 1$, and minima at $x = 1/2$. Also, $V_P(x)$ has higher maximum and lower minimum i.e., it is steeper as compared to $V_Q(x)$. Let us take a third player R which has a uniform value function $V_R(x) = 1$, for all $x \in [0, 1]$.

Before we apply the algorithm, it is evident that P gets the leftmost piece, Q will receive the middle piece and R will get the rightmost piece of the cake.

We will look into how to find values of p and q that gives maximal envy-free allocation. Firstly, the 1/3 and 2/3 marks will appear as given, where r_1 will be at $x = 1/3$ and r_2 at $x = 2/3$.

0– 1
p_1 q_1 r_1 r_2 q_2 p_2

Here we can see that p_1 preceeds q_1 and r_1 so we will start by looking at the P's trisection that whether it yields an envy-free allocation or not. According to this trisection Q and R prefer the middle piece that is $[p_1, p_2]$.

By applying the squeezing procedure, the middle piece $[p_1,\ p_2]$ will be squeezed from both the sides i.e., left and right, and the first player whose valuation of the squeezed middle piece ties with the left and right piece will be Q, who places more value towards the endpoints than R.

Both the equations (5) and (6) are applicable for finding the values of p and q when the tie occurs for the first piece with Q. The equation (1) ensures that the cutpoints are at equal distance from 0 and 1. The equation (2) ensures that Q's middle piece whose value is given by left hand side of the equation (2), ties with the right piece, whose value is given by the right hand side of the equation (2).

$$\int_0^p (-4x + 2)\, dx = \int_q^1 (4x - 2)\, dx, \tag{1}$$

$$\int_p^{1/2} (-2x + 3/2)\, dx + \int_{1/2}^q (2x - 1/2)\, dx = \int_0^p (-2x + 3/2)\, dx. \tag{2}$$

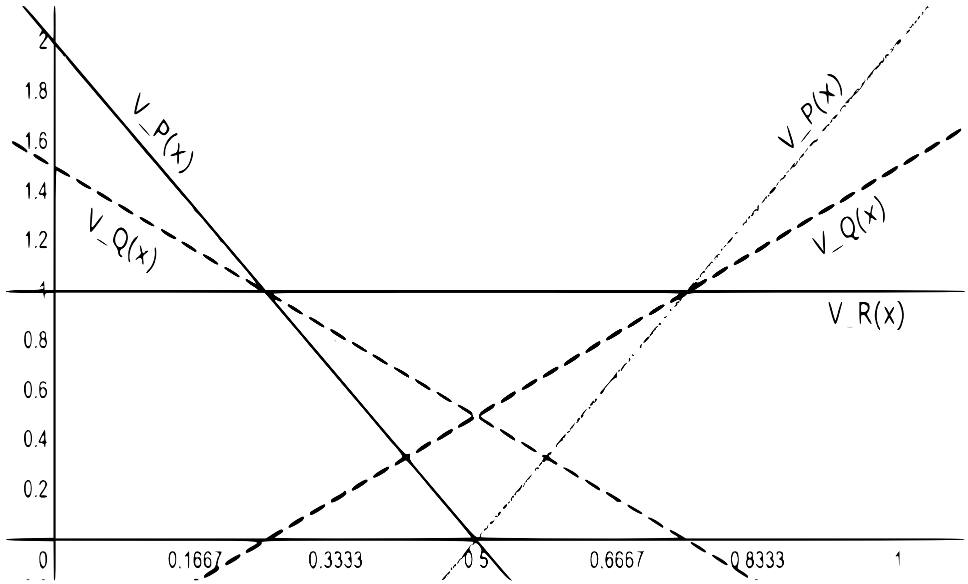

Figure 3.1: Value functions $V(x)$ of players P and Q drawn in Desmos

Solving both the equations (1) and (2) we get,

$$\begin{aligned} -2p^2 + 2p &= -2p^2 + 2q, \\ 2p^2 - 3p &= -q^2 + q/2 - 1/2. \end{aligned}$$

Now, we get the values of $p = 0.271$ and $q = 0.729$ which gives P a share of 39.6% for the subinterval [0,0.271], Q gets a share of 36.2% for the subinterval [0.729,1] and R gets a share of 45.8% for the subinterval [0.271,0.729].

We can further allocate more part of the cake to the worst off player that is Q by further squeezing the middle portion of R to [1/3,2/3]. This will increase the portion that Q and P will get. In this example Q is the one who receives the least share, the referee needs to increase the share. This is done by further squeezing R's portion until it ties with Q's portion by maintaining the envy-freeness. More specifically the referee should ensure that the squeezer P equally values the left and right enlarged pieces using equation (3) which is same as equation (1) as well as ensuring that Q's left share and R's middle share are equal using equation (4).

$$\int_0^p (-4x + 2)\, dx = \int_q^1 (4x - 2)\, dx \tag{3}$$

$$\int_0^p (2x - 3/2)\, dx = \int_p^{1/2} dx + \int_{1/2}^q dx \tag{4}$$

After evaluating the integration in equation (3) and equation (4) we get,

$$
\begin{aligned}
-2p^2 + 2p &= -2q^2 + 2q, \\
-p^2 + (5/2)p &= q.
\end{aligned}
$$

After solving the above equations we get $p = 0.314$ and $q = 0.686$. After squeezing, P's share will be 43.1% for the subinterval [0,0.314] to the left, Q's share will be 37.2% for the subinterval [0.686,1] to the right and R will receive 37.2% for the subinterval [0.314,0.686].

This allocation is still envy-free because R's reduced middle piece is still greater than what P and Q receive from other two sides. Since this allocation maximises the minimum share that each player receives, it is the maximin envy-free allocation. Further reducing R's share would increase P and Q's share but then the envy-free allocation will not be maximin.

We also know that the allocation is maximally equitable when all the players receive equally valued share. If looking through Brams, Jones, and Klamler [5], when P's share is equal to R's, R's share is equal to Q's, this share in our example is 39.3% but this allocation won't be envy-free as this requires P to be closer to 0 than Q is to 1 and the horizontal share of R is the share of each player.

We can summarize our results in the table below:

	P	**Q**	**R**
$Envy-free\ allocation$	[0,0.271] 39.6%	[0.729,1] 36.2%	[0.271,0.729] 45.8%
$Envy-free\ allocation\ (maximin)$	[0,0.314] 43.1%	[0.686,1] 37.2%	[0.314,0.686] 37.2%
$Equitable\ allocation\ (maximal)$	[0.,0.269] 39.3%	[0.662,1] 39.3%	[0.269,0.662] 39.3%

Table 3.1: Summary of the percentage share of each player drawn in LaTeX

3.1 Envy-free and Equitable Algorithms

The envy-free algorithm is implemented in the five steps specified next, where the value functions (i.e., probability density functions) of P, Q, and R are respectively $f_p(x), f_q(x)$ and $f_r(x)$.

Envy-Freeness:

We begin by assuming Case 75 specified above. But a referee determines whether P's marks result in an envy-free allocation, and Q and R get their pieces (they value different pieces), which concludes the algorithm.

Suppose if it is indeterminate whether cuts p_1 and p_2 yield an envy-free allocation, then we follow the steps below:

Step 1: The players now submit their pdfs over [0,1]. A referee calculates the value that each player obtains from the different pieces, defined by the marks at p_1 and p_2. If Q and R most value different pieces, each player receives the piece that they value most, and this concludes the algorithm.

Step 2: If both Q and R value the same piece, say the right most piece, we follow the next step:

Right-most piece squeezed by P's equal pieces to the left: Solve for the lower and upper limits of integration as two pairs of integral equations, simultaneously, the first given by equation (5) and equation (6).

$$\int_0^p V_P(x)\,dx = \int_q^1 V_P(x)dx \quad \text{and} \quad \int_p^q V_Q(x)\,dx = \int_0^p V_Q(x)dx \tag{5}$$

$$\int_0^p V_P(x)\,dx = \int_q^1 V_P(x)dx \quad \text{and} \quad \int_p^q V_Q(x)\,dx = \int_p^q V_Q(x)dx \tag{6}$$

The pieces left to those of equations (5) and (6), which are the same, ensure that the value of the left and middle pieces of P are equal. Equations to the right of equation (5) and equation (6) ensure that the value of the right piece for Q equals:

1. The value of the left-most piece
2. The value of the middle piece

Next, determine the upper and lower limits of integration for two pairs of integral equations, simultaneously, the first given by equation (7) and equation (8), but V_r is substituted for V_q.

$$\int_0^p V_P(x)\,dx = \int_p^q V_P(x)dx \quad \text{and} \quad \int_1^q V_R(x)\,dx = \int_0^p V_R(x)dx \tag{7}$$

$$\int_0^p V_P(x)\,dx = \int_p^q V_P(x)dx \quad \text{and} \quad \int_1^q V_R(x)\,dx = \int_p^q V_R(x)dx \tag{8}$$

The referee chooses the pieces, either left or right, where the solutions to the above equation (5) and (6) for p and q gives the larger value of $\int_q^1 V_R(x)\,dx$.

Compare the larger values given by equations (5) and (6), and by the solutions of equations (7) and (8), and choose which is greater (if it ties, either may be chosen). This determines whether Q or R receives the bigger piece-on the left or the middle, that ties with the diminished piece. Assume it is Q that still receives the enlarged piece; then R will receive the remaining enlarged piece on the left or in the middle. This concludes the envy-free algorithm.

Middle piece squeezed by P's equal pieces to the left and right: Solve for the lower and upper limits of integration as two pairs of integral equations, simultaneously, the first given by equations (9) and (10).

$$\int_0^p V_P(x)\,dx = \int_q^1 V_P(x)dx \quad \text{and} \quad \int_p^q V_Q(x)\,dx = \int_0^p V_Q(x)dx \tag{9}$$

$$\int_0^p V_P(x)\,dx = \int_q^1 V_P(x)dx \quad \text{and} \quad \int_p^q V_Q(x)\,dx = \int_p^q V_Q(x)dx \tag{10}$$

The equations of pieces to the left of equations (5) and (6), which are the same, ensure that the value of the left and middle pieces of P are equal. Equations to the right of equations (9) and (10) ensure that the value of the right piece for Q equals:

1. The value of the left-most piece
2. The value of the piece to its right.

Next, determine the upper and lower limits of integration for two pairs of integral equations, simultaneously, the first given by equations (9) and (10), but V_r is substituted for V_q.

$$\int_0^p V_P(x)\,dx = \int_q^1 V_P(x)dx \quad \text{and} \quad \int_p^q V_R(x)\,dx = \int_0^p V_R(x)dx \tag{11}$$

$$\int_0^p V_P(x)\,dx = \int_q^1 V_P(x)dx \quad \text{and} \quad \int_p^q V_R(x)\,dx = \int_1^q V_Q(x)dx \tag{12}$$

The referee chooses the pieces, either left or right, where the solutions to the above equations for p and q gives the larger value of $\int_p^q V_R(x)\,dx$.

Compare the larger values given by equations (11) and (12), and by the solutions of equations (9) and (10), and choose which is greater(if it ties, either may be chosen). This determines whether Q or R receives the bigger piece-on the left or the middle, that ties with the diminished piece. Assume it is Q that still receives the enlarged piece; then R will receive the remaining enlarged piece on the left or in the middle. This concludes the envy-free algorithm.

4 Conclusion

We described above 3-person, 2 cut algorithm for getting the envy-free allocation where the players submit their value functions instead of moving knives. This gives an efficient allocation and connected pieces as well.

With the help of the value functions of each player given to the referee and with certain calculations we can have the envy-free allocation. This procedure raises the value that the worst off player receives which makes it more fairer than Barbanel Brams (2004) [4] envy-free allocation. In this way, a referee can use the value functions of the players to find a maximally equitable allocation which gives each player that portion that the player values the most.

References

[1] Aziz H., Mackenzie, S.: *A Discrete And Bounded Envy-free Cake Cutting Protocol For Any Number Of Agents*, 57th Annual IEEE Symposium on Foundations of Computer Science, 2016, pp. 416–427 (2016).

[2] Brams, Steven, Landweber and Peter S., *3 Persons, 2 Cuts: A Maximin Envy-Free and a Maximally Equitable Cake-Cutting Algorithm*, February 2018.

[3] Amanatidis G., Christodoulou G., Fearnley J., Markakis E., Psomas C.A. and Vakaliou E.: *An Improved Envy-free Cake Cutting Protocol For Four Agents* 2018.

[4] Julius B. Barbanel, Steven J. Brams, *Cake Division With Minimal Cuts: Envy-free Procedures For Three Persons, Four Persons, And Beyond*, Mathematical Social Sciences,Volume 48, Issue 3, 2004, pp. 251-269, ISSN 01654896, https://doi.org/10.1016/j.mathsocsci.2004.03.006

[5] Brams Steven J.; Jones Michael A. and Klamler, *Divide-and-conquer: A proportional, Minimal-envy Cake-cutting Algorithm*, Christian New York University, American Mathematical Society, University of Graz 2010, http://mpra.ub.uni-muenchen.de/22704/

[6] Dehghani, Sina, Alireza Farhadi, MohammadTaghi HajiAghayi, and Hadi Yami 2018. *Envy-Free Chore Division for an Arbitrary Number of Agents*, Twenty-Ninth Annual ACM-SIAM Symposium on Discrete Algorithms. http://epubs.siam.org/doi/abs/10.1137/1.9781611975031.164

(Mentor) Nitin Sharma, Assistant Professor, Department of Mathematics, Lady Shri Ram College for Women, New Delhi
nitinsharma@lsr.du.ac.in

Deepti Bhardwaj, B.Sc.(H) Mathematics, 4th Semester, Lady Shri Ram College for Women, New Delhi
deeptibhardwaj1503@gmail.com

Naga Siva Gayatri Dittakavi, B.Sc.(H) Mathematics, 4th Semester, Lady Shri Ram College for Women, New Delhi
sivagayatridittakavi.maths2021@gmail.com

Éclat, A Mathematics Journal
Volume 14, 2022-23 (83-95)

Transit-Oriented Development (TOD): A case study of Delhi Metro

Jyoti Darbari, Aditri Srivastava and Iqra Akhlaq

Abstract

Transit Oriented Development (TOD) is a concept that helps in getting easy access to public transits for people by establishing optimal neighbourhoods. This paper proposes a Node-Place (NP) Model that aims to find the TOD Readiness of stations on the yellow line of the Delhi metro rail-transit system. Multiple Criteria Decision-Making (MCDM) techniques like Analytic Hierarchy Process (AHP) and Technique for Order of Preference by Similarity to Ideal Solution (TOPSIS) have been applied to identify the stations that are ready for Transit-Oriented Development (TOD). We also aim to examine the extensions of the NP model, which can be further established if other factors like ridership and time value are considered.

Keywords: Transit Oriented Development, NP Model, MCDM, AHP, TOPSIS

1 Introduction

Due to enormous population size of Delhi, the transportation system in the city is under immense burden. Therefore, transit systems like metro rail, Bus Rapid Transit System (BRTS), etc., are being implemented to cater to the growing travel demand. Moreover, the ever-increasing number of private vehicles in Delhi is a major cause of concern as vehicular emissions contribute to 70% of the air pollution in Delhi. It has thus become inevitable to consider Transit Oriented Development (TOD) for all such cities which have an existing mass transit system.

Delhi has a long history of auto-centric planning which led to segregated land uses, low density sprawl and large unwalkable streets [2]. The availability of extra wide roads with heavily encroached footpaths/cycle tracks, discourages non-motorised modes of transport and ensures that the citizens are dependent on their own vehicles all the time. However, due to the exponential growth in the use of private vehicles, the vehicular movement in these cities have increased tremendously, leading to traffic jams and pollution. In this alarming situation, it is essential that a rapid paradigm shift is undertaken in order to move people away from private vehicles towards the use of public transportation. This is possible through TOD. TOD is an urban paradigm with the potential to achieve urban competitiveness, environmental sustainability and equality in the society. With policies to promote a culture of walking to work, incorporating key elements of mixed-use development, non-motorized transport and pedestrian-first, Delhi sees TOD as a solution to its mobility and air quality challenges.

Delhi is at a defining moment in terms of preparing itself for the next few decades with its Master Plan 2021 which includes city and sub-city level plans, comprehensive traffic and transportation plan, circulation network plans, traffic management schemes, environment management schemes etc. As the Master Plan for Delhi 2021 (or MPD 2021) is looking at innovative concepts to tackle urbanisation, implementation of TOD becomes a rational and probable choice for transportation planners [18].

1.1 Objective

As the TOD application in Delhi is found sparingly, the aim of this study is to analyze the TOD readiness of selected Delhi Metro stations on the Yellow Line. In this paper, we attempt to imitate an NP value model on the current Yellow Line of the Delhi metro transit system to further analyse the TOD readiness of these stations. This involves identification of the key indicators that reflect the TOD principles, i.e., design, diversity and density to model the travel behaviours of the commuters around the area of transit stations. The data for these indicators have been collected from reliable sources such as Delhi Metro Rail Corporation (DMRC) portal, Delhi Development Authority (DDA) portal, etc. By using MCDM techniques such as AHP and TOPSIS, we finally rank the stations that are TOD ready. We also aim to examine the extensions of the NP model which can be further established if other factors like ridership and time value are considered.

1.2 Preliminary Terms

1. **Transit Oriented Development (TOD):** TOD is basically any macro or micro development centered around a transit hub that facilitates full access to transit facilities and encourages people to walk or use public transport instead of private transport. The primary goal of TOD is to reduce and/or discourage private vehicle dependency and induce public transport use alongwith providing easy public transport access to maximum number of people within walking distance.

2. **Node-Place (NP) Model:** The NP model is a commonly used method for TOD evaluation and classification, which essentially designs an analytical framework for assessing station areas in both transport (node) and land use (place) aspects. One of the fundamental principles of this model is to provide the accessibility and conditions necessary for the location to develop its transportation provision. The system of transportation is then improved as a result of rising transportation demand. The principal aim of the NP model is to balance land use with transportation [9].

3. **Analytic Hierarchy Process (AHP):** In decision making, AHP is a structured technique for organising and analysing complex decisions, based on mathematics and psychology. This method was developed by Thomas L. Saaty in the 1970s. AHP can be used to establish measures in both the physical and social domains. In using AHP to model a problem one needs a hierarchic or a network structure to represent that problem and pairwise comparisons to establish relations within the structure [11].

4. **Technique for Order of Preference by Similarity to Ideal Solution (TOPSIS):** TOPSIS is a multi-criteria decision analysis method based on the concept that the chosen alternative has the shortest geometric distance from the Positive Ideal Solution (PIS) and the longest geometric distance from the Negative Ideal Solution (NIS). It was originally developed by Ching-Lai Hwang and Yoon in 1981 [19].

2 Literature Review

TOD was introduced by Peter Calthrope in his book "The Next American Metropolis" [15]. A NP value was introduced in 1999 [10] that used two parameters i.e., the quality and attractiveness of the transit station area or the place value, and the importance of the transit station in the public or the node value. The place value determines how public interaction is related to the diversity of urban activities. On the contrary, the node value indicates the accessibility of the node. This model was used to evaluate the public transit stations with the principal aim to balance land use with transportation and economic growth.

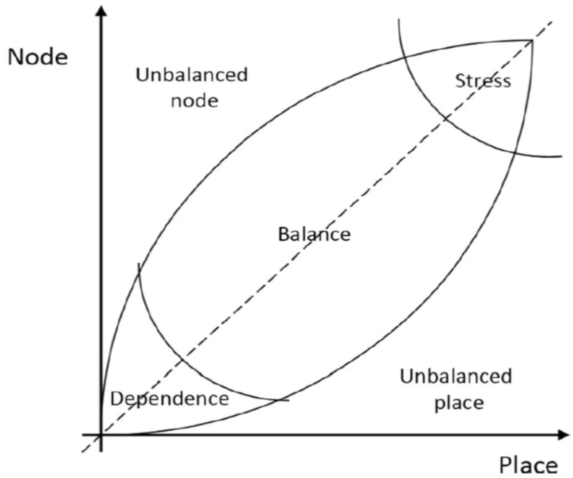

Figure 2.1: The Node-Place Model [10]

In the Figure 2.1, the place value and the node value correspond to the X-axis and the Y-axis respectively. Bertolini identifies five possible situations through the diagram.

The central diagonal area indicates the 'balance' area. That is, if the node and location values are similar and of equal strength, the station is considered accessible or balanced. In the Balanced Zone, infrastructure and land use harmonise without stress, sustaining the environment and systems. The 'stress' region is over-composed of different transport modes and activities, indicating that the critical nodes have the greatest physical human interaction. This constitutes an important value. Stations located in stress zones have numerous potential facilities that allow for more efficient land use. The dependent area represents stations that have matching node and location values but are poorly configured. The zone lacks demand for public transport. Vacant land is plentiful, but there is no reasonable need for infrastructure due to low demand for public transport. A station is an 'unbalanced node' if transportation is more readily available than city activities. In this area, land use facilities are relatively low compared to public transport coverage, resulting in traffic congestion, extensive transportation, and environmental degradation. If the opposite situation actually exists, the station is considered an 'unbalanced site'. Land use activities are more readily available compared to public transport coverage.

If the node and/or place value is increased or decreased, it would bring an unbalanced station in the balanced area ([3],[7]). Thus, researchers have confirmed that a two-dimensional NP model cannot cover all aspects of analysis for a station. A comprehensive model of node, place, ridership and time should be considered to include practical values. Network access at a station consists of two main factors: options accessible via train station and transportation options available ([1],[8],[12]) to reach the station. Accessible opportunities and network centrality have recently been added to the value of nodes by Zhejing Cao et al. [5].

Bertolini measured the importance of his proposed node location model based on the land use around the station and the number of residents and employees in the economic area. Other researchers added other indicators after Bertolini to place values, such as population density, land value, unemployment rate, number of dwellings, and central urban area [4]. Diversity of activities and density are the main factors in measuring location value, but other important metrics, such as parking lots, electric buses at stations, and pedestrian zones, need to be considered. Zhejing Cao et al. [5] also included the features of the built environment in the value of the place. Additionally, they considered ridership of the transits as the third dimension of the node-place value model.

3 Case Study

3.1 Approach

The metro network emerged in response to an alleviated travel demand patterns along Delhi's arterial roads, but these travel patterns have remained unchanged. The road-related congestion that has been a concerning factor in big Indian cities has been eased by accommodating the growing number of commuters through metros. This is why for this case study, metro lines have been taken as the popular transit choice among the people. For the purpose of this study, we consider 15 stations of the Yellow line of Delhi Metro to create an NP Model and calculate TOD Readiness Score of stations of Yellow Line. We provide a list of Node and Place indicators. Different data sources were used to collect data for our indicators. AHP is applied to find weights of different indicators and further TOPSIS is used to assign values to the selected stations for the given indicators. Finally, the TOD Readiness for each station is analyzed and the stations are ranked from highest to lowest based on their TOD Scores.

3.2 Study Area and Indicators

The need for a mass transit in Delhi was first mentioned in 1969 in a traffic and travel characteristics study done by the Central Road Research Institute (CRRI) [6]. Since then, several studies have been conducted by various government agencies to explore possible technologies for such mass transit transportation. However, metros were not selected as a suitable technology for mass transit until the 1990s, based on feasibility reports prepared by Rail India Technical and Economic Services (RITES) [6].

Inaugurated on 24th December 2002, Delhi Metro is a Mass Rapid Transit (MRT) system serving Delhi and its satellite cities Ghaziabad, Faridabad, Gurgaon, Noida, Bahadurgarh and Ballabgarh, in the National Capital Region of India. This transit network includes 10 colour-coded lines serving 255 stations with a total length of 348.12 kilometres, and has a daily ridership of 2.78 million (2019–20) [17]. It is India's second-oldest metro rail system after the Kolkata Metro and by far the biggest and busiest. The network uses both broad-gauge and standard-gauge to connect a variety of underground, at-grade, and elevated stations. Each day, the Delhi Metro runs more than 2,700 trips!

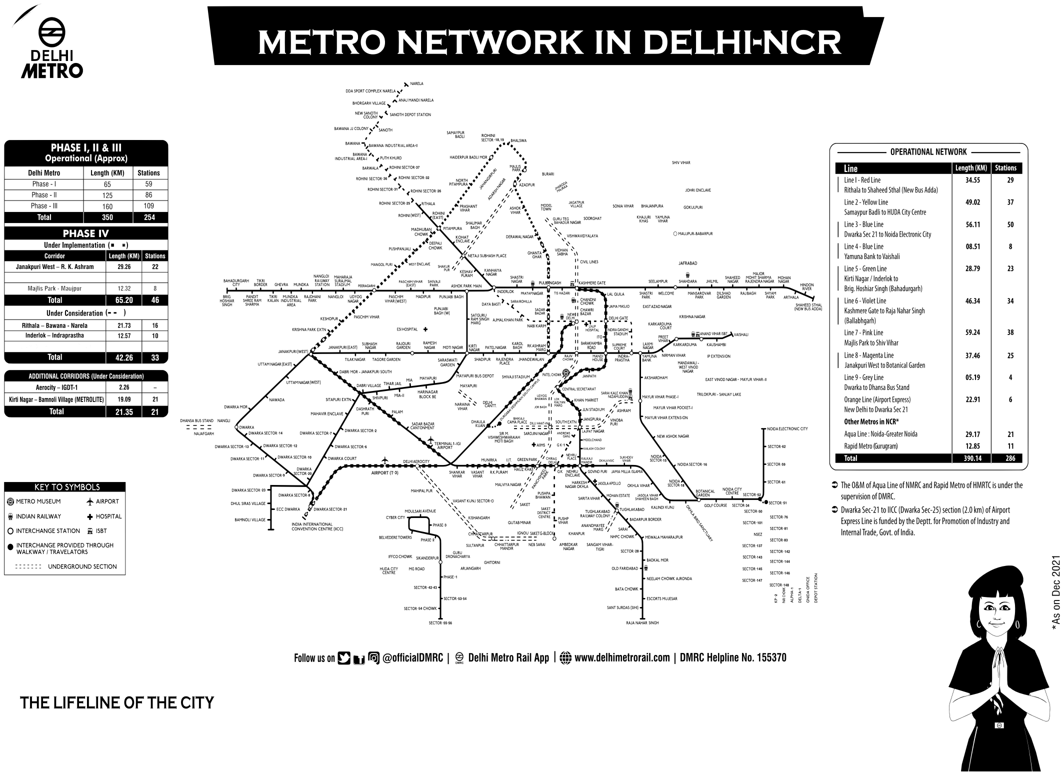

Figure 3.2.1: Map of delhi metro (Source: DMRC [16])

For the purpose of research, we have considered the Yellow Line of Delhi metro. The Yellow Line consists of 37 stations from Samaypur Badli in Delhi to HUDA City Centre in the neighbouring city of Gurgaon in Haryana. The 49.02 kilometre long line runs under one of Delhi's busiest areas and is mostly underground. It is the second line of Delhi Metro to become operational after the Red line and is the 3rd longest metro line on the Delhi Metro network. This line covers North West Delhi, North Delhi, through Central Delhi, New Delhi, South Delhi and finally the city of Gurgaon in Haryana. The Yellow line has interchanges with the Red, Blue, Violet, Pink and Magenta lines of the Delhi Metro, as well as with the Old Delhi and New Delhi railway stations of the Indian Railways. The Line also connects with the Airport Express Line at New Delhi metro station.

To simplify the case study, 15 stations have been selected, spread in the northwest, north, central, New Delhi and southern districts of Delhi, that are- Samaypur Badli, Haiderpur Badli Mor, Azadpur, Vishwa Vidyalaya, Kashmere Gate, Chandni Chowk, New Delhi, Rajiv Chowk, Patel Chowk, Central Secretariat, Jor Bagh, Dilli Haat - INA, Hauz Khas, Saket and Qutab Minar. A few stations were eliminated in this case study because of unavailability of sufficient data.

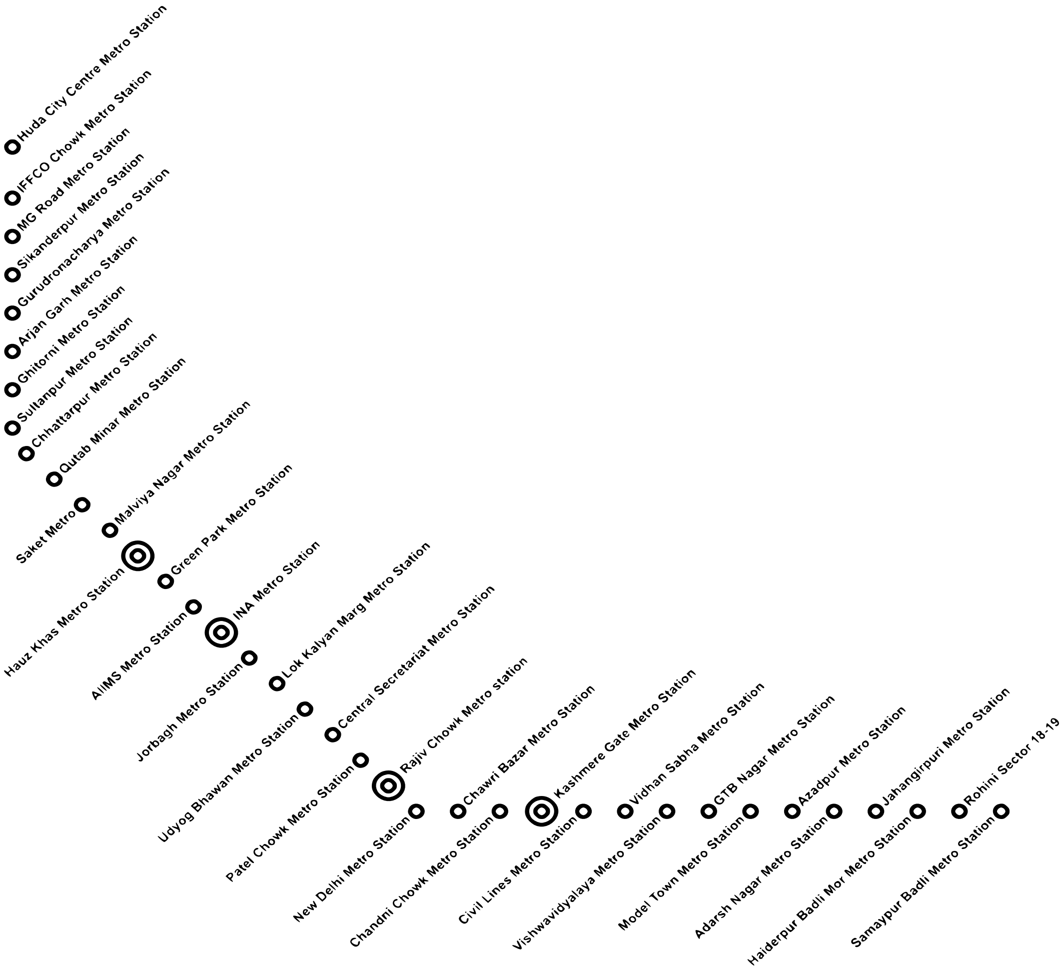

Figure 3.2.2: Map of Yellow line of the Delhi Metro (Source: DMRC [16])

3.3 Indicators

A literature review was conducted to shortlist the required indicators to conduct a TOD readiness study [13]. Further, these indicators were analysed to decide its fitness in this case study of Delhi metro system. The following indicators have been considered in this case study. The data has been collected from different sources and has been compiled on Excel for further analysis.

ASPECT	STATION COMPONENT	DEFINITION	SOURCE
NODE	Waiting time	Average time between the arrival of two metros in a transit station	Google maps
	Connectivity	Number of platforms in a transit station, indicating the number of lines that are connected at the station	Delhi Metro Rail Corporation (DMRC)
	Design / station facilities	Extend of services at the transit station that provides support and ease to commuters using the services, car parking, no. of entrances and exits, connectivity to other modes of transport, etc. **Note:** Due to limited availability of data, we have selected the following parameters to judge the extent of transit facilities. 1. wheelchair accessible car park 2. toilets 3. 24 hour public transport services available 4. Parking 5. ATM 6. Food outlets	Delhi Metro Rail Corporation (DMRC)
PLACE	Distance from commercial activity	Distance between the transit station and nearest commercial area like markets, offices, etc.	Delhi Metro Rail Corporation (DMRC) and Google Maps
	Key attractions	Popular places to visit around the transit station. For instance, accessible public places like monuments, shopping complexes, airports, etc.	Delhi Metro Rail Corporation (DMRC) and Google Search
	Population Density	Number of people per square kilometre residing in a 500 m radius around the metro station. **Note:** Due to lack of data availability, we considered the population density of the district in which the transit station lies.	Census 2011 by Government of India

Figure 3.3.1: Indicators (Tabulated on MS Excel)

4 Methodology and Approach

4.1 Survey

To understand how metro users rate the different judgement criteria while comparing two stations, a short survey was conducted where the users were interrogated to further develop a pairwise comparison matrix of these indicators.

The data was collected from 8 respondents who were randomly selected based on elements like their purpose of travelling, the frequency of using the transit mode in a week, the residential area, the time at which they usually travel and the terminal station of their journey through metro.

The questionnaire was predominantly a 6×6 matrix in which both rows and columns represented indicators. Respondents were first asked to arrange the indicators from most important to least important based on their preferences. They were then asked to fill the cells of the matrix based on their preferences such that the indicator on the row was some rational number times more important than indicator on the column.

4.2 Application of AHP - TOPSIS technique

4.2.1 AHP

The respondents assigned pairwise comparison score to indicators on a scale from 1 to 9 with 1 being of equal importance and 9 of extreme importance. The criteria were compared pairwise on a scale of 1-9 representing subjective judgements for the levels of importance. The numeric values '1-3-5-7-9' represented "equally important-moderately important-important-very important -extremely important", with the intermediate subjectivities represented by 2,4,6 and 8.

Once the pairwise comparison matrices are obtained from the survey of metro users, the geometric mean of elements in all the matrices is calculated, to create an aggregate pairwise comparison matrix.

Indicators	Waiting Time	Distance from commercial activity	Connectivity	Design	Key attractions	Population density
Waiting Time	1.00	0.80	0.71	5.46	0.86	2.04
Distance from commercial activity	1.25	1.00	1.04	4.46	0.97	3.01
Connectivity	1.40	0.95	1.00	4.46	1.40	1.97
Design	0.19	0.22	0.22	1.00	0.24	0.36
Key attractions	1.15	1.03	0.71	3.95	1.00	1.88
Population density	0.48	0.32	0.48	2.60	0.52	1.00

Figure 4.2.1: Geometric Mean of elements of individual matrices obtained from user survey (Tabulated on MS Excel)

We then normalise this matrix and generate the priority vector which is the principal eigenvector. Ultimately, we check the consistency of the matrix by utilising the following equations:

$$CR = \frac{CI}{RI} \qquad \text{and} \qquad CI = \frac{(\lambda_{max} - N)}{(N-1)},$$

where CI is the Consistency Index, CR is the Consistency Ratio and RI is the Random Index.

The matrix with $CR < 0.1$ is acceptable, which implies that the overall inconsistency less than 10% is acceptable else, the judgement is reviewed and the steps are repeated till an acceptable consistency ratio is derived.

The priority vector gives us the weights of the corresponding indicators.

4.2.2 TOPSIS

Once the weights are obtained, TOPSIS is applied to calculate the weights of different stations for the selected indicators (whose weights were calculated above in the subsection 4.2.1).

Construct a normalised decision matrix followed by a weighted normalised decision matrix.

Weighted Normalized Matrix									
Weights-	0.045	0.233	0.193	0.232	0.197	0.100			
Stations	Design	Distance from commercial activity	Waiting time	Connectivity	Key Attractions	Population Density (in km^2)	Euclidean Distance from best	Euclidean Distance from worst	Performance Index
Samaypur Badli	0.014	0.022	0.055	0.034	0.000	0.011	0.108	0.083	0.433
Haiderpur Badli Mor	0.011	0.030	0.047	0.034	0.000	0.011	0.110	0.075	0.405
Azadpur	0.008	0.067	0.047	0.068	0.026	0.019	0.089	0.059	0.398
Vishwa Vidyalaya	0.016	0.067	0.047	0.034	0.026	0.019	0.107	0.048	0.312
Kashmere Gate	0.016	0.037	0.047	0.103	0.078	0.037	0.031	0.128	0.806
Chandni Chowk	0.008	0.037	0.047	0.034	0.052	0.037	0.080	0.091	0.532
New Delhi	0.014	0.063	0.047	0.103	0.052	0.037	0.062	0.101	0.618
Rajiv Chowk	0.014	0.022	0.055	0.068	0.078	0.037	0.037	0.123	0.767
Patel Chowk	0.011	0.097	0.055	0.034	0.052	0.037	0.116	0.062	0.349
Central Secretariat	0.008	0.048	0.047	0.068	0.052	0.037	0.061	0.090	0.597
Jor Bagh	0.008	0.075	0.055	0.034	0.078	0.005	0.101	0.084	0.454
Dilli Haat - INA	0.011	0.007	0.047	0.068	0.026	0.005	0.071	0.106	0.600
Hauz Khas	0.011	0.041	0.055	0.068	0.026	0.015	0.075	0.078	0.510
Saket	0.008	0.082	0.047	0.034	0.078	0.015	0.104	0.082	0.440
Qutab Minar	0.008	0.104	0.047	0.034	0.026	0.015	0.132	0.028	0.174

Figure 4.2.2: Weighted Normalised Decision Matrix (Tabulated on MS Excel)

We determine the Positive Ideal Solution (PIS) and Negative Ideal Solution (NIS) from the weighted normalised decision matrix and then calculate the separation measures for each alternative. The separation measures from PIS and NIS alternatives are calculated using Euclidean distance method. Finally, we calculate the relative closeness to the ideal solution for each alternative.

Indicators-	Design	Distance from commercial activity	Waiting time	Connectivity	Key Attractions	Population Density (in km^2)
Ideal Best(B) / Worst(W) Values	B	W	W	B	B	B
Euclidean Distance from worst	0.008	0.104	0.047	0.034	0.000	0.005
Euclidean Distance from best	0.016	0.007	0.055	0.103	0.078	0.037

Figure 4.2.3: Euclidean distance figures (Tabulated on MS Excel)

Rank the preference order of alternatives on the basis of their relative closeness to the ideal solution.

5 Results

TOD approach in Delhi will help in bringing people closer to public transport, leading to much-needed land-use and transport integration in the city. A compact, walkable, multi-purpose settlement will be created within the sphere of influence of the transit station. This important paradigm shift can improve public transport utilization, reduce traffic congestion, and reduce greenhouse gas emissions and pollution in the long term [17].

Through this case study, we obtained a list of stations that need to be prioritised for TOD. The following rank table is obtained after the application of AHP and TOPSIS.

Stations	Rank
Kashmere Gate	1
Rajiv Chowk	2
New Delhi	3
Dilli Haat - INA	4
Central Secretariat	5
Chandni Chowk	6
Hauz Khas	7
Jor Bagh	8
Saket	9
Samaypur Badli	10
Haiderpur Badli Mor	11
Azadpur	12
Patel Chowk	13
Vishwa Vidyalaya	14
Qutab Minar	15

Figure 5: Rank table (Tabulated on MS Excel)

From the table we can analyse three groups of stations:
Category 1- Kashmere Gate, Rajiv Chowk, New Delhi, Dilli Haat-INA and Central Secretariat.
Category 2- Chandni Chowk, Hauz Khas, Jor Bagh, Saket and Samaypur Badli.
Category 3- Haiderpur Badli Mor, Azadpur, Patel Chowk, Vishwa Vidyalaya and Qutub Minar.

In category 1, we get a list of stations that are most likely to be TOD ready since they bring about qualities such as ease of transport services, good population growth, frequent travelling or visiting the area and a potential for scaled economic activities. These stations can be further developed with the vision of TOD that will further bring together elements such as urban regeneration, real estate development, land value capture, urban design, land use planning, transport planning, and infrastructure implementation.

In category 2, we can see a list of stations whose primary objective is the feature to have a key attraction that influenced people to travel there. These stations are a frequent visit stop for commuters but this might be occasional and not a necessity. So they can be prioritised second on the scale. One of the common features of these stations can be the closeness to commercial activities further indicating its importance in TOD.

Addressing Delhi's growing pollution, congestion problems and housing shortages for the poor and middle class, it was unveiled in 2007 as part of Master Plan Delhi 2021 [20] that the TOD policy will be added for the first time, to attempt reorienting Delhi to modern needs. This decision was based on the recognition that travel through transit has become a central avenue for future urban redesign or renovation. Every day, millions of settlements move for work, education, commerce, health and entertainment, turning large cities into a landscape of chaotic traffic, long distances, space and great inequalities of land value and opportunity. There have been many attempts to transform the limited land already available in cities [14] to create sustainable, walkable, livable and equitable areas for all strata of society so as to live and work together. Habitat professionals who have at least a little understanding of the physical planning requirements and the available frameworks, therefore, have been developing a viable, equitable and workable environment, promoting TOD in Indian cities. As recently as 2015, the Planning Authority (Delhi Development Authority or DDA) made a conscious effort to formulate a comprehensive transport-oriented development policy to redevelop station areas and neighborhoods along the metro corridor [21].

In category 3, we have a list of stations that lie lower on the scale. A lot of information cannot be drawn from this analysis as it might lack the vision of few parameters like the offices and other travelling objectives that people might have to use the metro. We might also need to consider the ridership factor of these stations to understand the current scenario of the metros clearer.

6 Extension of the NP Model

We observe that the NP model is a region-scale model that focuses on rail transit networks and stations to classify TOD typologies. One of the basic ideas of this model is to provide accessibility and location conditions for developing transportation modes. The increased transportation demand leads to faster location growth and strengthening of the transportation system. However, it looks like we need more dimensions as nodes and place values that have not been considered yet. Ridership refers to the use of transit centres and infrastructure by public transport users, which is related to land use and time. To get a comprehensive model, we need to collect data during peak and off-peak hours. This is because the aforementioned parameters and number of passengers are functionally related to time. Many researchers have further suggested more complex models like Node-Place-Ridership (NPT) and Node-Place-Ridership-Time (NPRT) models. Analysing the adjustments between NPRT values helps transportation planners better understand this model.

7 Conclusion

In this paper, we conducted a case study on the Yellow Line of Delhi metro rail-transit stations to present the relationship between node and place. After collecting the data and providing all the influential parameters, it was applied to create an NP model to further understand the TOD readiness of these stations. For this, we used AHP and TOPSIS techniques of MCDM to model the coordination and relationship between the effective parameters of the NP model. We further analysed how these results can be developed into research studies for the policymakers, city planners and governments which will help them to analyse the efficiency of these metro transit stations. When considering the NP model, it seems to give less accurate results than other models like NPRT and NPR models presented by previous researchers. There is a bi-directional relationship between the dependent and independent variables as it is an effect of ridership on node and place values. For further studies, a multi-characteristic model which considers the effect of the economy, ecology and socio-demographic characteristics (such as transit mode share, household going-out rate and age composition) would be essential to achieve accuracy.

References

[1] Geurs K.T. and Van Wee, B., *Accessibility Evaluation of Land-Use and Transport Strategies: Review and Research Directions*, Journal of transport geography, Volume 12, No. 2, 2004, pp. 127-140.

[2] Chorus P. and Bertolini L., *An Application of the Node Place Model to Explore the Spatial Development Dynamics of Station Areas in Tokyo*, Journal of transport and land use, Volume 4, No. 1, 2011, pp. 45-58.

[3] Zemp S., Stauffacher M., Lang D.J. and Scholz R.W., *Classifying Railway Stations for Strategic Transport and Land Use Planning: Context Matters!*, Journal of transport geography, Volume 19, No. 4, 2011, pp. 670-679.

[4] Reusser D.E., Loukopoulos P., Stauffacher M., Scholz and R.W., *Classifying Railway Stations for Sustainable Transitions–Balancing Node and Place Functions*, Journal of transport geography, Volume 16, No. 3, 2008, pp. 191-202.

[5] Cao Z., Asakura Y. and Tan Z., *Coordination between Node, Place, and Ridership: Comparing Three Transit Operators in Tokyo*, Transportation research part D: Transport and environment, Volume 87, 2020, pp.102518.

[6] Randhawa P., *Delhi Metro Rail: Beyond Mass Transit*, Economic and political weekly, Volume 47, 2012, pp. 25-29.

[7] Lyu G., Bertolini L. and Pfeffer K., *Developing a TOD Typology for Beijing Metro Station Areas*, Journal of transport geography, Volume 55, 2016, pp. 40-50.

[8] Bhat C., Handy S., Kockelman K., Mahmassani H., Chen Q. and Weston L., *Development of an Urban Accessibility Index: Literature Review*, Report No. TX-01/7-4938-1, 2000.

[9] Amini Pishro A., Yang Q., Zhang S., Amini Pishro M., Zhang Z., Zhao Y., Postel V., Huang D. and Li W., *Node, Place, Ridership, and Time Model for Rail-Transit Stations: A Case Study*, Scientific reports, Volume 12, No. 1, article no. 16120, 2022, pp. 1-16.

[10] Bertolini L., *Spatial Development Patterns and Public Transport: The Application of an Analytical Model in the Netherlands*, Planning practice and research, Volume 14, No. 2, 1999, pp. 199-210.

[11] Saaty R.W., *The Analytic Hierarchy Process— What it is and How it is Used*, Mathematical modelling, Volume 9, No. 3-5, 1987, pp. 161-176.

[12] Guy C.M., *The Assessment of Access to Local Shopping Opportunities: A Comparison of Accessibility Measures*, Environment and planning b: Planning and design, Volume 10, No. 2, 1983, pp. 219-237.

[13] Supaprasert S., Lohatepanont M. and Visamitanan K., *The Transit-Oriented Development (TOD) Index and Its Application to Metro Stations in Bangkok*, Journal of international logistics and trade, Volume 19, No. 3, 2021, pp. 115-131.

[14] Shirke C., Joshi G.J., Kandala V. and Arkatkar S.S., *Transit Oriented Development and its Impact on Level of Service of Roads & Metro: A Case Study of Mumbai Metro Line-I*, Transportation research procedia, Volume 25, 2017, pp. 3035-3054.

[15] Calthorpe P., *The Next American Metropolis: Ecology, Community, and the American Dream*, Princeton architectural press, 1993.

[16] Delhi Metro Rail Corporation, *Delhi Metro Rail Map*, 2022, https://www.delhimetrorail.com/network_map

[17] Government of National Capital Territory of Delhi, *Economic Survey of Delhi*, 2021-22, pp. 217–219, 229, http://delhiplanning.nic.in/sites/default/files/E12_Transport.pdf#page=5

[18] Delhi Development Authority, *Master Plan for Delhi-2021*, 2021 https://dda.gov.in/sites/default/files/inline-files/Master_Plan_for_Delhi_2021_text_report.pdf

[19] Hwang C.L. and Yoon K., *Multiple Attribute Decision Making: Methods and Applications*, Springer-Verlag, New York, 1981, http://dx.doi.org/10.1007/978-3-642-48318-9

[20] Ministry of Housing and Urban Affairs, *National Transit Oriented Development (TOD) Policy*, 2021, /https://mohua.gov.in/upload/whatsnew/59a4070e85256Transit_Oriented_Developoment_Policy.pdf

[21] DMRC, Capita Symonds, *Transit Oriented Development (TOD)-Study for Existing Metro Corridor Between Chattarpur and Arjangarh of Delhi Metro Project of Phase II*, Academia.edu, 2019, https://www.academia.edu/6043488/Transit_Oriented_Development_TOD_Study_for_Existing_Metro_Corridor_Between_Chattarpur_and_Arjangarh_of_Delhi_Metro_Project_of_Phase_II_And.

(Mentor) Dr. Jyoti Darbari, Associate Professor, Department of Mathematics, Lady Shri Ram College for Women, New Delhi
jyotidarbari@lsr.du.ac.in

Aditri Srivastava, B.Sc.(H) Mathematics, 6th Semester, Lady Shri Ram College for Women, New Delhi
aditrisrivastava.math@gmail.com

Iqra Akhlaq, B.Sc.(H) Mathematics, 6th Semester, Lady Shri Ram College for Women, New Delhi
iqraakhlaq.math@gmail.com

Éclat, A Mathematics Journal
Volume 14, 2022-23 (96-100)

SOFIA KRUKOVSKY KOVALEVSKAYA

Reema Agarwal, Shiya Ramteke and Varri Krishna Priya

Abstract

This paper traces the life and contributions of Russian Mathematician, Sofia Kovalevskaya in Mathematics. She was the first woman in modern Europe to gain a doctorate in Mathematics and and the first to be appointed as professor of Mathematics. This paper will help to get a better understanding about her life and career. It also briefs about the Cauchy Kovalevskaya Theorem given by Sofia.

Keywords: Cauchy Kovalevskaya Theorem, Partial Differential Equation

1 Early Life and Family Background

Sofia Krukovsky Kovalevskaya, often called Sonya by close friends and family, was born into an aristocratic family in Moscow in 1850. Sofia, the youngest girl in the family, had an older sister, Anyuta, who later became one of her best friends and role model, and a younger brother, Fedya. When Sofia's father General Vasily Krukovsky's military career ended, he moved the family to an estate near the Lithuanian border called Palibino. It was the place where Sofia began regular schooling and eventually developed love for mathematics. It is said that Kovalevskaya ran out of wallpaper when decorating their new home and resorted to General Krukovsky's old Calculus notes for the walls in the nursery. Later Sofia claimed that the paper allowed her to become more familiar with calculus symbols even before learning the material.

Figure 1.1: Sofia Kovalevskaya in 1868 (source: Wikimedia Commons)

Sofia's brother Pyotr and Sofia discussed about mathematical concepts, such as squaring circles and asymptotes. It was these conversations that kindled Sofia's interest in Mathematical Sciences. Sofia's academic interests became greater. At the age of thirteen Sofia mastered Algebra and then wanted to study Physics. Her neighbour, Professor Tyrtov, decided to permit her to study from his books if she learnt trigonometry by herself, which was needed for the section on optics. When Tyrtov finally observed her work, he was amazed and called her by the name, 'New Pascal'. Sofia analyzed the sine function by constructing a chord on a circle using a development strikingly similar to that of the actual development of Mathematics. Tyrtov was so impressed with the intelligence of the girl that he convinced General Krukovsky to allow Sofia to go to Saint Petersburg to study Mathematics under Professor Alexander Strannoliusky [3].

2 Education

After finishing her studies, around 1867, Sofia became determined to pursue higher education. Since the universities in Russia were not open to women, Sofia's only option was to travel west. This task however, seemed to be insurmountable. Sofia was living in a society where women were completely dependent upon men. By law, a woman traveling alone had to have either her father or husband's permission. General Krukovsky did not allow his daughters to leave the country to study. The only option was to marry a man who would allow her to go. While Sofia was engaged in studies, her sister became an advocate for the liberation of women. In her discussions with some of the other revolutionaries of her generation, Anyuta her sister, realized Vladimir could allow Sofia to study after marriage [1].

Figure 2.1: Sofia Kovalevskaya A 19th century pioneer for women in mathematics (source: https://bhavana.org.in/the-theme-of-the-sad-and-unattractive-kovalevskaya/)

Vladimir, a twenty-six year old university student studying Geology, was mesmerized with Sofia. Vladimir and Sofia married in September of 1868 and soon moved to Petersburg where Sofia recieved permission to attend classes. Sofia was determined, and it was at Petersburg that she decided to pursue a career in Mathematics. In 1869, Kovalevskaya began attending the University of Heidelberg, Germany. Shortly after beginning her studies there, she visited London with Vladimir. There at the age of nineteen, she met Herbert Spencer and was led into a debate, at Eliot's instigation, on "Woman's Capacity for Abstract Thought". This was well before she made the notable contribution of the 'Kovalevsky top' adding to the brief list of known examples of integrable rigid body motion [3].

3 Journey as a Mathematician

Even after studying for a year at the University of Heidelberg, Sofia's thirst for Mathematical knowledge remained unquenched. She decided to seek out one of the most noted Mathematicians of the time, Karl Weierstrass. This quest led her to the University of Berlin, where once again she discovered that female students were not welcome. After Weierstrass saw her work, and personally requested that she should be allowed to attend his classes, the university still denied her this opportunity.

Weierstrass recognized Kovalevskaya's great Mathematical ability and offered to tutor her privately. This working mentorship lasted for four years, and the resulting friendship continued throughout most of her life. While under the tutelage of Weierstrass, Sofia completed three papers for a doctoral dissertation. They were: *'On the Theory of Partial Differential Equations'*,*'On the Reduction of a Certain Class of Abelian Integrals of the Third Rank to Elliptic Integrals'*, and *'Supplementary Remarks and Observations on the Laplace's Research on the Form of Saturn's Rings'*. Finally, in July 1874, Sofia Kovalevksy's hard work was rewarded, and she received a Ph.D. in absentia, *summa cum laude*, from the University of Gottingen. She became the first Russian woman to receive her

Figure 3.1: Sofya Kovalevskaya in 1880 (source: Wikimedia Commons [4])

doctorate in Mathematics [3].

Even after earning her Ph.D., Kovalevskaya was unable to have a job. As a result, Sofia returned home to Russia with Vladimir, Anyuta, and Anyuta's husband. She was invited by Russian Mathematician Chebyshev to present a paper at a scientific conference in Sweden. Her presentation was such a success that she was invited to teach at the University of Stockholm. Before Sofia moved to Sweden, she visited Weierstrass in Berlin and actively started her research in Mathematics.
In 1883, Sofia took on her first job as a lecturer at University of Stockholm. She was eventually appointed as a Professor of Higher Analysis. In addition to this, she became an editor for *Acta Mathematica* [2].

4 Cauchy Kovalevskaya Theorem

"*The Cauchy problem has a unique analytic solution locally if the functions occuring in the differential equation and all the initial data, together, are analytic*".
Whilst working under the supervision of Weierstrass, Sofia wrote three papers. The first and most highly acclaimed of these dealt with the theory of Partial Differential Equations. Weierstrass had previously worked on theorems involving ordinary differential equations and wished to extend some of them to Partial Differential Equations.

Her work included the formulation of what is commonly known as the Cauchy-Kovalevskaya Theorem, and it was said by Henri Poincaré that her work significantly simplified Cauchy's method of proof, and gave the theorem its final form.

Cauchy presented the first general existence theorem for Partial differential equations in year 1872. This theorem showed that Ordinary Differential Equations and some Partial differential equations have analytic solutions. An analytic function f in a neighbourhood of the point (t, v),

$$f(t, v) = \frac{dv}{dt}$$

with the initial conditions $v = v_0$ and $t = t_0$, then there exists a unique solution. Cauchy considered the following type of partial differential equation

$$\frac{\partial \mu}{\partial t} = F_i\left(t, x_1, \ldots, x_n : \mu_1, \ldots, \mu_n : \frac{\partial \mu_1}{\partial x_1}, \ldots, \frac{\partial \mu_m}{\partial x_m}\right),$$

the initial conditions $v_i(\theta, x_1, ..., x_n) = w_i(x_1, ..., x_n)$ for $i = 1, ..., m$ when $t = \theta$, and tried to find a solution which satisfied these conditions. He achieved this by finding a locally covergent power series solution by assuming F_i and w_i analytic. A simple analytic function then replaces F_i which has non-negative coefficients in the power series expansion. The coefficient are greater than or equal to the absolute value of the corresponding coefficients for F_i.
Sofia generalised this result in her dissertation to systems of order r with time derivatives $\frac{\partial^r \mu}{\partial t^r}$. One of the more precise forms of the Cauchy-Kovalevskaya Theorem tells us that an equation $\frac{\partial \mu}{\partial t} = f(t, x, v, \frac{\partial \mu}{\partial x})$, where f is analytic for values near $(t_\theta, x_\theta, v_\theta, \frac{\partial \mu}{\partial x})$. This equation has exactly one solution $v(x, t)$ which is analytic near (x_θ, t_θ). Sofia was influenced by Cauchy's use of majorants in his work in proving this theorem to obtain locally convergent power series solutions. She used majorants of the form

$$\frac{N}{1} - \left[\frac{t_1 + t_2 + \ldots + t_r}{\sigma}\right],$$

where N and σ are constants [7].

5 Other Significant Achievements and Legacy

Figure 5.1: Commemorative coin made in honour of Sofia Kovalevskaya (source: https://en.numista.com/catalogue/pieces 71562.html)

Figure 5.2: Bust of Sofia Kovalevskaya by Finnish sculptor Walter Runeberg (source: Wikimedia Commons)

In early 1891, at the height of her mathematical powers and reputation, Kovalevskaya died of influenza complicated by pneumonia. She had travelled to France and had fallen ill shortly after returning to Stockholm.
Sofia Kovalevskaya was the first woman in modern Europe to gain a doctorate in Mathematics. Sofia was the first person to join the editorial board of the scientific journal, *the Acta Mathematica*. Sofia was the world's first female professor of Mathematics. She was the first woman to be made a Corresponding Member of the Russian Academy of Sciences. In 1888, Sofia entered the French Academy of Science competition which entailed submitting a paper on the theory of the rotation of a solid body. Sofia's paper was so brilliant that she was awarded the Prix Bordin and the award amount was increased from 3,000 francs to 5,000 francs [5].
Kovalevskaya also gained a reputation as a writer, an advocate of women's rights, and a champion of radical political causes. The Alexander von Humboldt Foundation of Germany presents the Sofia

Kovalevskaya award in every two years. This prestigious award named in her honor is given to promising young academicians to further pursue their research in Sciences or Arts and Humanities. The School of Mathematics and Statistics at the Polytechnic University of Catalonia hosted a half-day conference devoted to their 'Mathematician of the Year' - Sofia Kovalevskaya in year 2018-19 [6].

Sofia Kovalevskaya impacted the world by not only discovering important Mathematical principles but also by opening the door for other female mathematicians. The action against prejudice against women would have been inevitable without her. Sofia changed the world, thanks to her unparalleled devotion to Mathematics and perseverance to overcome prejudice.

References

[1] Koblitz H.A., *A Convergence of Lives- Sofia Kovalevskaya Scientist, Writer, Revolutionary*, Rutgers University Press, 1993.

[2] Spicci J., *Beyond the Limit: The Dream of Sofia Kovalevskaya*, Forge Books, 1st edition, 2002.

[3] Stillman B., *Sofia Kovalevskaya, A Russian Childhood*, 1978, pp. 47-58.

[4] Lamb E., Review: Remembering Sofya Kovalevskaya, *Scientific American*, `https://blogs.scientificamerican.com/roots-of-unity/review-remembering-sofya-kovalevskaya/`

[5] Sofia Vasilyevna Kovalevskaya — Russian mathematician, *Britannica*, `https://www.britannica.com/biography/Sofya-Vasilyevna-Kovalevskaya`

[6] Sofja Kovalevskaja Award, *Alexander von Humboldt Stiftung*, `https://www.humboldt-foundation.de/en/apply/sponsorship-programmes/sofja-kovalevskaja-awar`

[7] Ellison L., Sofia Kovalevskya-Cauchy-Kovalevskaya Theorem, *MacTutor*, University of St. Andrews, `https://mathshistory.st-andrews.ac.uk/Projects/Ellison/chapter-5/`

(Mentor) Ms. Reema Agarwal, Assistant Professor, Department of Mathematics, Lady Shri Ram College for Women, New Delhi
reemaagarwal001@gmail.com

Shiya Ramteke, B.Sc.(H) Mathematics, 4th Semester, Lady Shri Ram College for Women, New Delhi
shiyaramteke.math2021@gmail.com

Varri Krishna Priya, B.Sc.(H) Mathematics, 4th Semester, Lady Shri Ram College for Women, New Delhi
krishnapriya.maths2021@gmail.com

CONTACT US

Email Id: eclat.lsr@gmail.com

Lady Shri Ram College for Women
(University of Delhi)
Lajpat Nagar, New Delhi - 110024